Thesis for Master's degree in chemistry

Cathrine Brecke Gundersen

Biodegradation and Characterization of Dissolved Organic Matter (DOM) along the Flowpath of a N-saturated Subtropical Forested Catchment in China.

60 study points

DEPARTEMENT OF CHEMISTRY

Faculty of mathematics and natural sciences

UNIVERSITY OF OSLO 06/2012

Abstract

Excessive input of anthropogenic reactive nitrogen (Nr) to forested ecosystems is associated with increased rates of denitrification and possible emission of the potentially harmful greenhouse gas nitrous oxide (N_2O). Denitrification is performed by heterotrophic bacteria, and Dissolved Organic Matter (DOM) is thus required for the process to proceed. Only a fraction of DOM is however assumed to be readily available for the bacteria. In a N-saturated subtropical forest in South China (Tie Shan Ping) potential denitrification rates and growth potential have been investigated in the framework of a study on N_2O emissions. Spatial variations were found, displaying higher denitrification rates at the unsaturated hill slope (recharge zone) as compared to the more hydromorphic groundwater discharge zone. These findings were explained by the denitrifiers being C-limited, which was especially evident at the groundwater discharge zone. It was hypothesized that the reduced transport of DOM from the densely vegetated hill slope to the groundwater discharge zone was attributed to rapid mineralization along the flow path. This would result in only the more recalcitrant fraction of DOM remaining in solution for transportation to the groundwater discharge zone.

The objective of this present study was to test this hypothesis by investigating differences in chemical characteristics and biodegradability of the DOM between the hill slope and the groundwater discharge zone. Soil-water samples collected along a topographic gradient, using suction lysimeters, were subject to both biological-, chemical-, and structural analyses. Measured biodegradability, using a batch experimental setup, suggested that the DOM from the groundwater discharge zone was far more biodegradable than the DOM from the hill slope. This was further corroborated with the structural characterization, using UV-Vis Absorbency and Fluorescence Spectroscopy, indicating small amount of more aromatic, and a low ratio of Humic to Fulvic acids in the DOM from the groundwater discharge zone as compared to the samples from the hill slope. This would imply that the attenuation of DOM along the flow path in Tie Shan Ping could not be attributed to mineralization. Instead, the loss of less biodegradable DOM is suggested to be explained by selective adsorption of the more aromatic, higher molecular weight, hydrophobic constituents of DOM to the clay-rich and organic-poor soils of the hill slope.

Preface

This research presented in this thesis was carried out as a part of the project "N_2O emissions from N saturated subtropical forest in South China", funded by the Research Council of Norway (NFR), Norklima program, Project Number 193725.

First of all, I would like to thank my supervisor Rolf D. Vogt for inspiring me to continue my studies at the University of Oslo, and for expanding my abilities to work as a scientist, both through my thinking and through my pen. Thank you to my co-supervisor Jan Mulder for letting me take part in this interesting project, and for expressing value in my results.

I would like to thank Zhu Jing for welcoming me to the wonders of China, and for helping me, together with Peter Dörch, to make me see the context of my results in the whole of the project. Thank you to Annelene Pengerud for sharing your experience and time with me for the development and execution of the biodegradation experiment, and to Katrin deKnoth for taking the time to introduce me to fluorescence spectroscopy. To Marita Clausen at the Analytical Laboratory I'm grateful for all of your answers to my newbie questions.

A great thank you to Reidun Sirevåg for introducing me to the field of microbiology, of which I'm now greatly found! Thank you for sharing your time and knowledge with me, and most of all for being an inspiration.

To all of you who have been a member of the Environmental chemistry group during the last two years, I would like to thank for laughs and the feeling of togetherness; Kaja, Pauline, Yikalo, Yemane, Muisha, Libargachew, and Bishnu. Especially thank you to Alexander Engebretsen for helping me with the IC, for introducing me to R, and for your encouraging words. To Christian W. Mohr for all your help and guidance, and for inquisitive discussions about organic matter. To Ruikae Xie for analyzing my samples with the ICP-MS, to Sahle Smur for helping me with the ICP-OES, and to Neha Parekh for analyzing my samples for P, and for becoming one of my best friends!

Thank you to my mom and dad for your unconditional love, support, and guidance. Thank you to the best friends in the whole entire world for support, laughs, and understanding. Especially thank you to my two roommates for the past year, Marianne and Ida. Finally, I would like to dedicate this master thesis to the memory of my beloved grandparents.

Table of Contents

1. Introduction

1.1 Emission of nitrous oxide (N_2O) from terrestrial Ecosystems and the role of Dissolved Organic Matter (DOM)

Anthropogenic disturbances of the biogeochemical cycles, which may lead to imbalance in the fluxes between the biosphere and the atmosphere, are perhaps today's greatest environmental challenge (Bakken and Dörsch 2007). The nitrogen cycle is conceivably the most profoundly affected (Galloway et al. 2008), resulting from an anthropogenic doubling of the total flux of reactive nitrogen[1] (Nr) to the environment, mainly from the application of synthetic fertilizers (NH_4NO_3) of which has increased exponentially from the 1940s (Vitousek et al. 1997).

Excessive application of fertilizers in agricultural areas may lead to increased deposition of Nr in nearby forested ecosystems. This occurs from volatilization and subsequent deposition of ammonia (NH_3). Forested soils which are inherently relatively acid, act as traps for ammonia by protonizing it to ammonium (NH_4^+). Although nitrogen is an essential element for all forms of life, an ecosystem may become N-saturated if the rate of Nr input exceeds that of the uptake by the biota, which is caused from exhaustion of other essential elements such as phosphorous (PO_4^{3-}) and calcium (Ca^{2+}) (Vitousek et al. 1997). In forest soils, the ammonium is readily converted to nitrate (NO_3^-) through the microbial mediated process of nitrification, resulting in an elevated pool of nitrate. Nitrate does neither form insoluble salts nor is readily adsorbed (Appelo and Postma 2005), but can be removed from the system through denitrification. This process, also mediated by microbes, involves reduction of nitrate to molecular nitrogen (N_2) by oxidation of organic matter. The process involves the intermediate species of nitrite (NO_2^-), nitric oxide (NO), and nitrous oxide (N_2O), in which the four steps are catalyzed by four distinct enzymes (vanSpanning et al. 2007). Although molecular nitrogen is termed the end product of denitrification, emission of the potentially harmful greenhouse gas, nitrous oxide, is frequently reported. This results from inhibition of the final

[1] Reactive nitrogen, Nr, includes the inorganic (NH_3, NOx, HNO_3, N_2O, and NO_3^-) and the organic (urea, amines, proteins, and nucleic acids) forms that readily participate in reactions of the N-cycle.

enzyme of the reaction sequence, which is generally attributed to environmental conditions such as low pH and shifting oxic/anoxic conditions (Firestone and Davidson 1989).

Nitrous oxide is estimated to have 310 times higher global warming potential than carbon dioxide (CO_2), due mainly to its long atmospheric lifetime of 114 years (Forster et al. 2007). Considering the strong forcing nitrous oxide has on the greenhouse effect, the estimated yearly global increase of 0.26 % may have tremendous consequences. With denitrification stated to be the main source of nitrous oxide emission (vanLoon and Duffy 2005), it is important to obtain knowledge about what factors are governing this process.

Denitrification is an alternative form of respiration performed by a number of facultative aerobic heterotrophic bacteria under anaerobic conditions, and a constant supply of organic matter is thus required for the process to proceed (Madigan et al. 2012). Organic matter constitutes a mixture of heterogeneous organic molecules derived from incomplete decomposition of plant material and animal remnants (vanLoon and Duffy 2005). Only a fraction of organic matter is readily available for microorganisms with the availability being governed by numerous interconnected factors which can be divided into the intrinsic DOM quality parameters (e.g. structural and functional), soil and solution parameters (e.g. ionic distribution, pH, flow regime), and external factors (e.g. vegetation, climate, land-use) (Marschner and Kalbitz 2003).

1.2 China in the context of global N_2O increase

In the global assessment of major sources of N_2O emission, tropical forests have received increased attention in recent years (IPCC 2001). The primary production in tropical forests is associated with P-limitation, as compared to the N-limited temperate forests, and will therefore experience a faster response to excessive deposition of Nr (Hall and Matson 1999). This, in addition to the higher temperature and moisture levels will result in higher rates of denitrification with possible associated emission of nitrous oxide (VanLoon and Duffy 2005).

Tie Shan Ping is a subtropical forested catchment located in the south-west of China, and has been found by the Sino-Norwegian interdisciplinary IMPACTS project to receive the highest loading of Nr among five monitored catchments in China during the years of 2001 – 2004 (Larssen et al. 2011). Despite N saturation and a high input of Nr there were relatively low fluxes of Nr in the runoff streams leaving the catchment. Based on these findings, this

forested catchment was selected as a study site for a research project assessing N_2O emissions from denitrification in acid forest soils. Within this project, Solheimslid (2011) investigated potential denitrification (and nitrification) rates in the catchment, and revealed spatial variations both in the denitrification potential and in the growth response of the bacteria. The more acidic and well-aerated recharge zone (hill slope) was found to portray higher rates of denitrification than the less acidic and waterlogged (groundwater) discharge zone. These findings contradict the theory in that denitrification is favoured in anaerobic and less acidic soils. This was however attributed to C-limitation, in which the bacteria from the discharge zone displayed zero growth without the addition of a readily available C-substrate. Solheimslid (2011) therefore hypothesized that the transport of Dissolved Organic Matter (DOM) from the more densely vegetated and DOM rich hill slope to the groundwater discharge zone is limited due to rapid mineralization of DOM along the flowpath of the catchment, resulting in only the more recalcitrant and thus less biodegradable DOM ending up in the discharge zone.

The objective of this thesis was therefore to investigate differences in both the quality and quantity of DOM along the soil-water flowpath through the Tie Shan Ping watershed, with special emphasis on parameters related to the biodegradability of DOM. Additionally, a sub-goal of revealing intrinsic DOM characterization parameters that governs its biodegradability was investigated. This was achieved by including two sets of previously characterized Reverse Osmosis (RO) isolated DOM reference samples in a biodegradation experiment. Empirical relationships between data on the DOM characteristics and the biodegradability of the DOM material were deduced.

2. Theory

2.1 Soil Organic Matter (SOM)

Soil Organic matter (SOM), also termed humus, affect numerous biogeochemical processes in soils, in which it is present in varying degree (Stevenson 1994). It originates from all organisms once living in a given area, and is formed through *incomplete* biotic and abiotic decomposition and transformation processes, in addition to secondary synthesis. The major source of SOM is that of plant origin, followed by microbial and animal remnants (Hayes 2009). Resulting from the numerous sources and transformation processes leading to its formation, SOM is characterized as a complex, dynamic, and heterogeneous mixture of organic compounds (MacCarthy 2001).

2.1.1 Formation of Soil Organic Matter (SOM) – "The humification process"

Collectively, all of the pathways leading to SOM formation are termed the humification process. The first steps are generally attributed to biotic decay, mediated by various species contributing in a subsequent manner depending on their metabolic adaptations (Huang and Hardie 2009). Microorganisms account for the majority of biotic decay (Wolters 2000), and include most of the saprophytic bacteria and fungi (Ross 1989). These organisms synthesize and secrete enzymes, not present in higher eukaryotes, which are specialized to degrade biomolecules into their constituent chemical subunits. During biotic decay, compounds of higher nutrient and energetic yield are utilized first (i.e. rich in nitrogen and carbohydrates), whereas the more recalcitrant and complex material remain. Biotic synthesis involves incorporation of organic compounds into biomass, which in addition to C lost through respiration (CO_2), leads to only a small fraction of the initial litter ending up as SOM. Abiotic decay and synthetic processes include the polymerization of phenolic compounds with concominant ring-cleavage, resulting in formation of more aliphatic polymers with higher content of carboxylic groups. Further abiotic processes cover incorporation of amino acids (Huang and Hardie 2009), and inorganic constituents from rock weathering into the SOM (Ross 1989). These abiotic processes are generally catalyzed by metal-oxides (Mn, Fe, Al, Si), clay minerals and dissolved metals (Kogel-Knabner and Kleber 2011). Finally, with the steady supply of fresh organic litter, the heterogeneity of OM arises.

2.1.2 Components of Soil Organic Matter (SOM)

The resulting SOM can be subdivided into two categories, termed non-humic and humic substances. Non-humic matter includes compounds that belong to known classes of biochemistry, such as amino acids, carbohydrates, fats, waxes, resins, organic acids, and other low-molecular-weight organic substances, whereas the latter category consists of higher molecular weight compounds not possible to characterize distinctively by current methods (Schnitzer and Khan 1972).

Humic matter (HM) constitutes the dominating fraction of SOM (Stevenson 1994), and can be described as "an extraordinary complex, amorphous mixture of highly heterogeneous...molecules" (MacCarthy 2001). The characteristic of HM is largely dependent on the source and environment of origin, with however, similarities being more pronounced than differences among samples from various sources (Gaffney et al. 1996). Thus, based on analysis of a wide variety of HM, general elemental-, structural-, and functional properties have been assigned. Dominating elements consists, not surprisingly, of the major elements of life; carbon (45 - 60 %), oxygen (25 - 45 %), hydrogen (4 - 7 %), and nitrogen (2 – 5 %) (VanLoon and Duffy 2005), distributed within a quite narrow range. Structurally, HM is composed of a skeleton of alkyl/aromatic units on which the following major functional groups are attached; carboxylic acid, phenolic and alcoholic hydroxyls, in addition to groups of ketone and quinone (Gaffney et al. 1996).

Characterization of this heterogeneous material has historically been based on fractionation, which has lead to the current fractionation scheme which divides HM into three categories based on solubility within the pH range (Stevenson 1994);

- Fulvic acid (FA) is soluble within the whole range of pH values
- Humic acid (HA) precipitates out at pH 2, while remains soluble at elevated pH
- Humin (Hu) is insoluble at all pH values (VanLoon and Duffy 2005).

These fractions are structurally similar to each other, but display larger differences in molecular weight, elemental analysis, and distribution of functional groups (Schnitzer and Khan 1972). Among the three fractions, the largest differences are found between the fulvic

and the humic acids, whereas humin closely resembles that of humic acids (Gaffney et al. 1996).

Generic molecular structures of humic and fulvic acids, proposed by Stevenson (1982) and Buffle (1977), respectively, are presented in Figure 1. Although structurally similar, fulvic acids possess more of an aliphatic character than the humic acids which are dominated by conjugated aromatic compounds (Gaffney et al. 1996). Fulvic acids are further characterized by lower molecular weight (1000 - 30,000) and higher O:C ratio, whereas the humic acids consists of higher molecular weight compounds (10,000 - 100,000) dominated by the remaining major elements (H, C, and N) (Stevenson 1985; Gaffney et al. 1996; Paul et al. 1996). The higher oxygen content of fulvic acids is attributed to a higher content of carboxylic (COOH) and phenolic (OH) functional groups, which results in a more acidic character of this fraction (Stevenson 1985). The humic acids have further been found to contain larger content of longer fatty acids, which result in more hydrophobic character of HA as compared to FA (Beck et al. 1993).

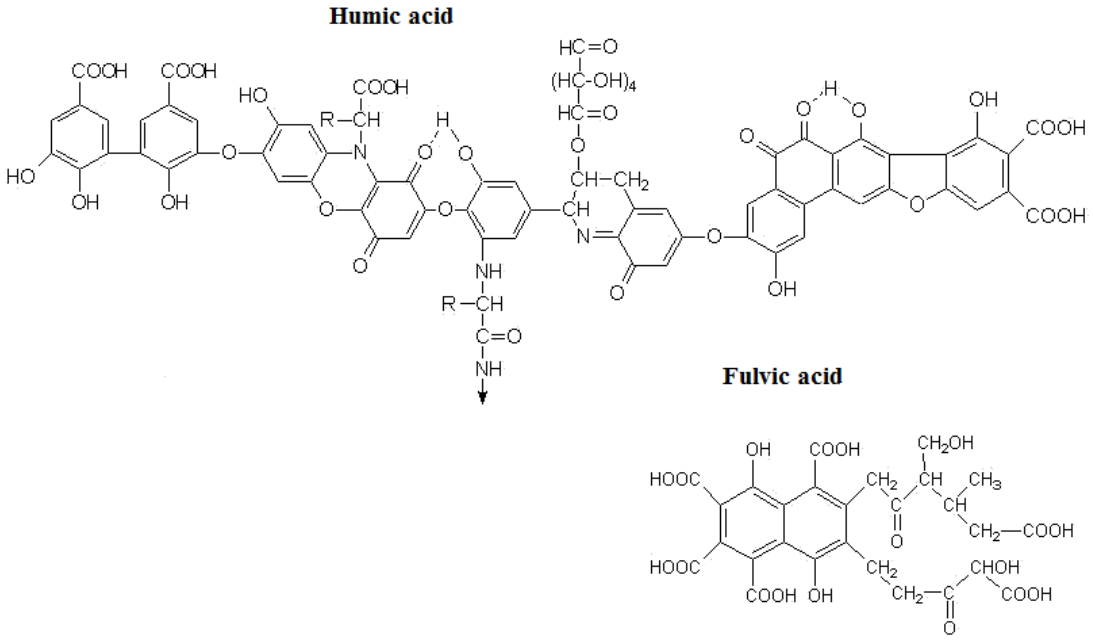

Figure 1: Generic molecular structure of Humic acid (Stevenson 1982) and Fulvic acid (Buffle 1977). Note that the difference in size between the two molecules in the figure is not representative for reported differences.

2.2 Dissolved Organic Matter (DOM)

Dissolved Organic Matter (DOM) is operationally defined as the part of SOM in the aqueous phase that passes through a filter paper of pore-size 0.45µm, while the remaining fraction in solution is termed Particulate Organic Matter (POM) (Thurman 1985). DOM is not the dominating OM fraction in soils (McGill et al. 1986), but is as its name implies, the most mobile and reactive constituent of SOM, and plays for this reason a significant role in several biotic and abiotic processes in soil ecosystems (Zsolnay 1996).

DOM consists of 50-75 % HM (Thurman 1985), with fulvic acid reported to be the dominating fraction in soils (Bolan et al. 2011). This may, at least partly, be explained by abiotic catalyzed processes rendering the character of the DOM from aromatic to more aliphatic, e.g. phenolic polymerization with concomitant ring-cleavage (Huang and Hardie 2009) (Chapter 2.1.1). The remaining constituents of DOM are ascribed to varying amounts of the identifiable compound classes making up non-humic matter (Bolan et al. 2011), which is stabilized to the HM through covalent bonding, hydrogen bonding, and electrostatic interactions. Thus, there is no clear distinction between the humic- and the non-humic fractions of DOM (Leenheer 1985). From Figure 2 it appears, that by definition, DOM also includes viruses, some ultra-small bacteria, and colloidal-OM, in addition to the "true" DOM. The colloidal DOM generally constitutes humic acids, and is commonly associated with clay minerals or oxides of iron and aluminium (Thurman 1985).

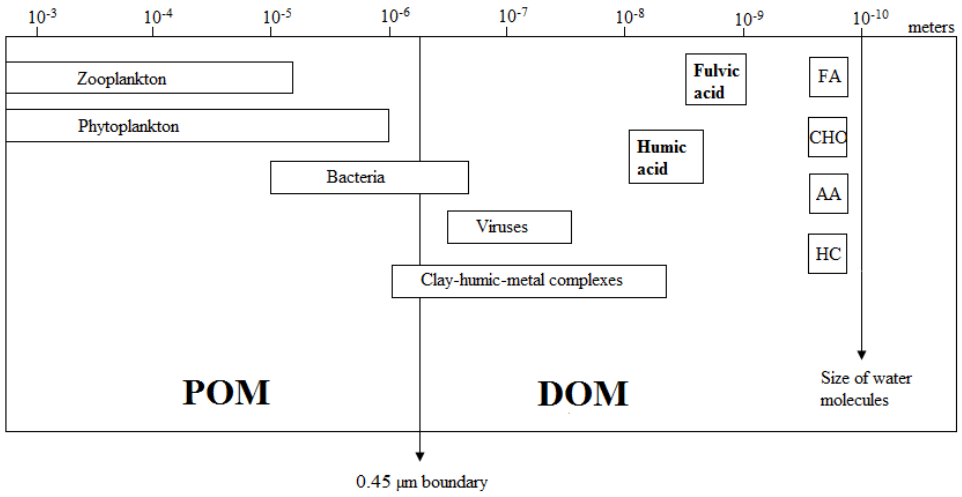

Figure 2: Size range of components included in the definition of Particulate Organic Matter (POM) and Dissolved Organic Matter (DOM), modified from Thurman (1985). FA = fatty acids, CHO = carbohydrates, AA = amino acids, HC = hydrocarbons.

2.3 Dynamics of DOM in Forested Soils as related to its properties

Both the quantity and quality of DOM in soils results from the balance between inputs and outputs, in addition to being governed by the numerous biogeochemical processes taking place in the any given area (Zsolnay 1996; Huang et al. 2009; Bolan et al. 2011). The dominating mechanisms regulating both the quantity and quality of DOM in forested soils are illustrated in Figure 3. Sources include organic compounds from 1) plant litter, 2) mobilization of SOM, and 3) from the rhizosphere, while sinks/transformation processes covers 4) transport governed by hydrological conditions, 5) adsorption to mineral phases, and 6) biodegradation. These biogeochemical processes are in turn interconnected, and depend on environmental factors such as temperature, precipitation and the physical/chemical characteristics of the soil, making it difficult to predict the fate of DOM in soils (Kalbitz et al. 2000).

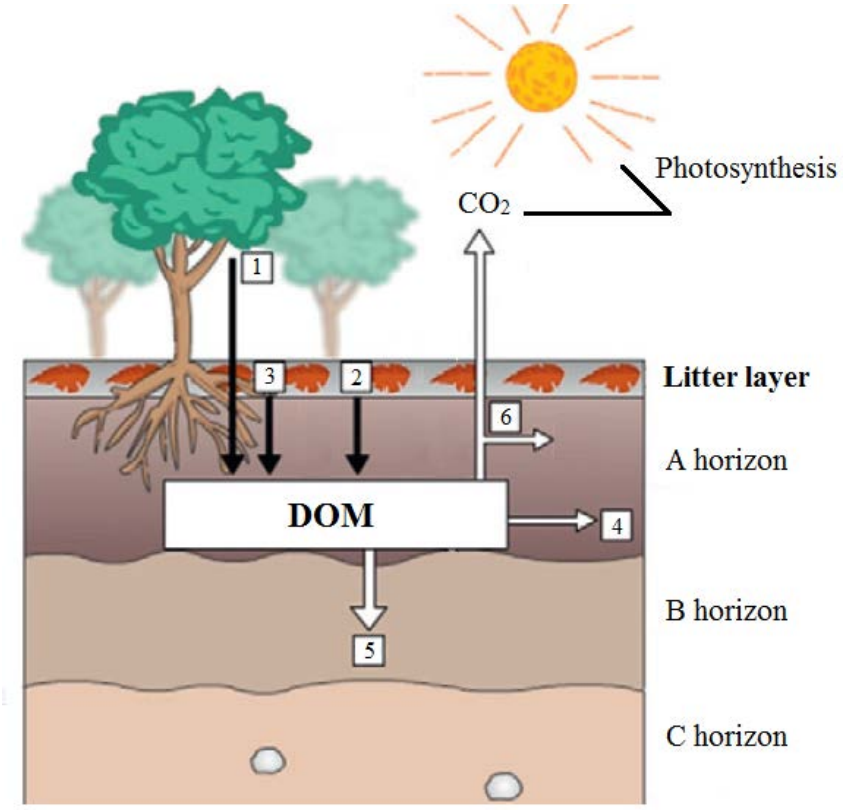

Figure 3: Illustrating the major processes governing DOM dynamics in soils, modified from Bolan et al. (2011). Sources include; 1) plant litter, 2) SOM mobilization, and 3) input from the rhizosphere, while sinks/transformation processes are represented by 4) flow transport, 5) adsorption, and 6) biodegradation.

2.3.1 Sources

The two major sources of DOM in soils are stated above to be from mobilization of SOM, and from plant litter (Kalbitz et al. 2000), while secondary sources may originate from the high biological activity of the rhizosphere (Bolan et al. 2011) (Figure 3, no. 1-3). Mobilized SOM is considered to be of recalcitrant nature in that it has already been exposed to humification processes in the soil. The extent of mobilization depends on the relative affinity of a molecule for the aqueous phase over the solid, and this tendency may further be altered through biotic (e.g. biotransformation of cellulose to glucose) and abiotic processes (Zsolnay 1996). Plant litter, on the other hand, is a source of "fresh" organics, and consist of varying degree of proteins, hemicellulose, cellulose, and lignin, in addition to lipids, sugars, organic acids, and amino acids (Paul and Clark 1996). Although these constituents display large variations in biodegradability, plant litter is considered as a source of labile DOM in that it has not been subject to extensive humification (Kalbitz et al. 2000). The relatively high biological activity of the rhizosphere further adds up as a secondary source of labile DOM, contributing with turnover of fine roots, plant and microbial exudates, in addition to microbial remnants (Zsolnay 1996; Bolan et al. 2011). Microorganisms generally consist of varying degree of lipids, chitin, and other biochemical components such as amino acids (Paul and Clark 1996).

2.3.2 Flow Transport

Transport of DOM (Figure 3, no. 4) generally follows the hydrological conditions in the catchment. As precipitation falls, organic material is flushed from the organic horizon, and may be further transported with the non-evapotransporated water, either by overland flow or through infiltration into the soil. Overland flow mainly occurs at high precipitation, in steeply sloped regions with shallow soils, or in saturated systems. Water that infiltrate the soil may leave the drainage basin as sub-surface runoff, or infiltrate further laterally until it reaches either the water table or an impermeable layer (Kalff 2002). The residence time of water will largely determine the fate of the DOM in that increased water fluxes will reduce the contact time between DOM and the soil/biota, limiting the possible transformation reactions (Kalbitz et al. 2000).

2.3.3 Adsorption to clay minerals

Clay minerals serve as excellent adsorbers in soils, which is related to its large and chemically reactive surface area (Appelo and Postma 2005). Organic matter adsorbed to clay minerals (Figure 3, no 5) typically represent more than 50 % of the total organic carbon in mineral soil (Chilom 2009), and the association is known to render both the properties of the clay (Cornejo and Hermosin 1996) and the quality of the organic matter remaining in the soil solution (DOM) (Chilom 2009). The exact mechanism of formation for this association is not clear, which is be due to the structural complexity of the organic matter (Cornejo and Hermosin 1996). However, based on the possible mechanisms found for adsorption of different types of specific organic molecules to clay minerals, the following possible mechanisms are proposed; physical adsorption (van der Waals forces), electrostatic bonding (chemical), H-bonding, and coordination with metals (Stevenson 1994).

To what extent DOM is adsorbed to clay minerals has been found to depend on several different factors, including solution properties, chemical- and physical properties of the clay mineral, and the intrinsic properties of the DOM itself (Chilom 2009). With regards to the chemical and physical properties of DOM, it is generally stated the more hydrophobic, aromatic, and higher molecular weight fractions containing N-functional groups are preferentially adsorbed to mineral surfaces, whereas the hydrophilic, less aromatic, low molecular compounds will remain in the solution (Kalbitz et al. 2000; Bolan et al. 2011).

Adsorption is further found to increase with increasing ionic strength of the water due to a combination of decreased solubility of DOM and charge neutralization of the clay surfaces. Increased temperature is found to increase adsorption that is of a chemical mechanism, and adsorption is further found to generally increase with decreasing pH due to reduced electrostatic repulsion between the negatively charged clay surface and the acidic functional groups of the organic matter (Chilom 2009).

Adsorption of DOM to clay minerals is stated to be the dominating process of DOM immobilization/transformation in the lower soil horizons (B horizon) (Zsolnay 1996), and is generally assumed to be a mechanism of partial stabilization against biodegradation (Insam 1996).

2.3.4 Biodegradation

All organisms require C for biosynthesis of cell material, and those which obtain this from organic compounds are termed heterotrophs (Madigan et al. 2012). Biodegradation of organic compounds may be complete, resulting in CO_2 and H_2O, or incomplete leading to fragmentation of the original compound. To what extent an organic compound is biodegraded is largely a function of its molecular properties, in the sense of the process being enzymatically controlled (Maier et al. 2009).

DOM, being composed of a mixture of different organic molecules is generally assumed to consist of at least three different pools with regards to biodegradability; a labile pool which is rapidly biodegraded, a more slowly biodegraded pool, and a pool of recalcitrant DOM which seems to persist biodegradation in laboratory experiments. These definitions should, however, only be used in relative terms since all organic molecules are believed to eventually be biodegraded. The chemical identity of the different pools are not certain, but it is generally assumed that labile DOM consists of simple carbohydrates, low-molecular acids, amino acids, amino sugars, and low-molecular weights proteins (Marschner and Kalbitz 2003), whereas the more recalcitrant pool is dominated by highly aromatic and complex compounds such as lipids and lignin (Kalbitz et al. 2003).

Highly branched molecules may further pose a problem for microbial attack in that the accessibility for the microbial enzymes may be hindered. The nature of the functional groups present on a molecule is moreover stated to affect the activity of the degrading enzymes through electronic interactions. In general, functional groups that are electron donating (e.g. CH_3) may induce biodegradability of a specific compound, whereas electron withdrawing groups (e.g. Cl^-) may have the opposite effect (Maier et al. 2009). Molecular size is frequently stated to be associated with biodegradability, probably due to the limited uptake of larger molecules by microorganisms. This effect of molecular size is however largely believed to result from the more easily biodegraded compounds being of lower molecular size (e.g. glucose, amino acids), rather than from the size itself (Wetzel 2001; Marschner and Kalbitz 2003). The elemental ratio of N:C is found to correlate positively with biodegradability of DOM (Bu et al. 2011), which may result from N being one of the essential elements for all microorganisms, and may thus also apply for O, H, P, and S (Madigan et al. 2012). The requirement for an aqueous phase for microbial uptake mechanisms may further lead to

preferential biodegradation of the more hydrophilic components of DOM (Maier 2000; Marschner and Kalbitz 2003).

A further dimension to the challenging task of predicting the extent of biodegradation of the DOM is added when Haider and Schäffer (2009) states that biodegradation of the pool termed recalcitrant may be increased though input of readily biodegradable organic compounds. This is explained by the wide spectre of metabolic solutions associated with bacteria; as readily biodegradable organic material is added, the more recalcitrant DOM is subject to co-metabolism.

2.4 Applications of DOM characterization

In order to characterize the mixture of heterogeneous organic molecules constituting DOM, several operationally defined parameters have been developed which are generally based on classical chemical procedures. To assess the environmental role of DOM, and to predict its fate in the environment, analysis procedures describing the behaviour of DOM is valuable. Such information is largely obtained from spectroscopic techniques. Certain challenges and shortcomings are however associated with analysis of this material, which include poor reproducibility due to the dynamic nature of DOM (Steelink 1985), in addition to a lack of conformity in the scientific community in terms of sample handling, pre-treatment, and due to slightly different operationally defined techniques.

While practically every available analysis techniques can be applied for DOM characterization purposes, the following section will include some of the generally applied methods, with emphasis on the interpretation of such results.

2.4.1 Elemental characteristics

Determination of the distribution of major elements (C, O, H, N) in the DOM is one of the most commonly employed methods for characterization, and is performed using classical chemical procedures (Huffman 1985). Although no structural formula can be obtained from such results, the relative distribution of O, H, and N to the total amount of C have been found to be indicative of the contribution of certain functional and structural groups in the DOM (Steelink 1985).

The O:C ratio indicates inherently the relative contribution of carbohydrates and carboxylic functional groups in the DOM, and has previously been stated to be one of the criteria distinguishing humic acids from the carboxylic-rich fulvic acids (Chapter 2.1.2). Aliphatic compounds will inherently contain more H to C than the aromatics, and thus, the H:C ratio functions as a proxy for the degree of conjugation. The N:C ratio is also stated to provide information of DOM (Steelink 1985), which include the contribution of nitrogen containing functional groups such as amines and amides, originating from amino acids and polypeptides (Thurman 1985).

2.4.2 Functional determination of DOM using spectroscopic methods within the UV-Vis region of the electromagnetic spectrum

Absorption of light within the UV (190-400nm) and visible (Vis; 400-800nm) region of the electromagnetic spectrum involves excitation of outer electrons from ground state to higher energy levels. When considering molecules, the absorbance is attributed to specific segments or functional groups that may contain σ-, π-, or η-electrons. These specific groups of atoms are termed *chromophores* (Pavia 2009), and are responsible for the characteristic colour of DOM (Stevenson 1994).

2.4.2.1 UV-Vis Absorption

The UV-Vis spectra of DOM are usually poorly resolved and contain few, if any, distinctive bands (Figure 4). The lack of resolution is typical for organic mixtures, and can be attributed to the numerous vibrational and rotational energy levels, in addition to strong intermolecular interactions among the various molecules (Stevenson 1994; Frimmel and Abbt-Braun 2009; Pavia 2009). Around $\lambda = 254$nm, however, a weak shoulder often appears which is assigned to chromophores of conjugated C=C and C=O double bonds (Frimmel and Abbt-Braun 2009) Absorbency at this specific wavelength is found to correlate strongly with the content of aromatic C found by NMR[2]-spectroscopy (Weishaar et al. 2003). By dividing the absorbency at this specific wavelength with the concentration of DOC in the sample, the Specific UV Absorbency index (sUVa) is obtained, which indicate the relative amount of aromatic C in the DOM (Vogt et al. 2008; Frimmel and Abbt-Braun 2009).

[2] Nuclear Magnetic Resconance Spectroscopy (NMR).

The absorbency of DOM decreases with increasing wavelength (Figure 4) (Stevenson 1994). Longer chained conjugated systems are responsible for the absorbency in the visible region, which is explained by the bathochromic shift[3] (Pavia 2009). Specific absorbance within the visible region can thus serve as a proxy for the amount of higher molecular weight chromophores, with the DOC normalized index termed sVISa (specific VISible Absorbance) (Vogt and Gjessing 2008).

In addition to the two indices of specific absorbency, two ratios are frequently presented for DOM characterization, which include the Specific Absorbency Ratio (SAR) and the E_4/E_6 ratio. The former is defined as the ratio of absorbency at 254 to 400nm, serving as a proxy for the relative contribution of lower to higher molecular weight chromophores (Vogt and Gjessing 2008). The latter ratio is defined as the absorbency at 465 to 665nm, and is found to decrease with increasing molecular weight and condensation. This ratio thus serves as an index of humification (Stevenson 1994). Absorption at a specific wavelength within the UV region, in particular $\lambda = 254$nm, has also been applied to quantify DOC (Frimmel and Abbt-Braun 2009). However, due to differences in the distribution of chromophores among samples, and also temporally within a given area, this method is only approximately (Tipping et al. 2009).

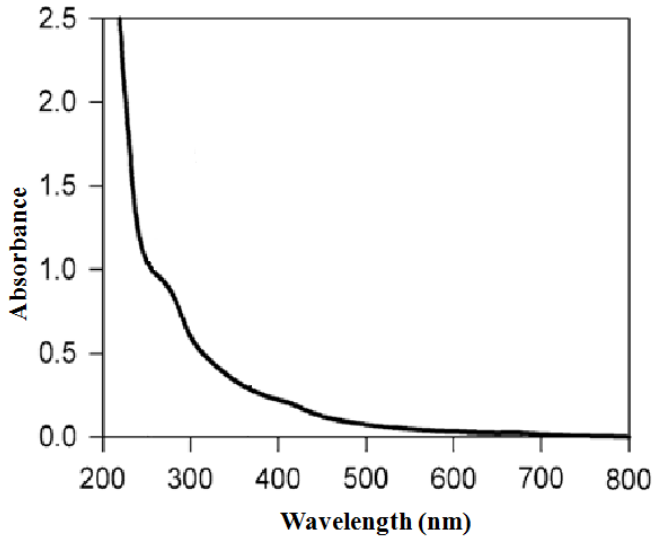

Figure 4: Typical UV-Vis absorbency spectra of DOM, edited from Leeben et al. (2010).

[3] Bathochromatic shift is a shift of absorbency towards longer wavelengths (red shift) induced by increasing length of conjugated systems.

2.4.2.2 UV-Vis Fluorescence

In contrast to the UV-Vis absorbency, fluorescence spectroscopy involves measurement of relaxation through emission of photons with lower energy (longer wavelength) than the incident light (Harris 2007). Not all molecules acquire this property, with the ability being largely a function of molecular structure, and generally attributed to those of double bonds (Frimmel and Abbt-Braun 2009; Martin-Neto et al. 2009).

Fluorescence spectroscopy has proven to be a rather useful method for characterization of DOM, with fluorescence being attributed to molecular systems such as C=O bonds, aromatic, phenolic, and quionine, in addition to more rigid unsaturated conjugated aliphatic entities. Several different types of spectra can be obtained, which include 2-D spectra of emission, excitation, and synchronous scan, in addition to 3-D fluorescence spectra. The latter is obtained by recording several emission spectra at different excitation wavelengths (Martin-Neto et al. 2009), offering several major advantages over single-scan methodologies in being independent of specific excitation and emission wavelengths (Coble 1996). Such spectra are generally termed Excitation-Emission Matrix (EEM) spectra, and the results can be presented in a 3 dimensional topographical manner with excitation and emission wavelength on the x- and y-axis, and the fluorescence intensity on the z-axis.

EEM spectra are able to capture the heterogeneity of DOM fluorescence. The interpretation of the > 10,000 wavelength-dependent fluorescence signals is however challenging. By combining the EEM spectra obtained for different types of DOM (model compounds, DOM-fractions, marine and freshwater samples), Chen et al. (2003) constructed four general areas of excitation and emission wavelengths in which fluorescence can be ascribed to specific compound classes of DOM (Figure 5);

1. Peaks at shorter wavelengths (< 250nm) and shorter emission wavelengths (<350nm) are related to simple aromatic amino acids such as tyrosine

2. Peaks in the intermediate excitation wavelengths (250- ~280nm) and shorter emission wavelengths (<380nm) are related to soluble microbial by-product like material

3. Peaks at longer excitation wavelengths (<280nm) and longer emission wavelengths (>380nm) are related to humic acid-like organics

4. Peaks at shorter excitation wavelengths (<250nm) and longer emission wavelength (>350nm) are related to fulvic acid-like materials

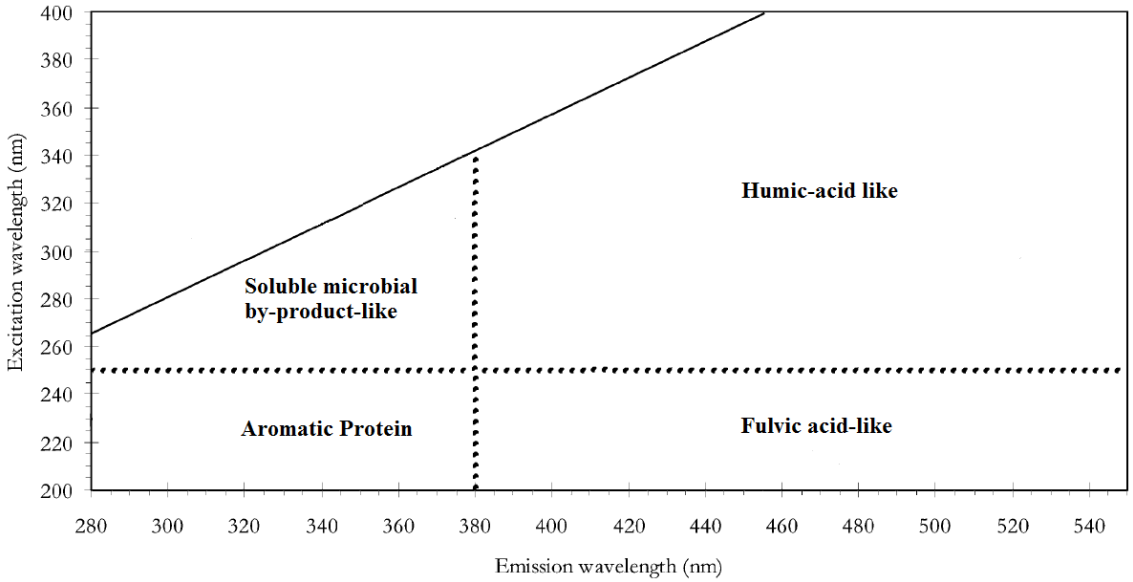

Figure 5: The sub-division of Excitation-Emission Matrix (EEM) spectra into four categories based on the specific excitation and emission wavelengths for the different compound classes of DOM. Modified from Chen et al. (2003).

2.4.3 Fractionation

The use of DOM fractionation techniques, based on properties such as solubility, molecular size, charge, and adsorption/de-sorption, has largely extended the knowledge of molecular properties and characteristics of DOM, in addition to aid in the application of analytical techniques (Swift 1985). Fractionation based on adsorptive properties of DOM has been the most successful method, and is frequently performed using chromatography through Amberlight XAD-8 resin. This non-ionic, acrylic polymer-material has excellent sorption properties for organic matter, and operationally defines DOM into hydrophobic and hydrophilic acids, bases, and neutrals of different strengths (Leenheer 1985).

From a review published by Bolan et al. (2011), an overview of the different compound classes found in these different fractions of DOM is presented (Table 1). Overall, the hydrophobic fraction of DOM comprise higher molecular weight compounds such as hydrocarbons, long-chained fatty acids, and humic-bound materials, whereas the lower molecular weight compounds containing elevated content of oxygen and carboxylic

functional groups are assigned to the fraction of hydrophilic DOM. One noteworthy aspect to this table is that both the humic and the fulvic acids are included in the category of strong hydrophobic material. This is contradicting to the fact that fulvic acids are distinguished from the humic acids in being of lower molecular weight and containing elevated amount of carboxylic functional groups, which should place this fraction among the hydrophilic compounds. Stevenson (1994) further states that fulvic acids are categorized as “weak hydrophilic acids” based on the same fractionation scheme. This indicates the inconsistency in DOM characterization, and that there exist few strict lines in categorizing the different fractions of this material. Moreover, with the dissolved form requiring some sense of hydrophilicity, these terms should be considered in a relative fashion rather than absolute.

Table 1: Components identified in specific fractions of dissolved organic matter (Bolan et al. 2011)

Fraction	Compound classes
Hydrophobic neutrals	Hydrocarbons
	Chlorophyll
	Carotenoids
	Phospholipids
Weak (phenolic) hydrophobic acids	Tannins
	Flavonoids
	Other polyphenols
	Vanillin
Strong (carboxylic) hydrophobic acids	Fulvic and humic acids
	Humic-bound amino acids and peptides
	Humic-bound carbohydrates
	Aromatic acids (including phenolic carboxylic acids)
	Oxidized polyphenols
	Long-chain fatty acids
Hydrophilic acids	Humic-like substances with lower molecular size and higher COOH/C ratios
	Oxidized carbohydrates with COOH groups
	Small carboxylic acids
	Inositol and sugar phosphates
Hydrophilic neutrals	Simple neutral sugars
	Non-humic-bound polysaccharides
	Alcohols
Bases	Proteins
	Free amino acids and peptides
	Aromatic amines
	Amino-sugar polymer (such as from microbial cell walls)

3 Materials & Methods

Complementing the soil-water samples from the study site in China, two sets of previously thoroughly characterized reference material of Reverse Osmosis (RO) isolated DOM were included in this study. This dry material is re-dissolved generating the reference samples. The following three sets of samples, are thus included in this study;

1. Soil-water samples containing DOM from Tie Shan Ping (TSP), China.
2. Reference Reverse Osmosis (RO) isolated DOM:
    a. Isolated (from surface waters in Norway) and characterized by and within the project entitled "Natural Organic Matter in drinking water" (NOM-typing) (Gjessing et al. 1999).
    b. Isolated (from surface waters in the Nordic countries) and characterized by the project entitled "Natural Organic Matter in the Nordic Countries" (NOMiNiC) (Vogt et al. 2001).

3.1 Field site description: Tie Shan Ping (TSP)

Tie Shan Ping (TSP; 29° 38' N, 106° 41' E) is a small (16.3 ha) forested catchment with acid soils that receives a high loading of airborne pollutants, including reactive nitrogen. It is located on the top of a ridge, with an elevation of about 450 – 500 m above sea level, running approximately 25 km northeast of the Chongqing city centre (Figure 6a). The site is situated within a national preserved forest (Dawei et al. 2001; Jin et al. 2006). The climate in the region is subtropical and humid with an average temperature of 18 °C. Minimum temperature is observed during January (8 °C) while maximum temperatures are reached in June (27 – 29 °C). Rainfall is characterized as monsoonal with most of the precipitation occurring from April to October, and with a mean annual precipitation estimated to about 1100 mm (Dawei et al. 2001). Haplic Acrisol (FAO[4]) is the main soil type of the area (Chen and Mulder 2007), which is characterized as clay-rich and with low base saturation. This soil type is typical for sub tropical forests (Driessen et al. 2001), and is representative for this southern part of China. The soil is further characterized as homogenous, and is dominated by the secondary clay minerals kaolinite, smectite, and some illite, and the primarily minerals quartz and feldspar

[4] Food and Agricultural Organization (FAO)

from the underlying sedimentary bedrock of mainly sandstone with some shale (Chen et al. 2007; Larssen et al. 2011). The vegetation of the catchment can be divided into three sections with regards to the dominating species. The highest situated part of the area is dominated by the coniferous tree specie Masson pine (*Pinus massoniana*), which was planted after the original deciduous forest was logged during the Great Leap Forward in the years of 1958-1962 (Jin et al. 2006). This is a typical forest history for large parts of China (Dawei et al. 2001). Deciduous shrubs and lianes are the dominant vegetation in the steep slopes in the middle level of the catchment, while the lower reaches, including the valley bottom, are covered by herbages dominated by ferns (Jin et al. 2006).

3.1.1 Sampling site description

The studied sub-catchment area within the field of TSP is 4.64 ha in size, and appears as a steeply sloped valley. With regards to morphological and hydrological conditions, the sub-catchment can be divided into a steep (approx. 34 %) hill slope region (recharge zone), and a groundwater discharge zone located in the valley bottom (Figure 6b) (Solheimslid 2010; Sørbotten 2011). The groundwater discharge zone consists of six to seven terrace levels originating from previous agricultural practices, with an overall slope of approximately 13 %. Clear pedological horizons are apparent in the soil profile of the hill slope (O, A, AB, B1 and B2), whereas none of these are visible in the groundwater discharge zone. The clay content in the soil profiles on the hill slope is found to increase with depth (A horizon: 21.09 %, B horizon: 24.47 %), and is substantially higher in the hill slope than in the groundwater discharge zone (14.83 %). In regards to other soil chemical and physical characteristics (% C, % N, pH, soil density, texture) the soil of the groundwater discharge zone is considered to be more similar to that of the subsoil on the hill slope (Solheimslid 2010). Hydrologically, a high proportion of interflow is allocated among the runoff at the hill slope, suggesting that the groundwater discharge zone receives considerable amounts of runoff from the hill slope. The groundwater discharge zone further appears more of as a wetland, with its surface-near groundwater table moving up and down following storm flow events, in addition to the presence of a small stream draining into a constructed pond located just below the study area. In terms of vegetation, the hill slope is dominated by quite dense woods, whereas the groundwater discharge zone is more sparsely vegetated by shrubs and pines (Solheimslid 2010; Sørbotten 2011).

Figure 6a: Location of the study area in the Southwest of China modified from Sørbotten (2011). The field of Tie Shan Ping (TSP) is outlined (green) in the inserted figure, and the studied sub-catchment is marked by a black line.

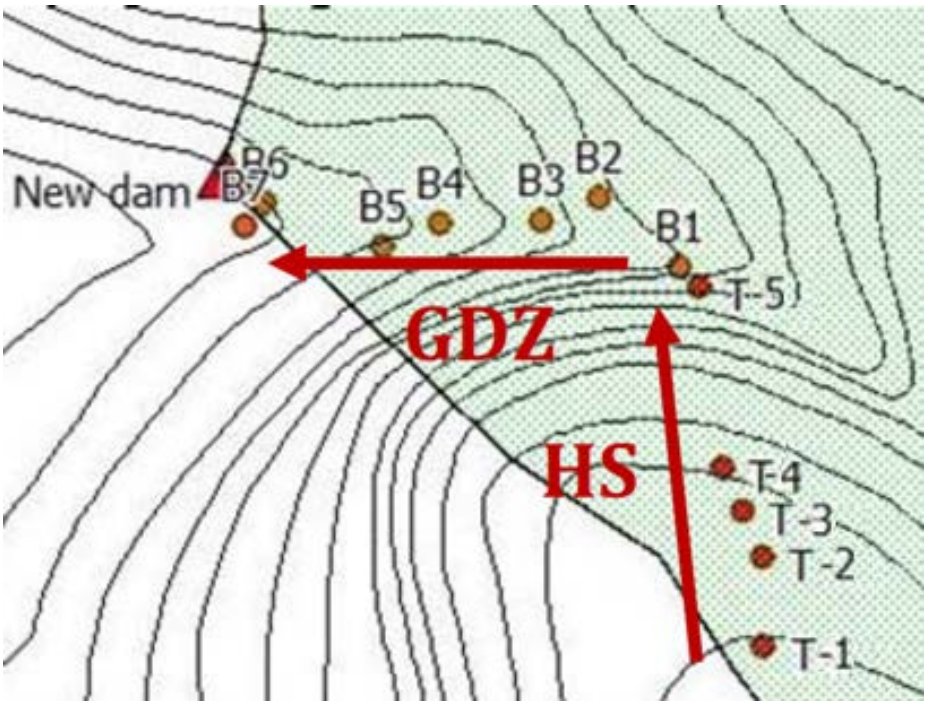

Figure 6b: Topographic presentation of the studied sub-catchment, including sampling plots from the hill slope (HS; T-1, to T-5, and B1) and the groundwater discharge zone (GDZ; B2 – B7). Modified from Solheimslid (2010).

3.1.2 Soil-water sampling

Soil-water sampling took place during the beginning of the raining season, from mid-April to the end of June 2011 by a local employee. Soil water were sampled from existing ceramic suction lysimeters installed in six plots on the hill slope (T1-T5 and B1) and six plots from the groundwater discharge zone (B2-B7) (Figures 6b and 7). On the hill slope, the lysimeters were installed in the following soil horizons; O/A, AB, B1, and B2 (top), whereas in the groundwater discharge zone, the lysimeters were installed at three different soil depths (20-30cm, 50-60cm, and 90-100cm) due to the lack of any clear soil horizons. These plots, including the different soil horizons/depths, were chosen to provide representative samples from the entire flow path of the studied sub-catchment. Samples were stored in plastic bottles and frozen immediately after collection. Freezing was selected as a preservation technique in that it stops biotic decay of the DOM, is non-additive and readily executable in the field. In early July, the samples were transported to the University of Oslo (UiO), Norway, in Styrofoam boxes equipped with frozen elements. Upon arrival, the samples appeared to have sustained nearly completely frozen, and were placed in a freezer (-18 °C) until analysis.

Figure 7: Sampling site at the hill slope (left) and in the groundwater discharge zone (right). Sampling glass bottles are displayed at both sites.

3.2 Reference samples of Reverse Osmosis (RO) isolated DOM

From the two previously conducted projects entitled “Natural Organic Matter in drinking water “ (NOM-typing) (Gjessing et al. 1999) and “Natural Organic Matter in the Nordic Countries” (NOMiNiC) (Vogt et al. 2001), a total of 19 DOM samples have been isolated by the method of Reverse Osmosis (RO). As both of these two projects shared the common sub-goal of establishing an inter collaboration for characterization of DOM, both sets of samples have separately been distributed to more than 20 research groups within Europe and North-America through their respective projects. Data generated was made available for this study and included results from a large number of methods for analyzing and characterization of DOM-properties including especially data on elemental distribution, functional group content, molecular size, and fractionation.

3.2.1 Field and Project description

Sampling sites selected for the two projects are presented in Figure 8, comprising eight sites within the Southern part of Norway (NOM-typing), and five sites within the Nordic countries of Norway, Sweden, and Finland (NOMiNiC). Based on the main aim of the NOM-typing project; “to develop a protocol for typing of DOM that could assist in the choice and optimization of water treatment processes”, the sites were carefully chosen to represent catchments that differed in properties such as climate, vegetation, retention time, etc., while at the same time not being under influence of neither agricultural nor industrial activities. The NOMiNiC project pursued the main aim of investigating the effect of anthropogenic loading on DOM, and the sites were selected to represent catchments from forested sites being similar in vegetation, soils, topography, and bedrock, while differing in climate and anthropogenic loading. Seasonal variations (spring/autumn) were further included in the NOMiNiC project, which resulted in a total of 10 samples. Note that two of the sampling sites were included in both of the projects (Humex B/Skjervatjern and Birkenes). For more detailed description of the various sampling sites, see Gjessing et al. (1999) and Vogt et al. (2001) for sites selected by the NOM-typing and NOMiNiC project, respectively.

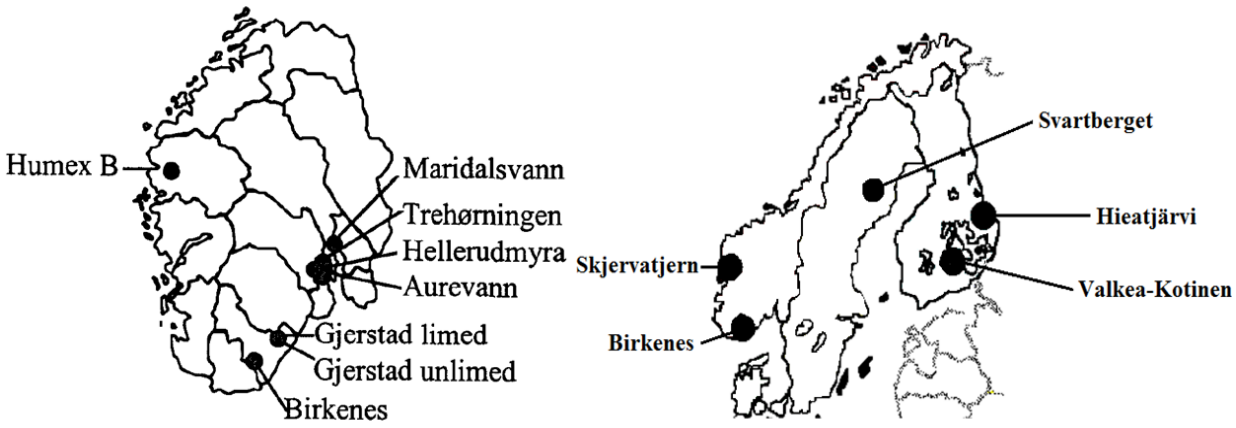

Figure 8: Sampling sites for the reference material. Left: sites within the Southern part of Norway selected for the NOM-typing project (Gjessing et al. 1999). Right: sites within the Nordic countries of Norway, Sweden, and Finland selected for the NOMiNiC project (Vogt et al. 2001).

3.2.2 Reference sample preparation by Reverse Osmosis (RO)

All reference materials were isolated from surface waters using the method of Reverse Osmosis (RO), in accordance with Serkiz and Perdue (1990). Through this method, nearly all of the dissolved inorganic and organic material from 500 – 3000 L of sample water is concentrated. This is performed in the field using a mobile RO-unit. The resulting water concentrate is filtrated through 0.45µm filters in the laboratory and concentrated further using a rotary evaporator. Samples are subsequently freeze-dried, resulting in the dry material of RO-isolated DOM (Figure 9).

Figure 9: Illustration of the appearance of Reverse Osmosis (RO) isolated samples of DOM.

This method has proven to be efficient for isolation and preservation of DOM with regards to its physico-chemical properties. One major alteration to the sample is however, that other cations in the raw-water are replaced with sodium (Na^+) through a cation exchanger in order to prevent precipitation of insoluble salts such as calcium carbonate ($CaCO_3$) and calcium sulphate ($CaSO_4$). For more information of the method and the equipment used for the isolation procedure, see Gjessing et al. (1999) and Vogt et al. (2001).

The total of 19 frozen RO isolates was thawed carefully by first placing them at 7 °C for 3h, followed by heating at room temperature (22 °C). Thawed samples were subsequently re-dissolved using 2 L of Type 1 water[5] to an estimated final concentration of 10 mg C L^{-1} based on their known content of carbon. In order to check for any concentration effects, three of the reference material was prepared to two additional estimated concentrations of 5 and 20 mg C L^{-1}. To ensure complete dissolution, samples were subject to stirring for approximately 72h in the dark using magnetic stirrers. After dissolution, samples containing reference material were filtrated through 0.2 µm membrane filters (cellulose acetate, Sartorius). This pore-size was selected as this was chosen as a sterilization technique for the TSP-samples with regards to the biodegradation experiment (Chapter 3.3.1). Although the microbial activity of these reference samples was assumed to be negligible, the same pore-size was used in order to compare the results from the two types of samples included in the study. Filtered samples were stored in prewashed LDPE[6] bottles in the dark, at 4°C until analysis.

[5] Type 1 water is ultrapure, de-ionized water (Milli-Q).
[6] Low Density Polyethylene (LDPE).

3.3 Sample pre-treatment

The frozen soil-water samples from TSP were thawed carefully by sequentially moving the samples from freezing temperature (-18 °C) to increasingly higher temperatures (24 h in 4 °C, 2 h in 7 °C, room temp.) until they reached room temperature.

3.3.1 Filtration

Once the samples reached room temperature, they were immediately filtrated through 0.2µm membrane filters (cellulose acetate, Sartorius) in order to separate out the fraction of particulate organic material (POM; > 0.45µm) (Thurman 1985), and as a means of sterilization (> 0.2µm) (Schnabel et al. 2002). Filtration was conducted using a water vacuum pump and filter papers were pre-rinsed using 150 mL Type 1 water. A greater loss of DOM than anticipated was observed during filtration. This was observed as a clear reduction in sample-solution-colour, and by apparent accumulation of material on the filter papers. The soil-water samples were collected through lysimeters, which are porous ceramic material with a pore size of about 1µm. The samples are therefore already filtrated through a coarse filter. Previous studies (Vogt, R. D. Pers. comm.) have shown that there is usually no difference between TOC and DOC in lysimeter samples. Fellman et al. (2008) found that freezing of surface water may lead to loss of DOC, DOP, and aromatic compounds (represented by sUVa). These samples were frozen in order to stop decomposition and preserve the organic material in the samples. The loss of material on the filters could therefore be the result of irreversible flocculation reactions induced by the up-concentration in pockets of brine occurring during the freezing. These findings are further stated by Fellman et al. (2008) to be especially applicable for samples containing DOC > 5mg C L^{-1} and/or samples with sUVa > 3.5-4 L mg-C^{-1} m^{-1}, which is characteristic for DOM with high content of more hydrophobic material. From analysis conducted post to filtration, four of the samples are found to contain DOC > 5mg C L^{-1}, indicating that possible loss of DOM from filtration could have occurred.

In order to control the effectiveness of the sterilization technique using filtration, sample aliquots of approximately 1 mL filtrated samples were plated on LB-agar[7] plates and incubated in room temperature. The samples used for this test had previously been plated as

[7] LB (Lysogeny Broth) agar is a nutritionally rich medium, used for growth of Bacteria.

unfiltered samples on the same type of agar plates to check for microbial activity in the context of inoculum preparation (Chapter 3.7.1). The amount of sample and the technique used to apply unfiltered and filtered samples to the agar plates differed. A generally larger amount of sample volume was plated for the filtered samples than for the unfiltered samples, and for certain of the unfiltered samples, the filter paper itself was applied directly on to the agar plates. By comparing results for unfiltered and filtered samples in Figure 10, it can be seen that the formation of colonies was greatly reduced by filtering the samples through a 0.2µm membrane filter. The sterilization was thus termed successful.

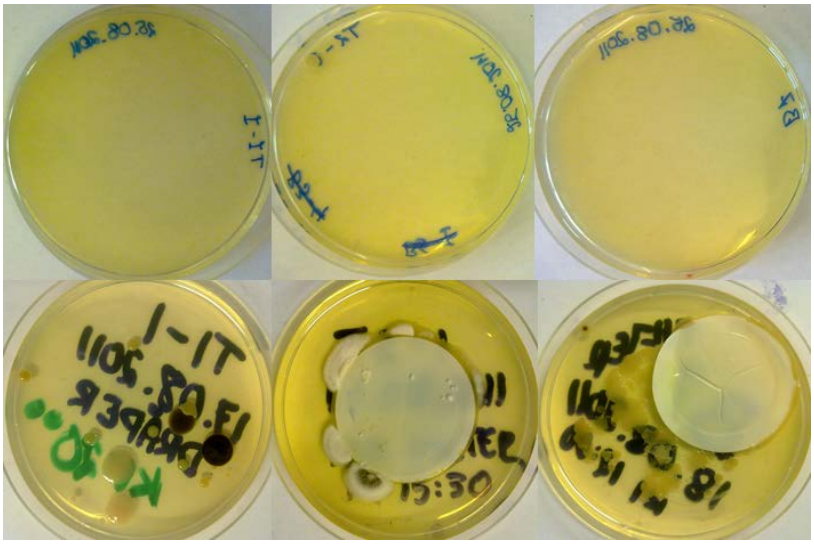

Figure 10: Results from plating filtered (above) and unfiltered (below) soil-water samples from Tie Shan Ping (TSP) on LB agar plates under the same set of conditions. Note that the filter paper was applied directly onto the agar plate for two of the unfiltered samples (below to the right).

3.3.2 Pooling of samples

Volume of soil-water being transportable from China was limited, thus it was decided to pool the samples based on their spatial and horizontal origin in the field. This resulted in a total of 11 samples representing two different soil horizons from the hill slope; O/A + AB and B1 + B2, and two different soil depths from the groundwater discharge zone; 20-30cm + 50-60cm and 90-100cm. An illustration of the origin and composition of the final 11 samples is presented in Figure 11. Pooling of the samples is justified since previous analysis in the field has proven similarities in the chemical characteristics in the soil-waters of the horizons/depths chosen to be combined, while including samples from all plots account for the hydrological connectivity among the sampling sites (Mulder, J. Pers.comm.).

The final samples were named based on their origin in the field, with 1) HS or GDZ indicating origin from the Hill Slope or the Groundwater Discharge Zone, 2) numbering (1-4) illustrating the origin along the transect of the hill slope or the groundwater discharge zone, and 3) the letter B being assigned to the samples originating from soil horizon B. Note that samples from the deeper soil depth (90 – 100 cm) of the groundwater discharge zone is assigned the letter B even though no soil horizons are evident in this area. The pooled samples were stored in prewashed LDPE bottles in the dark, at 4°C until analysis.

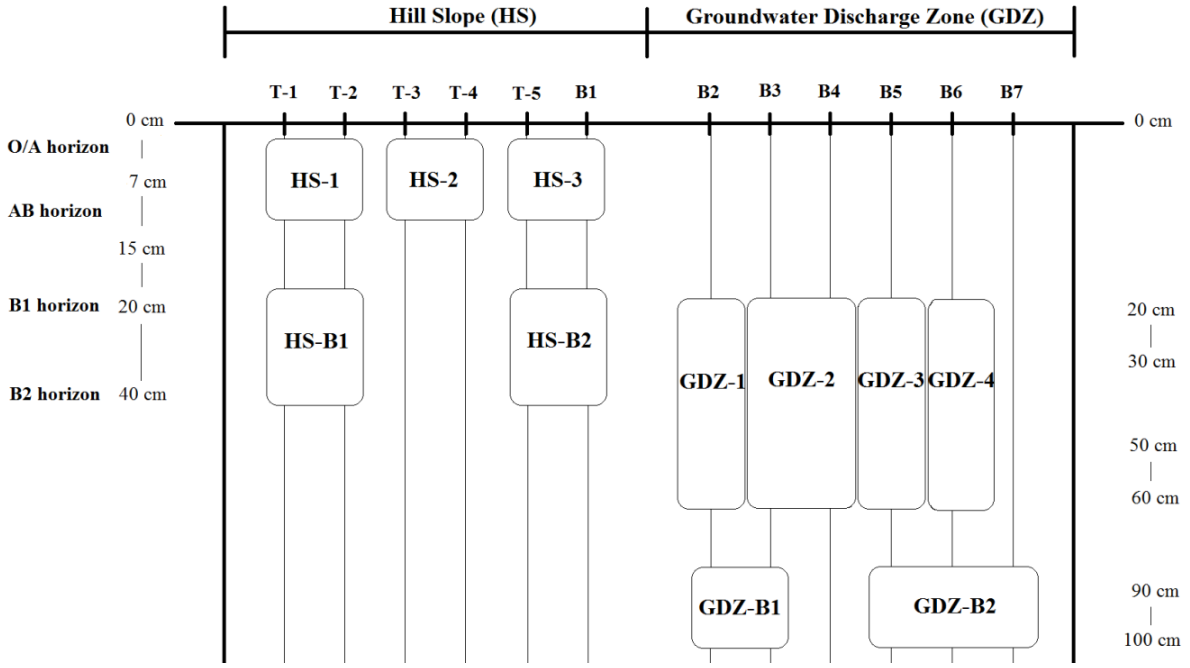

Figure 11: Illustration of the spatial and horizontal origin of the final 11 samples from the field. Samples from the hill slope (left) were pooled to represent two different soil horizons (O/A + AB and B1 + B2), while the samples from the groundwater discharge zone represent two different soil depths (20-30cm + 50-60cm and 90-100cm). Samples were further named based on their spatial and horizontal origin in the field; HS or GDZ, no 1-4, and the letter B for the deeper soil horizon/depth.

3.4 Water characterization

Analyses for the following water characterization parameters were conducted on filtrated samples prior to the biodegradation experiment. Measurements of conductivity and pH were repeated post to the biodegradation experiment.

3.4.1 Conductivity and pH

Conductivity and pH measurements were conducted according to ISO 7888 and ISO 10523, respectively. Sample aliquots of approximately 20 mL was first analyzed for conductivity using a Mettler-Toledo AG FiveGo™ electrode (temperature included), followed by pH analysis using an Orion pH-meter equipped with a combined Ross electrode. Calibration was performed using a standard solution of 85 µS cm^{-1} for the conductivity instrumentation, and the pH-meter was calibrated using buffer solutions with pH 4.00 and pH 7.00.

3.4.2 Alkalinity

Total alkalinity was measured on samples with pH above 4.5 by the method of titration using 0.02 M HCl, and with potentiometric end point (pH 4.5) detection, according to ISO 9963. Analysis was conducted using a Ω Methrom Swissmade 702 SM Titrimo instrumentation, and a pH meter calibrated for pH 4.00 and 7.00. Sample aliquots of ~50 mL were used.

3.5 Elemental composition and Speciation

The following analyses performed to determine the elemental distribution and speciation were performed on filtrated samples prior to the biodegradation experiment. The concentration of the major anions and organic-C was repeatedly determined post to the biodegradation experiment. Details concerning instrumental settings and calibration are presented in Appendix A-1 through A-5.

3.5.1 Major Anions

The concentration of major anions consisting of fluoride (F^-), chloride (Cl^-), sulphate (SO_4^{2-}), and nitrate (NO_3^-) were determined using a Dionex chromatograph system equipped with a

chemical suppression and an Anion Self-regenerating (AS) 18 column. The analysis was performed in agreement with ISO 10304-1 and the Dionex manual. The principle of ion chromatography is that the anions are retained in a charge-specific manner when travelling through the column filled with ion-exchange resin. Each anion is associated with a specific time of elution.

3.5.2 Major Cations

The concentration of calcium (Ca^{2+}), magnesium (Mg^{2+}), potassium (K^{+}) and sodium (Na^{+}), constituting the major cations, were determined using a Varian VISTA Inductively Coupled Plasma Optical Emission Spectrometer (ICP-OES), according to ISO 22036. The instrument is equipped with an Echelle polychromator, a Charge Coupled Device (CCD) for detection, and the emission was measured axially. The ICP-OES functions by measuring the light that is emitted after the analyte has been excited in the high temperature plasma (6000-10000K). The wavelength of the emitted light is specie-specific, and by using the plasma, both atom and ion lines can be obtained. Prior to analysis, all sample and standard solutions were conserved by acidification to 0.3 % (m/v) sulphuric acid (H_2SO_4). Cesium (Cs) was added as an ionization buffer to all of the samples and standards with a final concentration of 0.5 mg L^{-1}.

3.5.3 Total Organic Carbon (TOC)

Samples were analyzed for Total Organic Carbon (TOC) using a Shimadzu TOC-5000A total organic carbon analyzer, in agreement with ISO 8245 and the TOC-5000A instruction manual. The instrumental setting called Non-Purgeable Organic Carbon (NPOC) was applied, which include the preliminary step of removing inorganic carbon by purging acidified ($pH \leq 2$) samples with high purity air. Organic-C is decomposed (680˚C) to carbon dioxide (CO_2) by the aid of an oxidation catalyst. The final determination of CO_2 is carried out by a non dispersive infra-red (NDIR) gas analyzer.

3.5.4 Total Nitrogen

The concentration of total nitrogen was determined photometrically after oxidation by peroxodisulphate, in accordance with the Norwegian Standard, NS 4743. The principle of the method is that inorganic- and organic bound nitrogen is oxidized to nitrate (NO_3^-) by reacting with peroxodisulphate under high pressure ($pH > 7$). Nitrate is then reduced to nitrite (NO_2^-)

by copper-coated cadmium (pH 8.0 – 8.5), which under acidic conditions (pH 1.5 – 2) reacts with sulphanilamide to form a diazo-complex. This complex is then coupled to a N-(a-naphtyl)ethylenedamin to form a azo-coloured compound (N=N). Digestion was performed at the Norwegian University of Life Sciences (UMB), and analysis was conducted by the Institute of Plant- and Environmental sciences (IPM) at UMB, using Flow Injection Analysis (FIA).

3.5.5 Elemental Composition

Total concentration of aluminium (Al), iron (Fe), silicon (Si), manganese (Mn), and zinc (Zn), were determined using a Perkin Elmer Inductively Coupled Mass Spectrometer (ICP-MS), NexION™ 300x. Standard and kinetic energy discrimination mode was applied. The ICP-MS functions by ionizing the different analyte species in the high temperature plasma (6000-10000K). The analytes are separated from each other in the mass spectrometer based on their specific mass to charge ratio (m/z). Prior to analysis, all samples and standards were conserved by acidification to 2 % nitric acid (HNO_3).

3.5.6 Phosphate and Total Phosphorous

Concentrations of phosphate (PO_4) and total phosphorous (tot-P) were determined using a CNP-auto analyser (SKALAR San++ Automated Wet Chemistry analyzer) at the Norwegian Institute for Water Research (NIVA). Determination of phosphate and total phosphorous is based on the molybdate blue method, ISO 6878. In this method, phosphate is determined by reacting with molybdate and antimony ions in acidic solution to form antimony phosphomolybdate complex. The complex is subsequently reduced with ascorbic acid to form a strongly coloured molybdenium blue complex. Determination of the concentration of phosphate is conducted photometrically. For total phosphorous, the same method is applied, only that organic-bound phosphate is oxidized by peroxodisulphate prior to the procedure. Prior to analysis, all samples and standards were conserved by acidification to a concentration of 0.04 M sulphuric acid (H_2SO_4).

3.5.7 Aluminium fractionation

Fractionation of monomeric aluminium (Al_a) was conducted on samples with pH below 5.5, based on the solubility of gibbsite ($Al(OH)_3$). Monomeric aluminium was separated from

polymeric forms by complexation with 8-hydroxyquinone at pH 8.3 and subsequent extraction into MIBK organic phase. Further fractionation of the monomeric aluminium into organic (Al_o) and inorganic (Al_i) forms was conducted by trapping the Ali fraction in an Amberlight IR-120 ion exchange column. Concentrations of the resulting aluminium fractions were determined photometrically using a Shimadzu UV1201 UV-Vis spectrophotometer equipped with 1cm glass cuvettes. The procedure is based on the method of Barnes (1975), Driscoll (1984), and Sullivan et al. (1986).

3.6 Structural characterization

Structural characterization of the DOM samples was performed on filtered samples prior to the biodegradation experiment. Measurements of UV-Vis Absorbency were repeated for all of the samples post to the biodegradation experiment, whereas UV-Vis Fluorescence analysis was only repeated for the TSP-samples.

3.6.1 UV-/Vis Absorbency

Absorbency of the samples was measured at irradiance of light at wavelengths; 254nm, 400nm, and 600nm, using 1cm quartz cuvettes on a Varian Cary 100Bio UV-Vis spectrophotometer. Data were processes using Varian Cary software.

3.6.2 UV-\Vis Fluorescence Spectroscopy

Fluorescence analysis within the UV and Visible region of the electromagnetic spectrum was performed using a clear faced quartz cuvette on a Varian Cary Eclipse Fluorescence Spectrophotometer at the Norwegian Institute of Life Sciences (UMB). The light source of the instrument is a Xenon flash lamp. Excitation-Emission Matrix (EEM) spectra were generated by subsequently scanning the emission from 200 to 600 nm by incrementing the excitation wavelength by 10 nm from 200 to 450 nm. Excitation and emission slit widths were set to 10 and 5nm, respectively. Scan speed was set to 600nm min^{-1}. Data were processed using Varian Cary Eclipse software.

3.7 Biodegradation experiment

3.7.1 Inoculum

It is in the literature recognized that the origin and thereby the microbial composition of an inoculum will largely affect the results in a biodegradation experiment (Marschner and Kalbitz 2003). Therefore, based on the aim of this study, it was decided to prepare a mixed inoculum containing indigenous bacteria from all of the sampling sites within the field of Tie Shan Ping, based on the findings from Qualls et al. (1992) and Young et al. (2005). Prior to filtration (Chapter 3.3.1), 10 mL was withdrawn from each of the TSP-samples and pooled in a LDPE bottle. Sample volumes were also plated on LB[8] agar plates to confirm the presence of microbial activity, since the samples had been frozen for approximately two months. With the microbial density of the water samples being unknown, different techniques were used. This included the application of different volumes of sample (from a few droplets to 1 mL), as well as applying the filter papers directly to the agar plates. Plates were incubated in room temperature (22°C), and several morphologically distinct colonies appeared within a week (Figure 12). Based on these findings, the mixed TSP-inoculum was retained and subsequently filtrated through 5.0µm membrane filters (Nitrocellulose, Millipore) to exclude any microorganisms larger than bacteria (Kalbitz 2003).

Several preliminary biodegradation experiments were carried out, in order to optimize the method for the samples of subject, resulting in a depletion of the inoculum volume. It was therefore decided to supplement the inoculum with re-dissolved filtrate from the sterilization of the TSP-samples (Chapter 3.3.1). During the sterilization, all of the filter papers (except those plated on LB-agar plates) containing filtrate of high microbial activity were kept in known volume of Type 1 water[9] and stored in a LDPE[10] bottle in the dark at 4°C. This solution was used to supplement the inoculum. The inoculum was further diluted using Type 1 water to approximately 60 % of the original concentration. This was done to avoid excessive growth during the incubation experiment, and to reduce DOC concentration of the inoculum. The final inoculum was filtered through 5.0µm membrane filters (Nitrocellulose, Millipore) and stored in the dark at 4°C.

[8] LB (Lysogeny Broth) agar is a nutritionally rich medium, used for growth of Bacteria.
[9] Type 1 water is ultrapure, de-ionized water (Milli-Q).
[10] Low Density Polyethylene (LDPE).

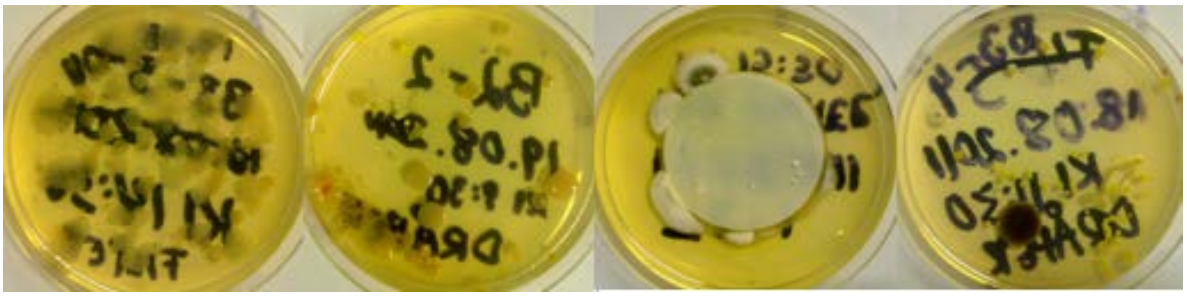

Figure 12: Results from plating unfiltered TSP-samples on LB agar plates to test for microbial activity with regards to inoculum preparation. Note that for one of the plates (number three from the left) the filter paper was placed directly on the agar plate.

3.7.2 Batch experiment

Biodegradable DOM was quantified as evolved carbon dioxide (CO_2) using a basic batch experimental setup (Figure 13). Water samples were incubated in triplicate using pre-combusted (550 °C), sealed glass jars with a total volume of 730 mL. Sample volume was set to 350 mL. This resulted in a void volume (380 mL) which was estimated to be sufficient to ensure aerobic environment within the sample jars, while at the same time not leading to substantial dilution of evolved CO_2. Samples were incubated with their original pH, ionic strength, and DOC concentrations, and the experiment was conducted in the dark at room temperature (22°C). As the samples were believed to comprise large differences in nutrient composition, inorganic nutrients were added to a final sample concentration of 0.1mM dipotassium phosphate (K_2HPO_4) and 0.1mM ammonium nitrate (NH_4NO_3) based on the method used by Kiikilä et al. (2011). Inoculum (Chapter 3.7.1) was added to a concentration of 1% (v/v), based on the review by Marschner and Kalbitz (2003), and two glass fibre filters (Borosilicate, AP25 Millipore) were added to each of the sample jars to provide the bacteria with a surface of growth and biofilm formation (Qualls and Haines 1992). Samples were gently swirled by hand for 1 min every third to fourth day during the experiment in order to ensure aerobic environment throughout the sample solutions (Marschner and Kalbitz 2003). For the last 10 days of the experiment, a shaking table was used (125 mot1 min^{-1}) to stir the samples with the same intervals used for the manual shaking.

The evolved CO_2 was collected by trapping it as carbonate in a strong alkaline solution (Reaction 1 and 2). A plastic tube (5mL, Axygen) containing 3 mL of freshly prepared 1M sodium hydroxide (NaOH) solution was placed inside each of the sample jars. The tubes were

kept floating in the sample solutions by means of a ring made of cross-linked polyethylene foam (New England Biolabs).

CO_2 (g) + OH^- (aq) → HCO_3^- (aq) (1)

HCO_3^- (aq) + OH^+ (aq) → CO_3^{2-} (aq) + H_2O (l) (2)

The duration of the experiment was set to 45 days with sampling being performed every ten days (except for the final analysis, performed after 15 days). This sampling scheme was conducted in order to obtain a mineralization curve for the various DOM-samples, and thereby distinguish between the labile and the more recalcitrant fractions of DOM (Marschner and Kalbitz 2003).

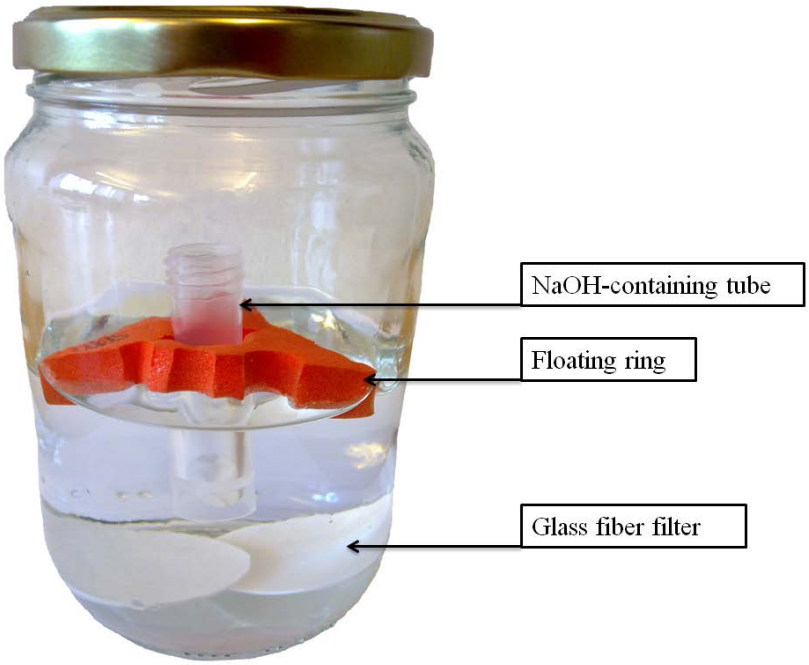

Figure 13: Experimental setup for the biodegradation experiment, displaying the sealed jar (730ml) used to incubate the sample solution (350ml). Evolved CO_2 was captured by placing 3 mL of 1M aqueous NaOH in a tube which sustained floating using a foam ring made of cross-linked polyethylene. Two pieces of glass fibre filters were further added to provide the bacteria with a surface of growth.

3.7.3 Control solutions

Three different types of control solutions were included in the biodegradation experiment (Table 2): 1) to test for microbial activity, a glucose solution of 10 mg C $L^{-1}$was prepared in triplicate, 2) blind solutions containing inoculum and type 1 water[11] were used to check for any CO_2 contribution from carbon mineralization of the added inoculum, and 3) the CO_2 contribution from the atmosphere from the void volume of the jars and that introduced each time the jar was opened for sampling (Chapter 3.7.4) was measured in blind samples containing Type 1 water only.

Table 2: An overview over the three different types of control solutions included in the biodegradation experiment, including content, purpose, and number of replicates.

Content	Purpose	No. of replicates
Glucose (10mg C L^{-1}) , nutrients, inoculum	Microbial activity of the inoculum	3
Inoculum, nutrients	C mineralization from the inoculum	9
Milli-Q water	CO_2 contribution from the atmosphere	4

3.7.4 Collection of evolved CO_2

At the day of analysis (except the final day), the tubes containing CO_2-NaOH were replaced with new tubes containing freshly prepared 1M NaOH. This procedure was performed in a reproducible manner, while avoiding direct exhalation into the tubes. The tubes on which analysis was to be performed were immediately capped, and subject to analysis the same day. These tubes have previously been proven to be completely air-tight for a shorter period of time (than what used in this experiment) by Ph.D student Annelene Pengerud (pers. comm) at UMB. The fresh NaOH solution was prepared the day prior to sample replacement by dissolving beads of NaOH in Milli-Q water. The beads had been excluded from any routine laboratory work in order to reduce absorption of CO_2 from the atmosphere. The NaOH solution was stored using an air tight "bag-in-box" which also allowed for withdrawal for

[11] Type 1 water is ultrapure de-ionized water (Milli-Q).

preparation of the calibration solutions needed for analysis. A total of four 1M NaOH solutions were prepared so that each set of samples could be analyzed using calibration solutions originating from the same stock of NaOH as the samples themselves. Calibration solutions were prepared at the day of analysis by dissolving sodium carbonate in 1M NaOH.

3.7.5 Quantification of evolved CO_2

Evolved CO_2 that was captured as carbonate in the floating alkaline tubes was quantified using a LI-820 Infra Red CO_2 Gas Analyzer (LI-COR®) at UMB. The instrumentation is equipped with a peristaltic pump which transports the liquid CO_2-NaOH solution into a mixing chamber where CO_2 is purged after acidification, protonating the carbonate to carbonic acid, which subsequently dehydrates into CO_2 and water (Reaction 3). A gas liquid separator further separates the released CO_2 (g) from the liquid which then is carried by the aid of argon carrier gas to the infrared detector for quantification.

$$CO_3^{2-}(aq) + 2H^+(aq) \rightarrow H_2CO_3 \rightarrow CO_2(g) + H_2O(l) \qquad (3)$$

The detector is an absolute, non-dispersive infrared (NDIR) gas analyzer based upon a single path, dual wavelength, and infrared detection system. Concentration of CO_2 is determined as a function of loss of IR energy as the gas molecules transverse the optical path. The sample channel is equipped with an optical filter centered at 4.24 µm, which corresponds to the absorption band of CO_2, while the reference channel contains an optical filter centered at 3.95 µm.

3.8 Calculations and statistics

3.8.1 Rate of biodegradation

The results from the biodegradation experiment were used to calculate the following biodegradation rate constant (first-order);

$$k = t^{-1} \ln \frac{S}{S_0},$$

where S_0 is the initial substrate concentration and S the substrate concentration after time t (days) (Paul and Clark 1996).

3.8.2 Significant difference

To test for significant change in the concentration of the major anions measured prior and post to the biodegradation, H_0: $\mu_{prior} = \mu_{post}$, the paired sample t-test was used;

$$t = \bar{x}\sqrt{\frac{n}{s_x}},$$

where $\bar{X}$ is the mean and S_x is the standard deviation of x values. The calculation was performed using the MiniTab® Statistical Software, and with a significance level of 95 % (p = 0.05).

3.8.3 Analysis of correlation

In order to investigate any correlation between the amount of DOM biodegraded and its solution- and intrinsic properties, the Spearman's rank correlation coefficient, r_s, was calculated. This choice of correlation coefficient was made based on the limited number of samples in each sample set (from n = 5 to n = 19), and with the assumption of non-linearity among several of the parameter values. The analysis for Spearman's rank correlation was performed using the R language and environment for statistical computing and graphics (R Development Core Team 2012), and the Hmisc package was installed (Harrell Jr. et al. 2012).

4. Results and Discussion

In the following discussion, the results will be presented in a timely manner, starting with the chemical and structural characteristics of the soil-water DOM samples from TSP. Following this, a brief presentation of the results obtained for the Reverse Osmosis (RO) isolated DOM reference samples will be given, which also includes an assessment of the ability of this material to function as reference samples. Results from the biodegradation experiment are there nest presented, with emphasis on the TSP-samples. Following this, a comparison of the results for the analyses conducted both prior and post to the biodegradation experiment is discussed, also with emphasis on the TSP-samples. Finally, the findings from the analysis of correlation between DOM biodegradability and its solution- and intrinsic properties are presented, with the aim of revealing parameters that governs the biodegradability of DOM. In this final section, only the reference samples are included, and the correlation analysis was performed using mainly the data of DOM characterization made available from the two respective projects in which these samples originate from (NOM-typing and NOMiNiC).

4.1 Soil-Water characterization

Overall, relatively large differences are found in the water chemistry between the soil-waters from the hill slope and from the groundwater discharge zone. Differences in water chemistry may influence the processes governing the fluxes of DOM (e.g. transport, adsorption, and biodegradation), in that parameters such as pH and the ionic strength of water may influence the physico-chemical properties of DOM (e.g. charge, structural confirmation) (Hayes and Swift 1978). Moreover, by investigating possible changes in the water chemistry along a flow path, processes governing mobilization and transport of DOM may be revealed.

4.1.1 pH and Aluminium

Values for soil-water pH are presented in Figure 14a, and display elevated acidity on the Hill Slope (HS; 3.63 – 3.90) as compared to the Groundwater Discharge Zone (GDZ; 4.26 – 4.90). This difference is largely attributed to the longer residence time of the soil-waters in the groundwater discharge zone, providing time for neutralization through weathering. The pH is

further found to increase down in the deeper soil horizon/depth at both of the two regions (samples outlined in brown), which is also attributed a longer residence time. For two of the plots in the groundwater discharge zone (GDZ-3 and GDZ-4), increased pH is observed. This may be explained by upwelling of water, as this has previously been described by Dawei et al. (2001).

The overall low pH values (< 5) in the soil-waters from TSP may influence the composition of DOM. This occurs through protonation of the acidic carboxylic- and phenolic functional groups (Hayes and Swift 1978), resulting in reduced molecular charge and thereby decreased water solubility. The hydrophobic moieties of DOM, containing fewer acidic functional groups, are thus more prone to immobilization through this process, and at pH < 3.8, the hydrophilic fraction is found to dominate (Zech et al. 1996). It can therefore be hypothesized that the soil-waters from TSP contain DOM that is dominantly hydrophilic, which would especially apply for the soil-waters from the hill slope.

The total concentration of inorganic bound aluminium is found to mirror the variations in pH (Figure 14b). This can be attributed to buffering of the soil-waters at pH < 5.5 by ion exchange, and indirectly by dissolution of aluminium containing minerals (e.g. primary silicates, clay minerals, and gibbsite ($Al(OH)_3$)). The very high total Al concentrations, ranging from 272.5 to 648.0 µM on the Hill Slope (HS) and from 19.5 to 62.8 µM in the Groundwater Discharge Zone (GDZ), may indicate that most buffering and mineral dissolution already takes place within these regions (Appelo and Postma 2005). Aluminium is kept in solution by the negative charge contribution of a mobile counter-ion, which in this environment is contributed by nitrate and sulphate, due to their high deposition in this area. The fraction of aluminium termed organic-bound exists in complex with DOM, which is formed with the acidic functional groups of DOM. This rather strong association (Burba et al. 2002) is further found to increase co-sorption of the Al-bound DOM to minerals (Vogt et al. 1994).

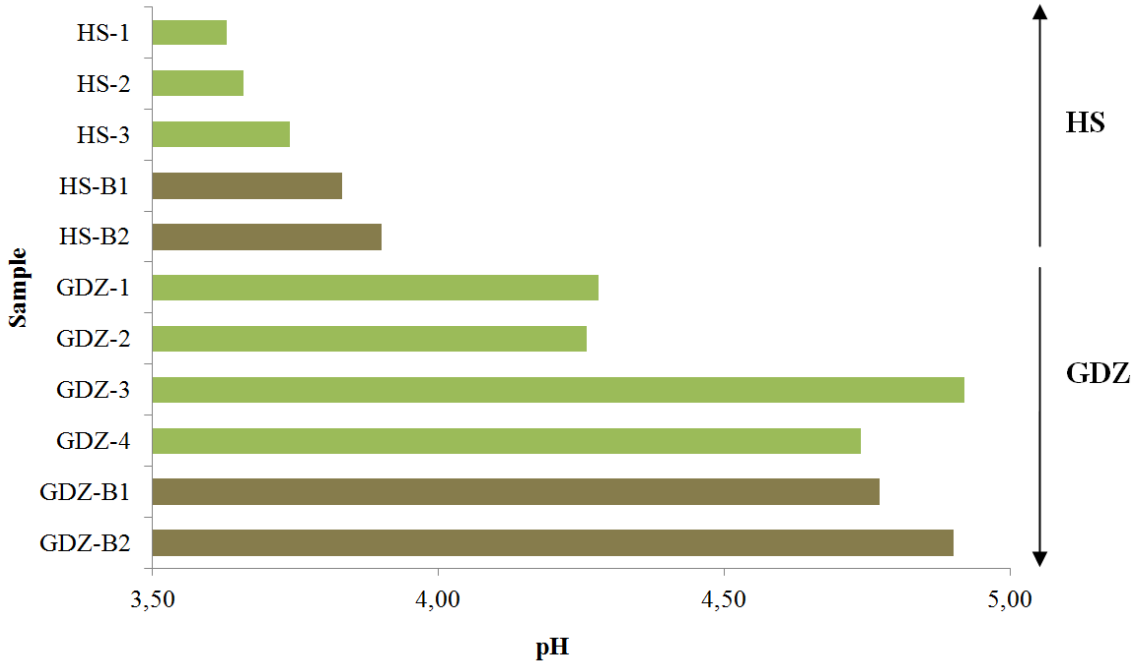

Figure 14a: Values of soil-water pH for samples originating from the Hill Slope (HS) and the Groundwater Discharge Zone (GDZ). Samples originating from the deeper soil horizon/depth are outlined in brown.

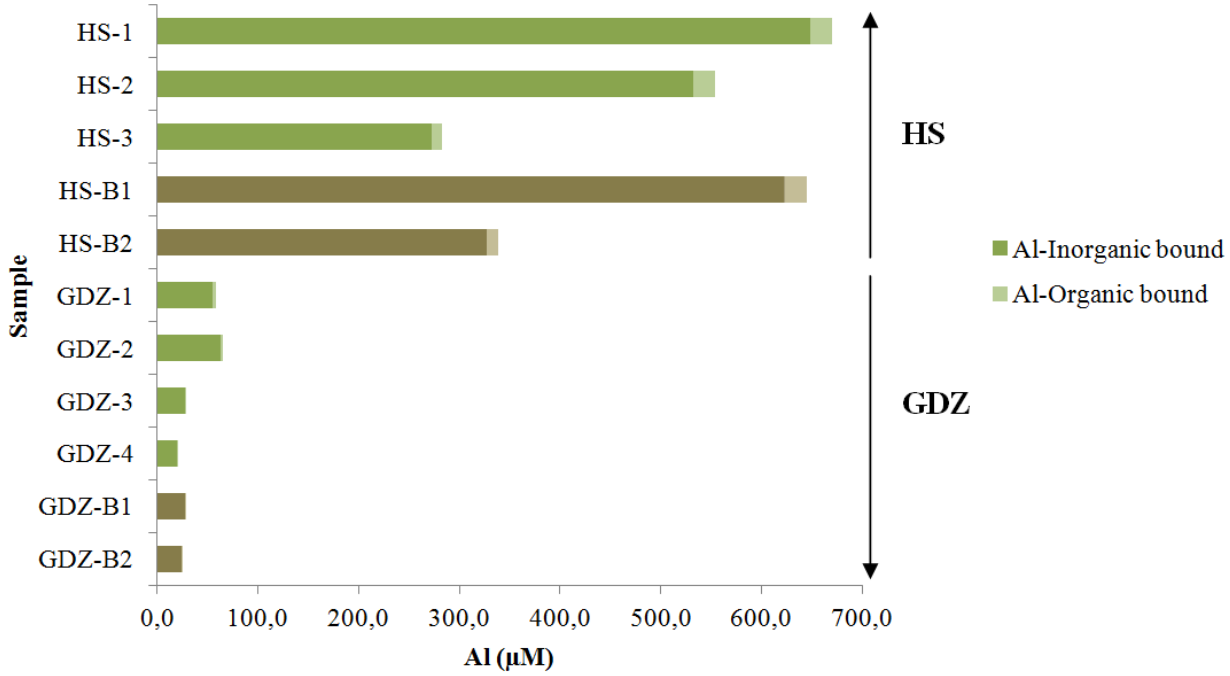

Figure 14b: Concentration (µM) of Inorganic- and Organic bound Aluminium in the soil-waters originating from the Hill Slope (HS) and the Groundwater Discharge Zone (GDZ). Samples originating from the deeper soil horizon/depth are outlined in brown.

4.1.2 Dissolved Organic Carbon

Concentrations of Dissolved Organic Carbon (DOC) in the sampled soil-waters from TSP are presented in Figure 15. The concentrations vary greatly on the Hill Slope (HS), ranging from 3.7 to 15.5 mg C L^{-1} , while in the Groundwater Discharge Zone (GDZ) the concentrations are low ranging only from 0.7 to 1.4 mg C L^{-1}. The hill slope, being vegetated by quite dense woods is prone to extensive litter fall, whereas the dominating source of DOM in the groundwater discharge is hypothesized to be discharge of water flow from the hill slope. The remarkable loss of DOC along the flow path can be attributed to a combination of the three processes; biodegradation and adsorption, as well as dilution. The first process is associated with the high microbial activity in the more surface near A horizon, whereas adsorption is believed to dominate in the relatively organic poor B horizon (Zsolnay 1996). Moreover, the more hydromorphic conditions in the groundwater discharge zone may lead to a further dilution of DOC, assuming that the incoming water contains low concentrations.

On the hill slope, concentrations of DOC are found to decrease down along the slope transect and down through the soil profile to soil B horizon (samples outlined in brown). From previous temporal analysis of the DOC in soil-water at TSP, the gradient in DOC along the slope is not found to be consistent (Jing, Z., pers. comm.). This trend, albeit coherent with general hydro-biogeochemical concepts must be considered to be mere reflection of the processes governing the fluxes of DOM at the time of sampling. Decreasing concentrations of DOC with soil depth is however frequently stated in the literature (e.g. Thurman 1985), with loss of DOC attributed to the combination of the three processes; biodegradation, adsorption, and decreasing concentration of SOM with depth. With regards to the groundwater discharge zone, no such clear trends in DOC concentration with depth appear. This may result from the overall low values of DOC found, in addition to that the soils are rich in clay and generally waterlogged, favouring horizontal rather than vertical transport of water. This inhibits soil (profile) forming processes rendering a more homogeneously soils in this zone. DOC concentrations from the groundwater discharge zone are close to or at the Limit Of Detection of the TOC-analyzer (LOD[12]: 0.8 mg C L^{-1}), resulting in rather large uncertainties associated with these values. In Table 3, the average values from measurement replicates (n = 3) are

[12] Limit of Detection (LOD) = 3*standard deviation of 10x measured blank samples (Type 1 water).

provided, in addition to the relative standard deviation (RSD %). It appears that the results for the samples originating from the groundwater discharge zone are associated with an uncertainty of up to 40 %. UV absorbency (λ = 254nm) is frequently stated to correlate with DOC (Frimmel and Abbt-Braun 2009), and a strong correlation exist for the samples from the hill slope (r^2 = 0.98), whereas only a very weak correlation is found for the samples from the groundwater discharge zone (r^2 = 0.12). This could underline the uncertainty of the DOC measurements, unless a more uneven distribution of chromophores exists among these samples.

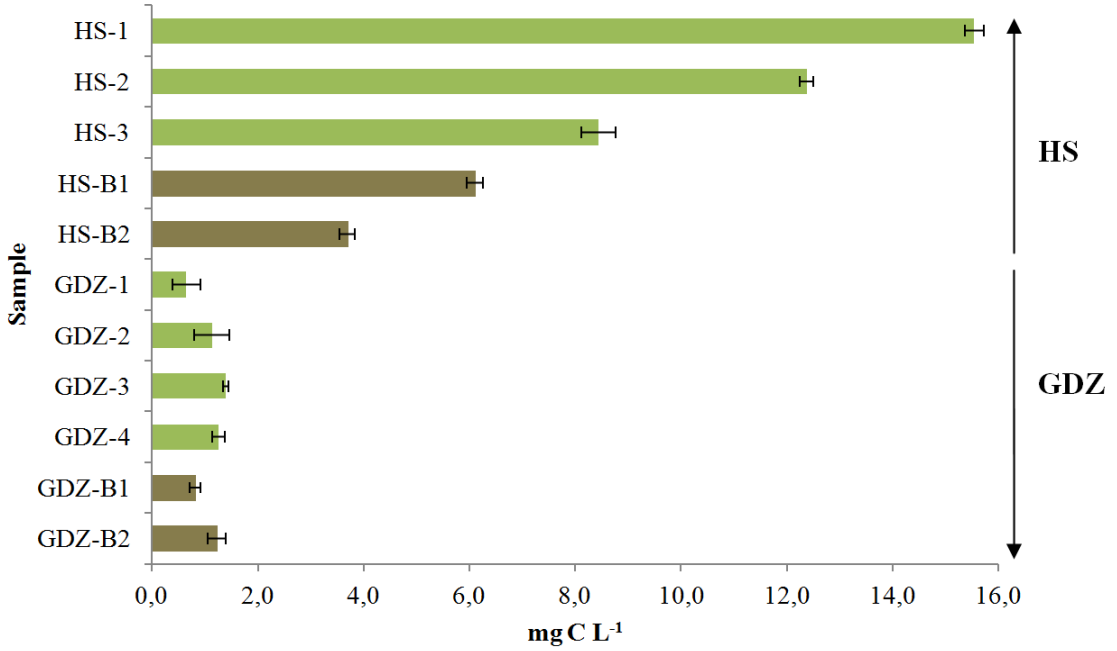

Figure 15: DOC concentrations (mg C L^{-1}) in the soil-water samples originating from the Hill Slope (HS) and the Groundwater Discharge Zone (GDZ). Variance in the analysis is illustrated by error bars. Samples originating from the deeper soil horizon/depth are outlined in brown.

Table 3: Average values and the Relative Standard Error (%) of DOC concentrations (mg C L^{-1}) from the analysis of the replicates (n = 3) of the samples originating from the Hill Slope (HS) and the Groundwater Discharge Zone (GDZ)

	Hill slope (HS)					Groundwater discharge zone (GDZ)					
Sample	1	2	3	B1	B2	1	2	3	4	B1	B2
Average	15.5	12.4	8.4	6.1	3.7	0.7	1.1	1.4	1.3	0.8	1.2
RSD (%)	1.2	0.7	3.8	2.5	3.9	41.3	29.4	3.9	9.8	12.9	13.4

4.1.3 Charge distribution of major anions and cations

The charge distribution of major anions (SO_4^{2-}, NO_3^-, Cl^-, Org. A^-, F^-) and cations ($Al^{2.4+}$, Ca^{2+}, Mg^{2+}, H^+, K^+, Na^+) is presented in Figure 16a. The charge contribution from organic acids (Org.A) was determined individually for the samples using the model developed by Oliver et al. (1983), and the charge contribution from aluminium, sulphate, and fluoride were obtained using the computer software, ALCHEMI (Schecher and Driscoll 1987). Overall, higher total charge concentrations are found at the Hill Slope (HS; 3645 – 8135µeq L^{-1}) as compared to the Groundwater Discharge Zone (GDZ; 1829 - 2610µeq L^{-1}), and the relative distribution of charge contributing species (Figure 16b) differ between these two regions, and also among the samples from the groundwater discharge zone.

The decrease in concentration of charge contributing species, from the hill slope to the groundwater discharge zone, has also been observed by others, without any concluding explanations (Larssen et al. 2011). At the hill slope, concentrations are further found to decrease down along the slope transect, and down to soil horizon B, which is in contrast to the more homogeneously distributed samples from the groundwater discharge zone. The variations between the two soil horizons of the hill slope could possibly be attributed to an up-concentration effect resulting from evapotranspiration at the O/A-AB horizons.

The very high charge concentrations, which are especially evident among the soil-waters from the hill slope, may further induce increased adsorption of DOC to the soils in this area (Chilom 2009). This in addition to the low pH and high concentrations of aluminium makes it reasonable to assume that the loss of DOC along the flow path from the hill slope to the groundwater discharge zone is largely attributed to adsorption mechanisms.

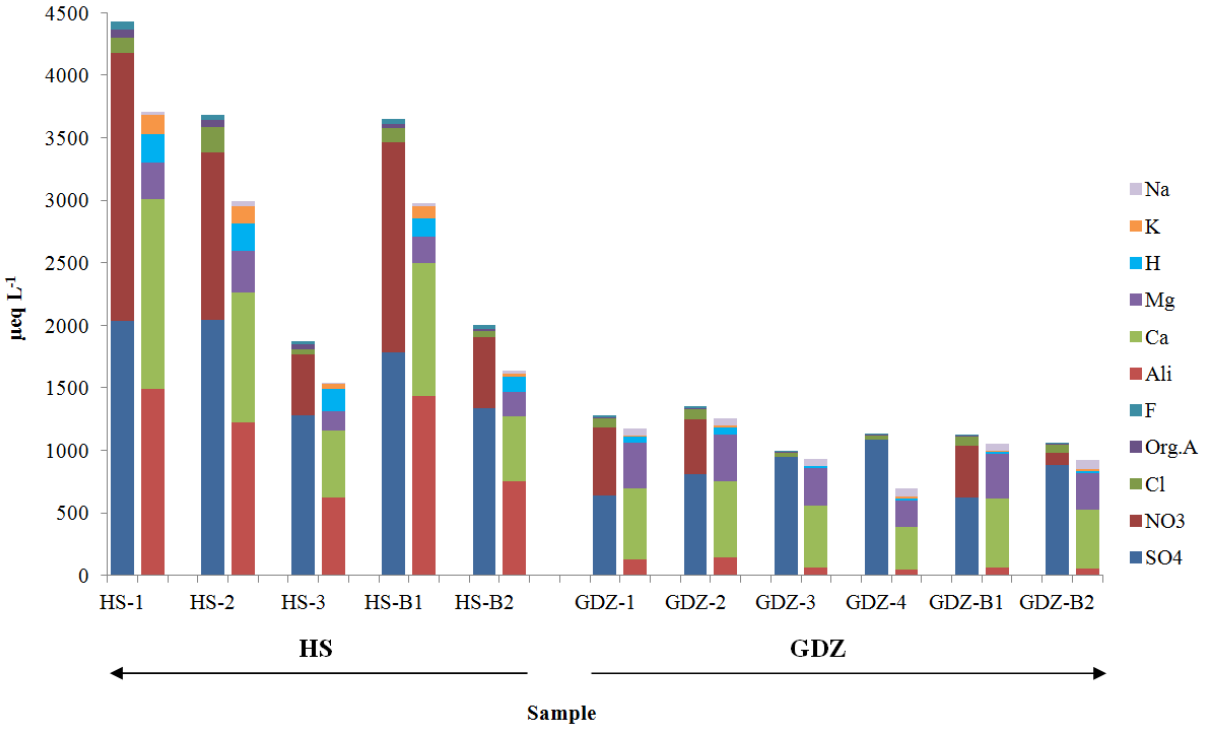

Figure 16a: Charge distribution of major anions and cations (µeq L^{-1}) for soil-water samples originating from the Hill Slope (HS) and the Groundwater Discharge Zone (GDZ).

In Figure 16b, the relative distribution (%) of the main charge contributing species are presented, and display a relatively large difference in the ionic composition between the soil-waters from the Hill Slope (HS) and the Groundwater Discharge Zone (GDZ). Overall, dominating anions include sulphate and nitrate, which is a result of exposure to heavy S- and N-deposition. Nitrate is the most dominating anion only at the most elevated site of the hill slope (HS-1), while gradually being exceeded by sulphate down the slope of the valley towards the groundwater discharge zone. The decrease in nitrate is most likely caused by the process of denitrification occurring in anaerobic micro-sites within granulates of the surface layer of the soils (Dawei et al. 2001; Solheimslid 2001). For two of the plots in the groundwater discharge zone (GDZ-3 and GDZ-4), the contribution of nitrate is even negligible. This most likely indicates that overall anaerobic conditions have evolved. Reducing conditions in these soils are also corroborated by a high concentration of iron found at one of these plots (GDZ-4; 946.6 mg Fe L^{-1}, complete data in Appendix C-1). When all the nitrate is exhausted as an electron donor, Fe (III) is reduced to Fe (II). This increases the solubility of iron allowing for elevated concentrations (Appelo and Postma 2005). With regards to dominating cations, high concentrations of calcium can be seen at all of the plots,

which is primarily caused by deposition (Dawei et al. 2001). Probable sources for this are proposed by Larssen et al. (2011) to be construction, dust, road traffic, and combustion. After calcium, aluminium dominates the cation charge on the hill slope, whereas magnesium is found to dominate in the groundwater discharge zone. The remarkably large differences in ionic distribution between the two regions may indicate dilution of the soil-waters in the groundwater discharge zone by incoming water, consisting of a different ionic composition.

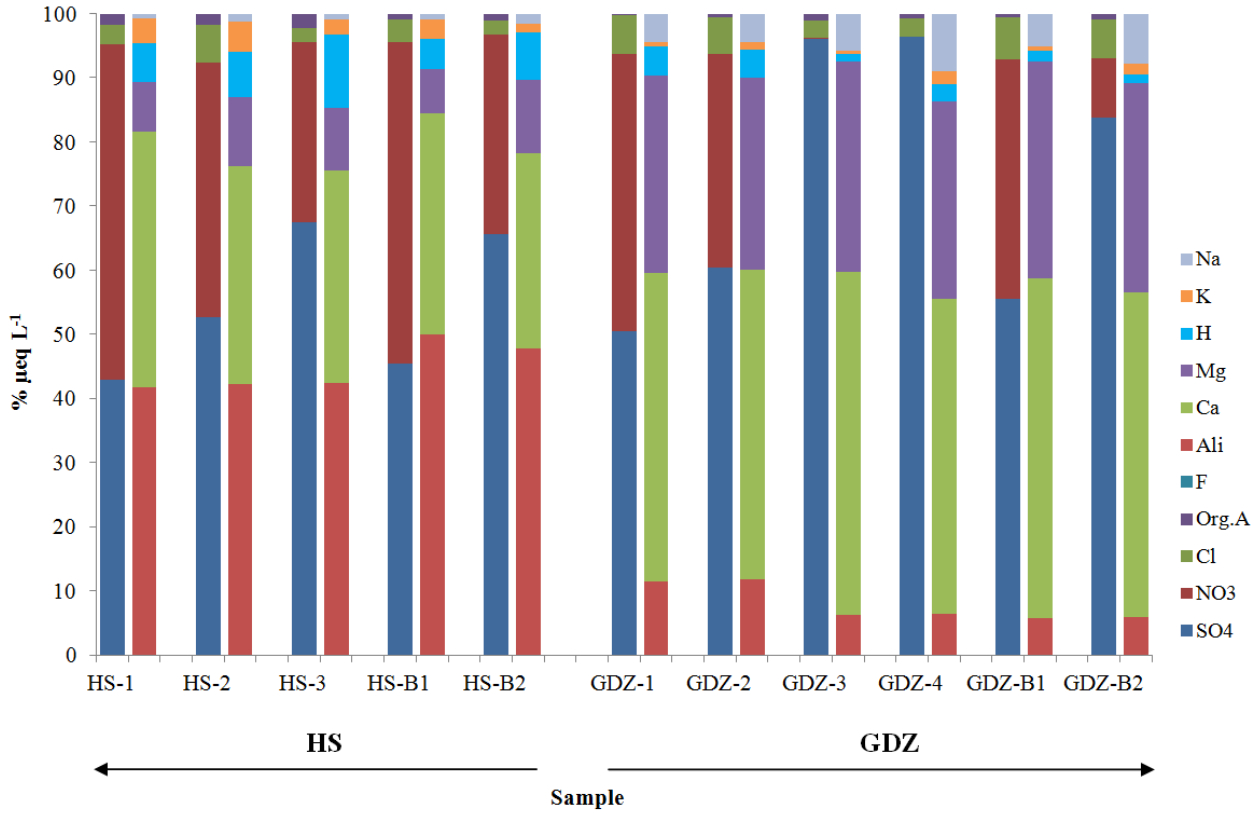

Figure 16b: Distribution (%) of charge contribution species in the soil-water samples originating from the Hill Slope (HS) and the Groundwater Discharge Zone (GDZ).

4.2 Structural Characterization of soil-water Dissolved Organic Matter (DOM)

Structural characteristics of DOM may largely determine the extent of the two processes; biodegradation and adsorption, stated in the literature to be the two main processes governing the fluxes of DOM in soils (Zsolnay 1996). The process of biodegradation is generally associated with preferential utilization of the less aromatic and hydrophobic DOM, while adsorption is frequently stated to involve the more aromatic and hydrophobic part of DOM. Thus, the thesis is that it may be possible to reveal the extent of these individual processes by investigating possible changes in these structural characteristics of DOM along the flow path in TSP.

4.2.1 UV-Vis Absorbency

Results for soil-water DOM absorbency of light within the UV (λ = 254nm) and visible region (λ = 400 and 600nm) of the electromagnetic spectrum are presented in Table 4. Values of absorbency at λ = 254nm and λ = 400nm are further used to calculate the two indices of Specific Absorbency, sUVa ((Abs_{254nm}/ [DOC])*100) and sVISa ((Abs_{400nm}/ [DOC])*1000), in addition to the Specific Absorbency Ratio, SAR (Abs_{254nm}/Abs_{400nm}). Values for absorbency at λ = 600nm are generally at the detection limit for all of the samples, indicating low content of higher molecular weight aromatics.

Table 4: Values of absorbency within the UV (λ=254nm) and Visible (λ=400 and 600nm) region of the electromagnetic spectrum for the soil-water samples originating from the Hill slope (HS) and the Groundwater Discharge Zone (GDZ).

λ (nm)	Hill Slope (HS)					Groundwater Discharge Zone (GDZ)					
	1	2	3	B1	B2	1	2	3	4	B1	B2
254	0.474	0.345	0.259	0.125	0.063	0.021	0.024	0.026	0.021	0.018	0.015
400	0.035	0.022	0.020	0.007	0.004	0.002	0.002	0.002	0.003	0.002	0.001
600	0.002	0.001	0.002	0.001	0.001	0.000	0.001	0.000	0.003	0.001	0.001

Results for the two indices of specific absorbency, sUVa and sVISa, are presented in Figures 17a and b, respectively. The uncertainty resulting from the DOC determination is illustrated by error bars. Values of sUVa, indicating the relative amount of aromaticity of the DOM, appear to be relatively higher among the samples from the Hill Slope (HS) as compared to those from the Groundwater Discharge Zone (except GDZ-1), and are also found to decrease down to soil horizon B in both areas (samples outlined in brown). This could indicate that the loss of DOC along the hill slope transect and down to soil horizon B, found in Chapter 4.1.2, results from selective adsorption of the aromatic compounds to clay minerals. This is conceptually sound as the aromatic fraction of DOM is considered to be more hydrophobic and thus more prone to be lost from solution. The relatively high value of sample GDZ-1, is assumed to result from the large uncertainty associated with the low DOC concentration of this sample (Chapter 4.1.2), since the value of absorbency is similar to the other samples from the groundwater discharge zone (Table 4). With regards sVISa, no clear variations appear between the samples from the hill slope and those from the groundwater discharge zone. This indicates no significant difference in the relative contribution of lower to higher molecular weight aromatics between these two regions. The peaking value of sample GDZ-4 is assumed to arise from interference of iron (Alberts 1982) which is found in high concentration in this sample (Chapter 4.1.3).

These findings can further be supported by the values of Specific Absorbency Ratio, SAR, presented in Figure 17c. From this figure, the B horizon of the hill slope appears to be more dominated by lower molecular weight aromatics as compared to the O/A-AB horizons (i.e. higher SAR). With regards to the samples from the groundwater discharge zone, no clear trend appears among the samples. The very low value for sample GDZ-4 may once again be attributed to the interference by absorbency of iron.

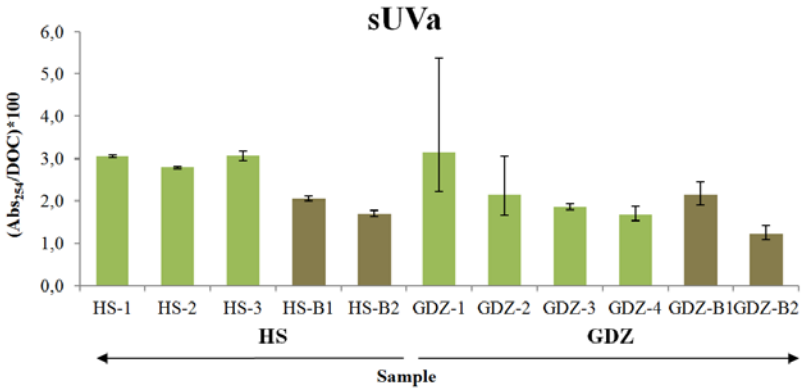

Figure 17a: Values for Specific UV Absorbency, ((Abs$_{254nm}$/ [DOC])*100), obtained for the samples originating from the Hill Slope (HS) and the Groundwater Discharge Zone (GDZ). Samples originating from the deeper soil horizon/depth are outlined in brown.

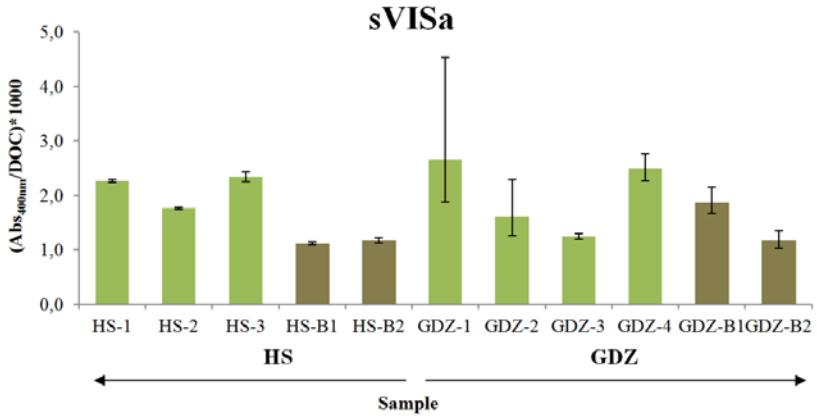

Figure 17b: Values for the Specific Visible Absorbance, ((Abs$_{400nm}$/ [DOC])*1000), for the samples originating from the Hill slope (HS) and the Groundwater Discharge Zone (GDZ). Samples originating from the deeper soil horizon/depth are outlined in brown.

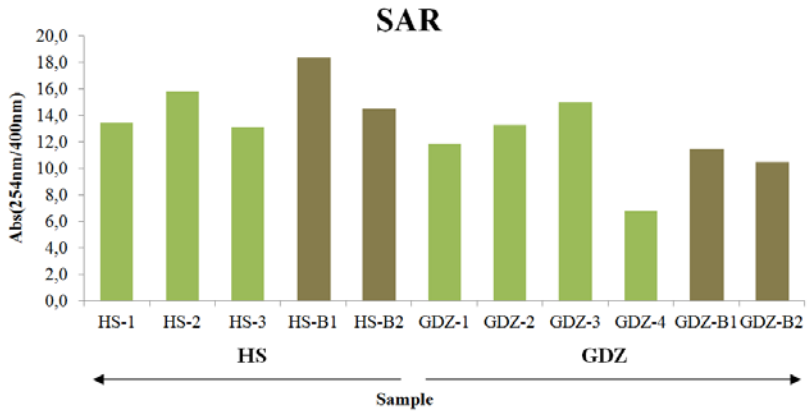

Figure 17c: Values for the Specific Absorbency Ratio, SAR, (Abs$_{254nm}$/Abs$_{400}$nm) for the samples originating from the Hill Slope (HS) and the Groundwater Discharge Zone (GDZ). Samples originating from the deeper soil horizon/depth are outlined in brown.

4.2.2 UV-/Vis- Fluorescence Excitation-Emission Matrix (EEM) spectra

Fluorescence excitation-emission matrix (EEM) spectra for the soil-water samples originating from the Hill Slope (HS) and the Groundwater Discharge Zone (GDZ) are presented in Figures 18a and b, respectively. The spectra appear quite different between the two regions of the studied area, with spectra for the samples from the groundwater discharge zone generally being of lower intensities and with less defined structures as compared to the spectra for the samples from the hill slope. The reason for this is most likely due to the very low DOC concentrations found in the samples from the groundwater discharge zone (Chapter 4.1.2).

The EEM spectra of the samples from the hill slope are generally broad which can be attributed to the continuum of different organic molecule structures which is an intrinsic property of DOM (Martin-Neto et al. 2009). Two major peaks, A and B, in addition to a weaker signal at shoulder C appear in the spectra of all of these samples, which are frequently reported for DOM (e.g. Blaser et al. 1999). Peak A, observed at $\lambda_{ex}/\lambda_{em}$ = 330-344nm/419-423nm is positioned within the area assigned to humic acids (Chen et al. 2003), with naturally occurring fluorophores of phenolic compounds being mainly responsible for the fluorescence (Blaser et al. 1999). The identity of peak B, located at $\lambda_{ex}/\lambda_{em}$ = 240-250 nm /402-426 nm, is generally attributed to fulvic acids (Mounier et al. 1999; Chen et al. 2003). Care should, however be applied for quantification purposes of this peak as it is located close to the Raman scatter of water. The shoulder termed C is further visible at longer excitation and emission wavelengths ($\lambda_{ex}/\lambda_{em}$ = 420/495), which is indicative of more highly conjugated aromatic compounds (Senesi et al. 1991; Blaser et al. 1999).

Fluorescence EEM spectra of the samples from the groundwater discharge zone generally display the same kind of shapes as those from the hill slope, even though the peaks are less pronounced. No fluorescence signal is detected in the region of shoulder C for these samples, which could possibly indicate lower, if any, amount of highly conjugated aromatics. At the area of shorter excitation and emission wavelengths ($\lambda_{ex}/\lambda_{em}$< 250/350nm), however, a weak shoulder is evident for certain of the samples from the groundwater discharge zone (GDZ-4, and GDZ-B2), with fluorescence in this area being attributed to the aromatic amino acids tryptophan and tyrosine (Determann et al. 1994). It is not known if this signal detected is due to the presence of microbially-derived material in these samples.

Absolute (I) and relative (I/DOC) intensities of peak A (humic acids) and B (fulvic acids), in addition to the peak ratio, A:B, are presented in Table 5 for the samples originating from the Hill Slope (HS) and the Groundwater Discharge Zone (GDZ). The table also include wavelength locations (λex /λem) for maximum fluorescence intensities of these two peaks, which seems to vary slightly among the samples. Note that the variance in the value of relative fluorescence intensity (I/DOC) include the spread in measurement replicates (n = 3) from the determination of DOC.

In the DOM from the O/A-AB horizon from the two highest elevated plots on the hill slope (HS-1 and HS-2), the intensity of the humic acid peak (A) dominate slightly over that of the fulvic acid (B), whereas the opposite appears when moving down the slope of the valley and into the groundwater discharge zone. A similar trend further appears when moving down through the soil profile from soil horizons O/A-AB to the B horizon, in that the peak ratio, A:B, decreases. This is most likely attributed to selective adsorption of the more aromatic, hydrophobic and higher molecular weight humic acids to clay minerals at the hill slope, resulting in transport of the more aliphatic, hydrophilic and lower molecular weight fulvic acids to the groundwater discharge zone. This is corroborated with the indices of absorbency in the UV and Visible region of the electromagnetic spectrum presented in Chapter 4.2.1, and the process may be enhanced with the low pH, and high ionic strength of these waters found in Chapter 4.1.1.

The wavelengths of excitation (λ_{ex}) and emission (λ_{em}) decrease down along the slope transect on the hill slope. This can possibly be attributed to the lower pH of the samples from the hill slope (Chapter 4.1.1), at least for peak A, as this is found to induce a shift towards longer wavelengths of emission at the longer wavelengths of excitation (Mobed et al. 1996). It should further be noted that the locations of the peaks are determined manually from the spectra, resulting in uncertainty related to the absolute wavelengths of excitation and emission. Moreover, with the rather weak intensities of emission obtained for the samples from the groundwater discharge zone, the locations of peak maximum for these samples should only be interpreted indicatively.

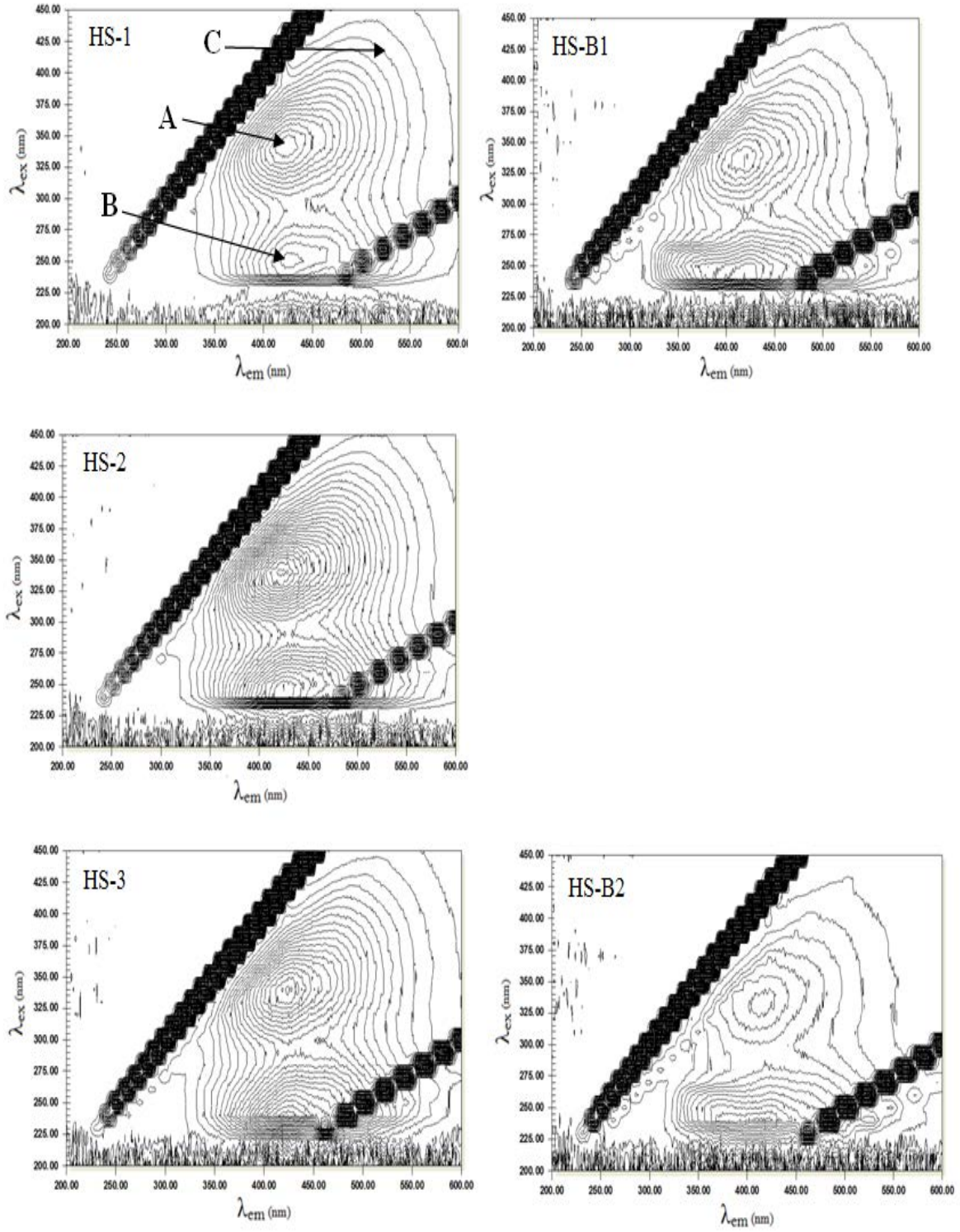

Figure 18a: Fluorescence Excitation-Emission Matrix (EEM) spectra obtained for the samples originating from the Hill Slope (HS). Locations of the two peaks A and B, in addition to shoulder C are indicated in the spectra of sample HS-1. Intensity maximum (I_{max}) is set to 100 for all samples, except from sample, HS-B2 (I_{max} = 40). Note that the spectra are presented in relation to the origin of the samples in the field.

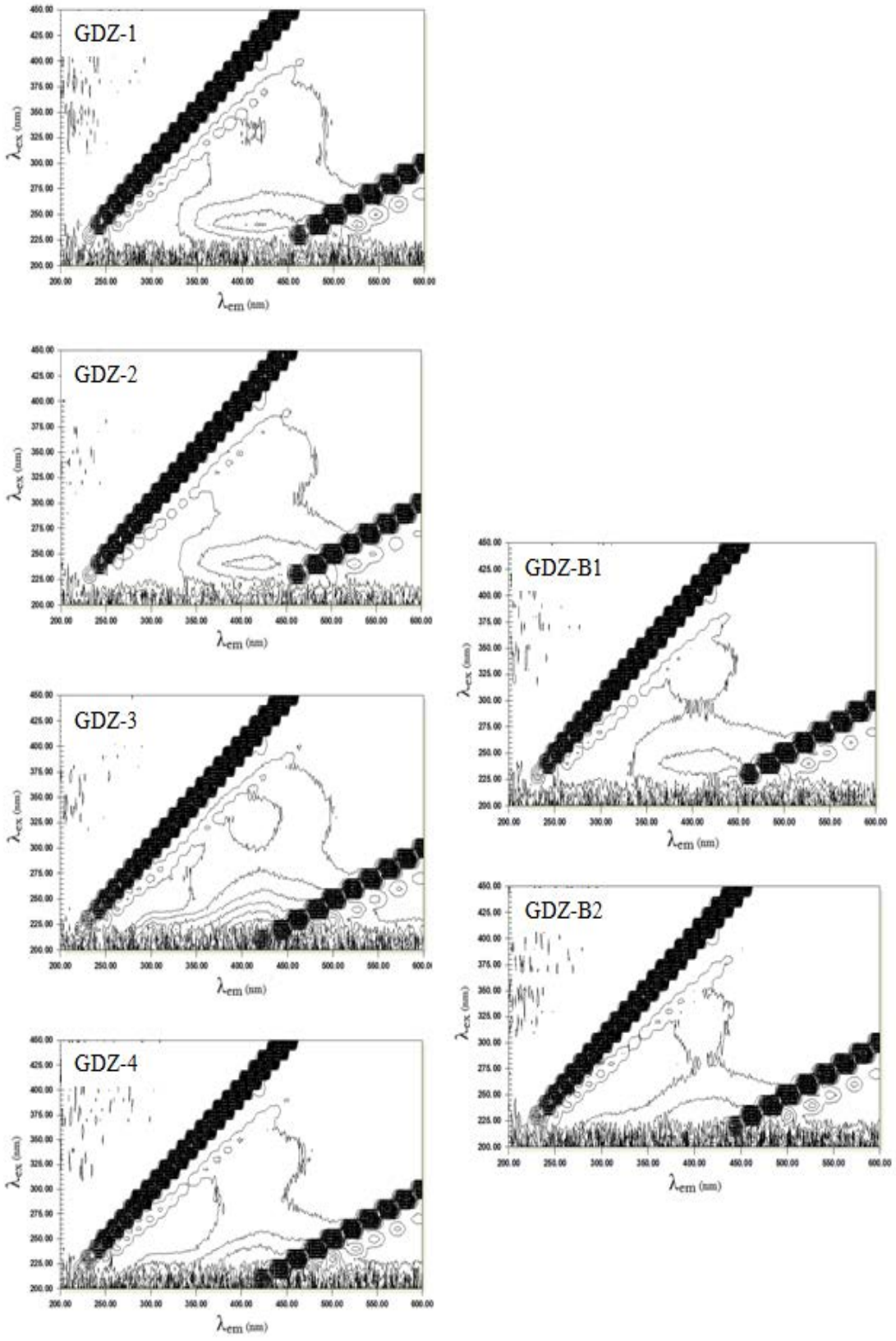

Figure 18b: Fluorescence Excitation-Emission Matrix (EEM) spectra obtained for the samples originating from the Groundwater Discharge Zone (GDZ). Intensity maximum (I_{max}) is set to 40 for all samples. Note that the spectra are presented in relation to the origin of the samples in the field.

Table 5: Locations (λex/λem), intensity (I), relative intensity (I /DOC) and peak ratio (A:B) for the two peaks, A and B, evident fluorescence EEM spectra obtained for the samples originating from the Hill Slope (HS) and the Groundwater Discharge Zone (GDZ).

	Peak A				Peak B				Peak ratio
Sample	λ_{ex}	λ_{em}	Intensity (I)	Rel. I (I/TOC)	λ_{ex}	λ_{em}	Intensity (I)	Rel. I (I/TOC)	A:B
HS-1	344	423	86	5.5±0.06	250	426	64	4.1±0.05	1.34
HS-2	342	423	75	6.1±0.04	250	425	68	5.5±0.04	1.10
HS-3	340	423	53	6.3±0.23	240	420	60	7.1±0.26	0.88
HS-B1	340	419	34	5.6±0.14	250	421	40	6.6±0.16	0.85
HS-B2	330	417	17	4.6±0.18	240	402	28	7.6±0.30	0.61
GDZ-1	330	420	6	10.3±3.96	240	420	10	17.1±6.66	0.60
GDZ-2	330	423	6	5.6±1.40	240	416	12	11.2±2.81	0.50
GDZ-3	330	422	7	5.0±0.19	230	422	16	11.5±0.44	0.44
GDZ-4	320	414	4	3.2±0.30	240	422	8	6.4±0.60	0.50
GDZ-B1	350	398	5	6.2±0.75	240	404	8	9.9±1.21	0.63
GDZ-B2	330	413	3	2.5±0.33	240	422	6	5.0±0.67	0.50

4.3 Reference samples: Re-dissolved Reverse Osmosis (RO) isolated Dissolved Organic Matter (DOM)

The main function of the Reverse Osmosis (RO) isolated DOM-samples in this study was to aid in the assessment of correlation between biodegradability and characteristics of DOM. For this reason, only a brief presentation of the water chemistry and the physical characteristics obtained in this study is included for these reference samples. Emphasis will further be given to the parameters believed to affect biodegradation of DOM, and to any major differences in these parameters as compared those obtained for the soil-water DOM samples from TSP.

Complete results of the characterization of the re-dissolved RO isolated DOM samples performed in this study are presented in Appendix C-2.

4.3.1 Water characterization

The re-dissolved reference samples range in pH from 4.59 (Heo) to 6.80 (Aur), in which the majority possess elevated values as compared to the soil-waters from TSP (Chap. 4.1.1; pH < 5). With the same inoculum (originating from TSP) being used for both the soil-water samples from TSP and for the reference samples in the biodegradation experiment (Chapter 3.7.1), the more elevated pH of the reference samples could possibly lead to reduced biodegradation, resulting from the bacteria of the inoculum most likely belonging to the category of microorganisms termed acidophiles[13] (Madigan et al. 2012).

With the RO-isolated reference materials being re-dissolved to a target value of 10 mg C L^{-1}, a slight spread around this value (± 3.5mg C L^{-1}) appeared in the final concentration of DOC among these reference samples. This is most likely due to the different physical properties (e.g. density) of the various RO isolates. This was further also found to be evident for the three reference samples selected to be re-dissolved to two additional concentrations.

Further differences between the reference samples and the soil-waters from TSP appear in the ionic strength and the distribution of major charge contributing species (Figure 19). The reference samples range in ionic strength from 300 (Svart S) to 711 µeq L^{-1} (Mar), which is

[13] Acidophiles are organisms which grow optimally at pH < 5.5 (Madigan et al. 2012).

generally an order of magnitude lower than what was found in the samples from TSP (1 829 – 8 135 µeq L^{-1}, Chapter 4.1.3). Major anions include sulphate (SO_4^{2-}), organic acids (Org.A), and chloride (Cl^-), of which the latter two are not found to contribute significantly in the samples from TSP. The greater contribution of chloride is due to sea-salt aerosols as the samples originate from coastal-near sampling sites. With regards to cations, sodium (Na^+) is found to be *the* most dominating ion in all samples. This results from the method of isolation by Reverse Osmosis, in which other cations are replaced with sodium in order to prevent precipitation of insoluble salts (Chapter 3.2.2).

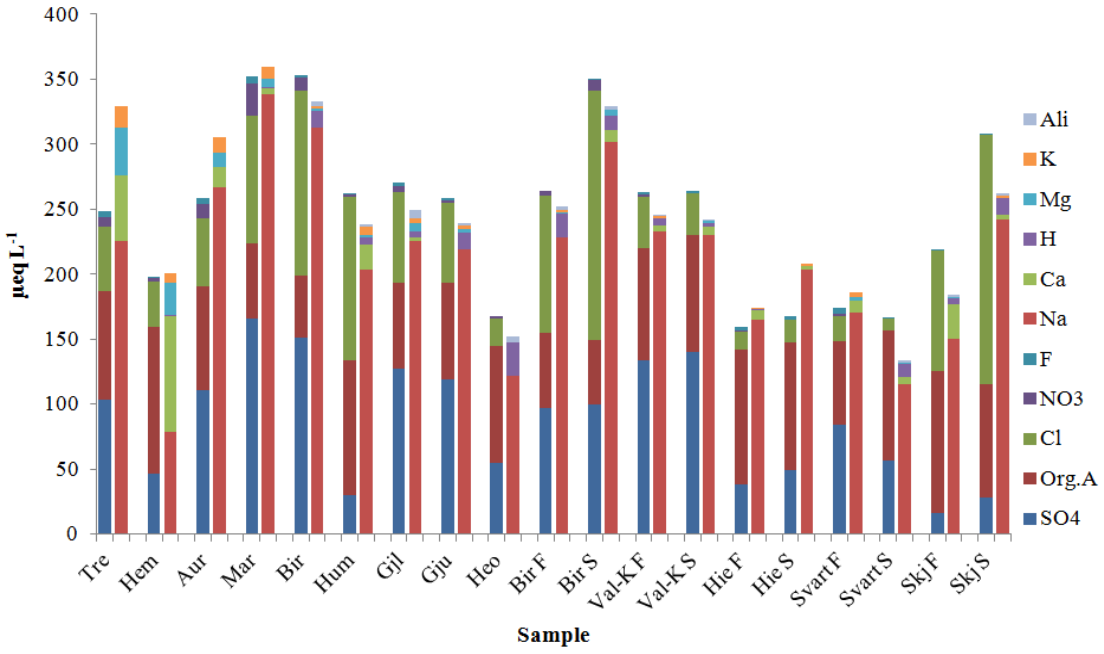

.

Figure 19: Charge distribution of major anions and cations (µeq L^{-1}) for the re-dissolved Reverse Osmosis (RO) isolated reference samples originating from the "NOM-typing" and "NOMiNiC" projects.

4.3.2 Structural Characterization

The reference samples generally display elevated values of the two indices of specific absorbency, sUVa (2.8 – 4.6) and sVISa (2.5 – 6.3), as compared to the soil-water samples from TSP (sUVa: 1.2 – 3.2, sVISa: 1.1 – 2.7. This indicates higher relative amounts of both lower and higher molecular weight aromatics in the reference samples. Values of the specific absorbency ratio, SAR, are however lower in the reference samples (7.1 – 11.2), than in the samples from TSP, indicating larger contribution of higher molecular weight aromatics as compared to the samples from TSP (SAR; 6.7 – 18.4). This is further supported by higher values of absorbency at the far visible region of the spectrum, λ = 600nm, ranging from

0.0015 – 0.0114 as compared to the close to zero values obtained for the samples from TSP (~ 0.001).

From fluorescence analysis, the EEM spectra obtained for the reference samples appear similar to those of the TSP-samples originating from the hill slope, in being broad, and containing the two distinct peaks, A and B, in addition to a weak signal at the location of shoulder C. The location of peak A is found at $\lambda_{ex}/\ \lambda_{ex}$ =237-343nm/432-459nm, which is shifted towards longer wavelengths of emission as compared to the EEM spectra obtained for the samples from TSP ($\lambda_{ex}/\ \lambda_{ex}$ = 330-344nm/419-423nm). Peak B is located within $\lambda_{ex}/\ \lambda_{ex}$ = 231-244nm/421-433nm, which is situated at shorter wavelengths of excitation and longer wavelengths of emission as compared to the soil-waters from TSP ($\lambda_{ex}/\ \lambda_{ex}$ = 240-250nm/402-426nm). These shifts towards longer wavelengths of emission (red shift) could be explained by the DOM-material of the reference samples being more humified (Ohno 2002), which could further be supported by the higher values of sUVa found among the reference samples. As discussed above for the shifts observed among the TSP-samples (Chapter 4.2.2), the difference in pH between the reference samples and the soil-water samples could further be an additional explanation of this shift towards longer wavelengths, especially for peak A. Moreover, for all but two of the reference samples (Svart S and Skj F), the relative intensity of peak B was larger than for peak A, which is in accordance with most of the TSP-samples.

4.3.3 Reverse Osmosis (RO) isolated DOM as reference material

Results from characterization of the re-dissolved RO isolates are compared with results from the same parameters previously analyzed by the two projects from which the sample materials originate (Gjessing et al. 1999; Vogt et al. 2001). This is done in order to investigate the stability of these RO isolated DOM samples, in the context of relating DOM-characteristics to biodegradability by using the characterization data previously obtained by the two projects and the biodegradation data obtained in this study. Values are standardized based on present and previous DOC concentrations (except for pH and SAR). Intercalibration correlations between previously reported data and data generated in this study are expressed with values of correlation (r^2) and the inclement of correlation presented in Table 6. It should be noted that filtration through pore size 0.2 µm prior to analysis was performed in this study in order to remove any original microbial content (Chapter 3.2.2), whereas pore size 0.45 µm was used prior to the previously conducted measurements.

Overall, the RO isolated DOM appears to be remarkably well suited as reference material, with correlation values (r^2) around 0.8 and 0.9 for most of the parameters, and with an corresponding inclement of around 1. Exceptions to these strong correlations are found for calcium for both sets of samples ("NOM-typing": 0.373, "NOMiNiC": -1.602), in addition to nitrate (0.239) and potassium (0.346) for the samples originating from the "NOMiNiC" project. The poor correlation with these three ions is most likely related to that the concentrations are very low. Correlation for the structural parameters further seems weaker for both the "NOMiNiC" samples (sUVa; 0.407, sVISa; 0.495, SAR; 0.623) and the "NOM-typing" samples (sUVa; 0.549). The reason for this is unknown, and beyond the scope of this study.

From fluorescence analysis, the EEM spectra obtained previously for the reference samples were available from the "NOMiNiC" project only. These spectra are found to display similarities with those obtained from present the analysis. Locations of the two peaks, A and B, are presented in Table 7, are found to lie within more or less the same range of excitation and emission wavelengths. The somewhat deviating values of wavelengths may however be attributed to the different instrumental settings applied for the two analyses, and the fact that the locations of the peaks in this study are determined manually.

Table 6: Values for the strength (r^2) and the Inclination describing the relation between the results obtained for water- and DOM characterization parameters obtained previously and in this present study.

	NOM-typing		NOMiNiC		All samples	
Parameter	r^2	Inclination	r^2	Inclination	r^2	Inclination
pH	0.783	0.963	0.852	0.979	0.810	0.972
Conductivity	0.977	1.212	0.980	1.104	0.971	1.169
Chloride (Cl^-)	0.979	1.122	0.958	0.972	0.971	0.972
Sulphate (SO_4^{2-})	0.993	1.182	0.960	1.067	0.981	1.068
Nitrate (NO_3^-)	0.994	1.385	0.239	1.609	0.303	1.600
Calcium (Ca^{2+})	0.373	0.813	-1.602	1.238	0.146	1.236
Magnesium (Mg^{2+})	0.946	1.198	0.367	2.143	0.675	2.138
Potassium (K^+)	0.965	1.067	0.346	5.022	0.494	4.885
Sodium (Na^+)	0.992	1.127	0.850	0.901	0.951	0.901
sUVa	0.549	1.079	0.407	1.031	0.405	1.052
sVISa			0.495	1.101		
SAR			0.623	0.978		

Table 7: Ranges in the locations (λ_{ex} and λ_{em}) of peak A and B from the previously and presently obtained fluorescence Excitation-Emission Matrix (EEM) spectra for the re-dissolved RO isolated DOM samples originating from the "NOMiNiC" project.

	Peak A		Peak B	
Analysis	λ_{ex} (nm)	λ_{em} (nm)	λ_{ex} (nm)	λ_{em} (nm)
Present	237-343	432-459	231-244	421-433
Previous	327-337	435-445	225-235	428-432

4.4 Extent and dynamics of biodegradation

Relatively large differences are found in the amount of biodegraded DOM among the soil-water samples from TSP and the reference samples, with by far largest differences existing among the TSP-samples. For all of the TSP- and the reference samples (except Svart F), the largest pool of biodegradable DOM is found be mineralized during the first time period of the experiment (day 0 – day 10), while decreasing during the second (day 10 – day 30). This could indicate rapid mineralization of a labile pool of DOM during the first 10 days, while biodegradation of the more slowly mineralized pools are initiated thereafter. For the two subsequent time periods, however, the extent of mineralization seems to vary among the samples, and is not generally found to decrease with time. This is assumed to be attributed to the uncertainty of the biodegradation experiment, which appears to increase with time. For this reason, emphasis in the assessment will be given to the results obtained from the two first incubation periods (day 0 – day 20) of the biodegradation experiment. The extent and consequences of the uncertainty will be discussed further in Chapter 4.4.4.2.

The following discussion of the results obtained from the biodegradation experiment will focus on the TSP-samples. Results obtained for the reference samples are presented in Appendix D-3.

4.4.1 Visible change in the incubated samples

Through the course of the biodegradation experiment, visible changes in the appearance of several of the incubated samples appeared (Figure 20a-d). Such alterations include the appearance of white or yellow-like suspended particles (Figures 20a and c), and opaqueness of the sample solutions (Figure 20b). The development of what is described as suspended particles is only observed among certain of the samples from TSP (HS-B1, GDZ-2, and GDZ-4), and was further apparent in only one of the three replicates of one of these samples (GDZ-4, Figure 20c). With the samples from TSP possessing elevated ionic strength as compared to the reference samples, this is most likely attributed to precipitation of metal cations. Opaqueness of the sample solutions results on the other hand from disintegration of the added glass fibre filters. This is only observed among the reference- and the control samples, with disintegration possibly being induced by the relatively low ionic strength of these waters. Finally, for certain of the samples, no visible changes were detected (Figure 20d). These

findings could indicate that over time, different (chemical) environments developed among the samples and also among the replicates of certain samples. It was nevertheless not found to be any effect in the results of the biodegradation experiment.

Figure 20: Photos illustrating the different appearance of the sample solutions which developed throughout the course of the biodegradation experiment; A) development of what described as suspended particles, B) opaqueness of the sample solution caused by disintegration of the added glass fibre filters, C) difference in the appearance of three sample replicates of one sample, and D) no visible change in the appearance of the sample solution. Note that the brownish-colour of the sample solution in figure B is caused by the DOM.

4.4.2 Control samples

4.4.2.1 Blank samples

From the two types of blank samples, with and without inoculum, average values (excluding possible outliers[14]) of measured CO_2 (mg C) during the four days of analysis in the biodegradation experiment are presented in Table 8. No apparent difference was found between the values of the two types of blanks, indicating that CO_2 evolution from the added inoculum was negligible. This demonstrates that the microorganisms of the inoculum were not subject to significant growth without the addition of the DOM-samples. Sources of CO_2, other than that from mineralization of DOC, include dissolved carbonate species (CO_2 (aq), H_2CO_3, HCO_3^-, CO_3^{2-}) in the sample waters (350 mL) and CO_2 present in the void volume of each jar (380 cm^3). While assuming that the blank solutions were in equilibrium with the atmosphere (pH = 5.6), calculated CO_2 contribution is estimated to be 0.14 mg C-CO_2. From Table 8, it appears that measured CO_2 from the two types of blank samples at the first day of analysis (day 10) agree very well with this theoretical value. From the three subsequent days of analysis, the measured contribution of CO_2 seems to increase slightly. This may be

[14] Possible outliers determined by the 1.5*IQR (Interquartile Range) rule of suspected outliers.

explained by that repeated opening of the jars for analysis may have lead to a defect in the lid of the jars, resulting in increased leakage of air from the atmosphere into the jars.

Only the average values from the inoculum-containing blank samples were used to correct for CO_2 contamination in the samples. Complete list of replicate values are presented in Appendix D-1.

Table 8: Average values (excluding possible outliers) CO_2 measured (mg C) in the two types of blank samples, with and without inoculum, during the four time periods of the biodegradation experiment (day 0-10, day 10-20, day20-30, and day 30-45).

Time period (days)	0 – 10	10 – 20	20 - 30	30 - 45
Inoculum-containing blank (n = 9)	0.13 ± 0.01	0.20 ± 0.05	0.17 ± 0.03	0.21 ± 0.02
Non-inoculum containing blank (n = 4)	0.14 ± 0.02	0.16 ± 0.05	0.18 ± 0.04	0.21 ± 0.04

4.4.2.2 Glucose control

For the control solution containing glucose (10 mg C L^{-1}), a total mineralization of 64-66 % initial C was observed for the three replicates (Figure 21). This confirms the microbial activity of the inoculum. Surprisingly, however, a lag phase was observed for the biodegradation of this control solution during the first time period of the biodegradation experiment (day 0 – day 10). Only 3-4% of the total mineralized C is biodegraded in this initial period, whereas as much as 73-78 % is biodegraded during the second time period of the experiment (day 20 – day 30). One possible explanation for this could be to be due to the quite large difference in pH between the control solution (pH ~7) and the inoculum (pH ~ 4). However, as no such lag phase is observed for any of the DOM-samples, including the reference samples with pH values approaching 7, this hypothesis is rejected. Apart from this, the only reasonable explanation for such a lag phase is assumed to be based on microbial adaption to different types of substrates. For a microbial community originating from forested soils, such as the inoculum, a large verity of species possessing different metabolic adaptations will be present. While assuming that the majority of the species in the inoculum are adapted to substrates of a more recalcitrant nature than glucose, a lag phase may be needed for the glucose-utilizing microbes to develop in significant amounts.

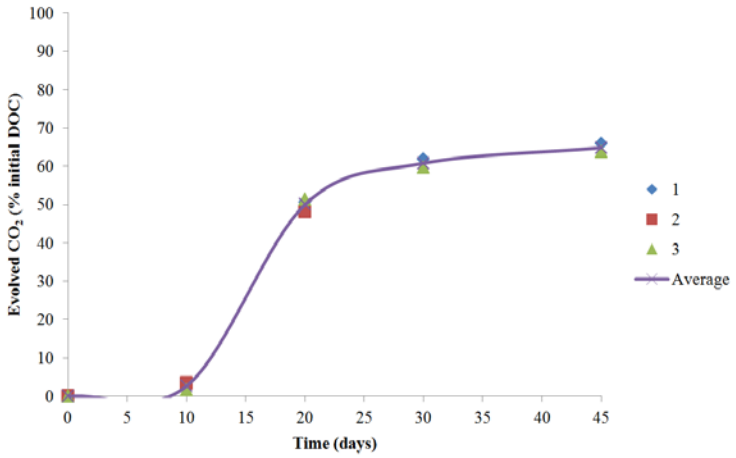

Figure 21: Mineralization curve illustrating the relative amount (%) of mineralized glucose-C as evolved CO_2 (mg C) to the initial amount of glucose-C (mg) during the time course of the biodegradation experiment. Individual values for the three sample replicates are illustrated by dots, while the average value of the three is presented by a solid line.

4.4.3 Soil-water DOM samples from Tie Shan Ping (TSP)

Overall, quite large differences are found in biodegradability of the soil-water DOM samples from Tie Shan Ping (TSP), with total mineralization ranging from 11 to 59 % among the samples from the hill slope, and with more than 100 % mineralization for all of the samples originating from the groundwater discharge zone. This unreasonably high mineralization of the samples from the latter region is attributed to a combination of uncertainties related to the biodegradation experiment, which is especially pronounced in these samples with very low initial concentrations of DOC in these samples (Chapter 4.1.2). The uncertainties related to the biodegradation experiment will, as previously stated, be further presented and discussed in Chapter 4.4.4.2. For now, it can however be stated that the very large differences in biodegradability between the DOM from the hill slope and the groundwater discharge zone is not believed to be accounted for by these uncertainties.

4.4.3.1 Rates of mineralization

Mineralization curves, presenting the relative amount of biodegraded DOM as relative (%) amount of CO_2 evolved (mg C) to the initial concentration of DOC (mg C), are presented for the soil-water samples originating from the Hill Slope (HS) and the Groundwater Discharge Zone (GDZ) in Figures 22a and b, respectively. For the samples originating from the hill slope, the values from the three incubation replicates are illustrated as dots and the average value by a solid line, whereas values from the three replicates of the samples from the

groundwater discharge zone are illustrated by solid lines. Note that the scaling on the y-axis varies between the samples from the two regions and also for one of the samples from the hill slope (HS-3).

With regards to the samples originating from the hill slope, a slight relative increase in the rate and extent of biodegradation can be seen when moving down the slope, and down through the soil to horizon B. This could be explained by the findings from the structural characterization of these samples, in which the relative amount of aromaticity, represented by UV-absorbency and fluorescence humic acids, was found to increase in the opposite manner (Chapter 4.2). This is further in accordance with the literature, stating preferential biodegradation of the less aromatic DOM (Bolan et al. 2011). The increase in biodegradability along the flow path and down into the B horizon can further be illustrated with the first order rate constant, k (day^{-1}), describing the rate of mineralization during the two first time periods of the experiment (Table 9a). These values are further found to be in accordance with the range in values calculated and presented by Zsolnay (1996) from data originating from various different studies on biodegradation of DOM.

Table 9a: First order rate constants, k (day^{-1}), describing the rate of mineralization during the two first time periods of the biodegradation experiment (day 0 - day 20) for the samples originating from the Hill Slope (HS).

Sample	HS-1	HS-2	HS-3	HS-B1	HS-B2
k (10)	$-4.4*10^{-3}$	$-6.2*10^{-3}$	$-10.2*10^{-3}$	$-15.0*10^{-3}$	$-23.0*10^{-3}$
k (45)	$-2.5*10^{-3}$	$-4.72*10^{-3}$	$-6.46*10^{-3}$	$-7.81*10^{-3}$	$-19.8*10^{-3}$

Complete mineralization appears to have occurred for all of the samples originating from the groundwater discharge zone within the first time period of the experiment (day 0 – day 20). No consistent trend can be seen in the modest variations among the samples, with regards to neither spatial nor horizontal origin in the field. This is however in accordance with the results obtained from other characterization parameters, and is attributed to the more homogeneous soils with no clear soil horizons of this region. With all of the initial DOC mineralized before or close to the day of the first analysis (day 10), first order rate constants are only available for two of the samples, with these being obtained for the first time period of the experiment (Table 9b). These values are moreover extremely high, and exceed by far the values reported

for biodegradation of DOM by Zsolnay et al. (1996). No further information can be obtained for these samples due to the lack of analysis performed prior to the tenth day of incubation.

Table 9b: First order rate constants, k (day^{-1}) , describing the rate of mineralization during the first time period of the biodegradation experiment (day 0 - day 10) for the samples originating from the Groundwater Discharge Zone (GDZ).

Sample	GDZ-1	GDZ-2	GDZ-3	GDZ-4	GDZ-B1	GDZ-B2
k (10)	-	$-187 * 10^{-3}$	$-389 * 10^{-3}$	-	-	-

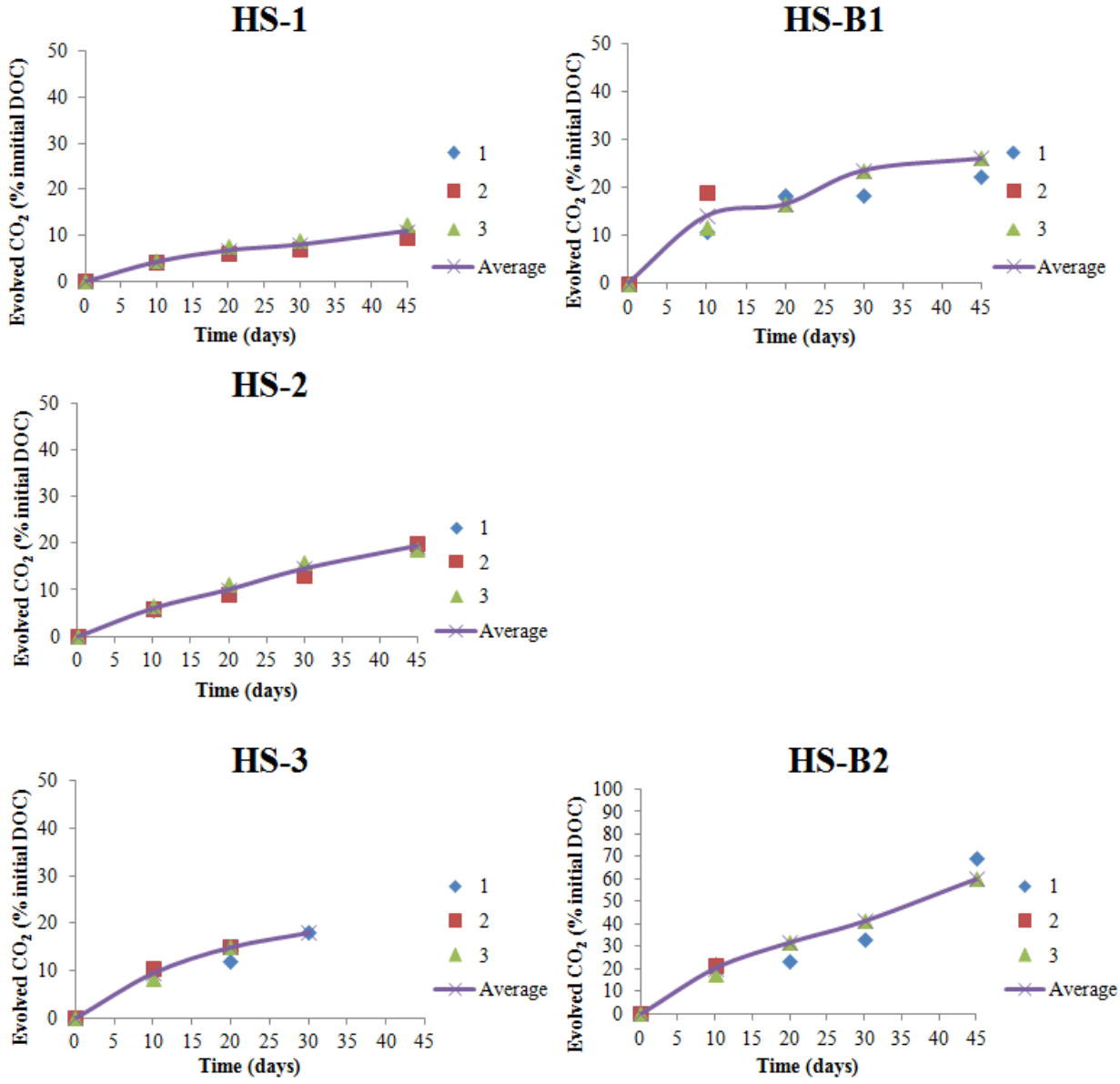

Figure 22a: Mineralization curves illustrating the amount of DOM biodegraded as relative (%) amounts of evolved CO_2 (mg C) to the initial amount of DOC (mg) during the time course (days) of the experiment for the samples originating from the Hill Slope (HS). The curves for each sample are presented in the order of origin in the field, with the O/A-AB horizon to the left, and the B horizon to the right. Note that a different scaling is applied for sample HS-B2. For sample HS-3 no values are available for the last time period of the biodegradation experiment due to contamination of the sample solution by NaOH. Values for sample replicates are marked as dots, while a line is drawn though the average values of the replicates.

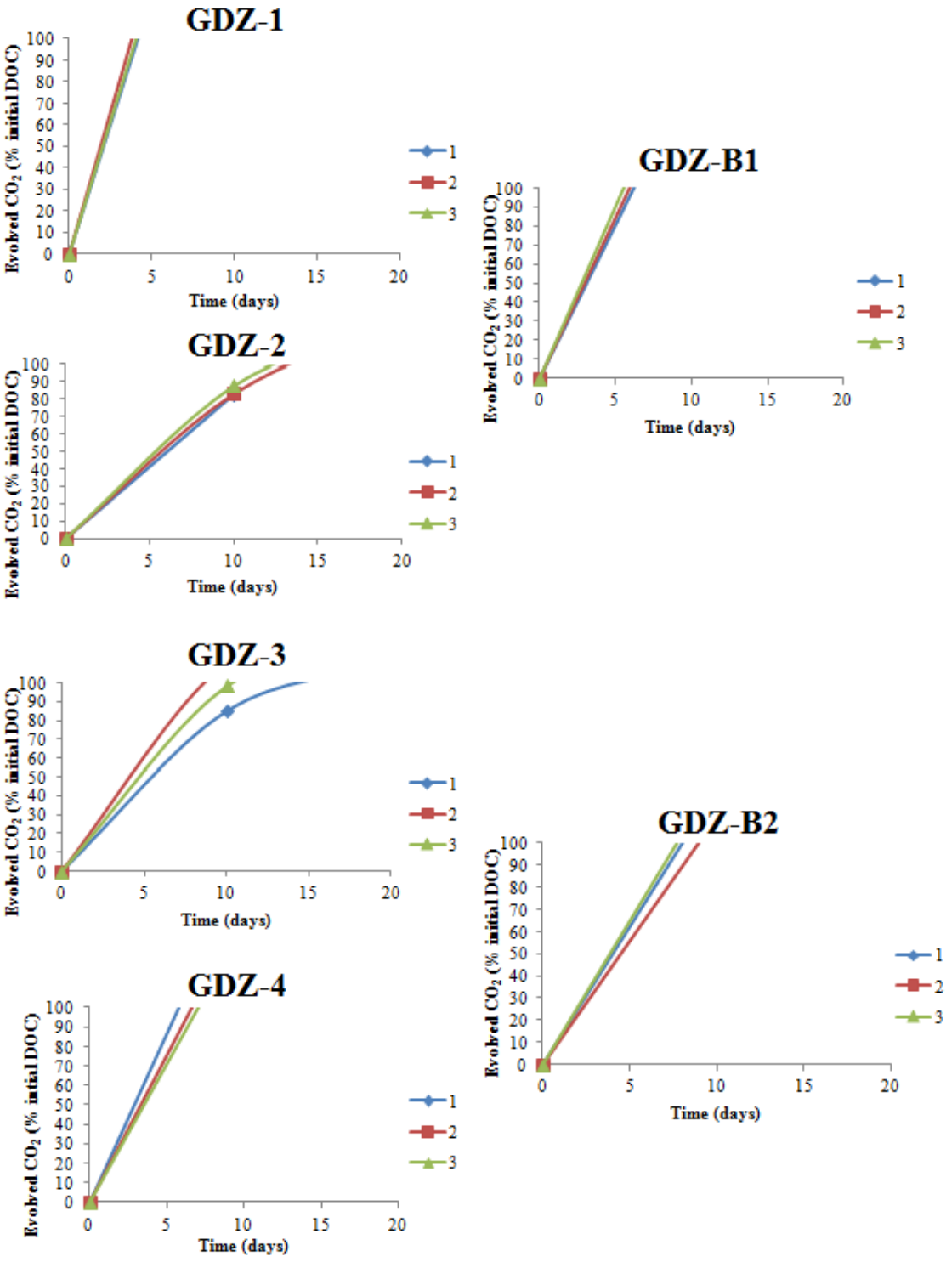

Figure 22b: Mineralization curves illustrating the amount of DOM biodegraded as relative (%) amounts of evolved CO_2 (mg C) to the initial amount of DOC (mg) during the first 20 days of the experiment for the samples originating from the Groundwater Discharge Zone (GDZ). The curves for each sample are presented in the order of origin in the field, with the overlying soil depths to the left (20 – 60cm), and the deeper depths to the right (90 – 100cm). Values for the three sample replicates are marked by solid lines.

The differences in biodegradability of DOM among the samples originating from the hill slope and the groundwater discharge zone is remarkably, and becomes even clearer with the average values for the three replicates of each sample presented by mineralization curves together in Figure 23. In this figure, the trend of increasingly more biodegradable DOM when moving down along the flow path of TSP is evident. From these findings it can be hypothesized that the microorganisms of the hill slope and the groundwater discharge zone exist in two different types of ecosystems with regards to supply of organic C. At the hill slope, the large amount of litter fall serves these bacteria with a constant supply of fresh organic matter of both labile and more refractory DOM. Along the flow path to the groundwater discharge zone, the more refractory pool, consisting mainly of aromatic and hydrophobic entities are selectively immobilized through adsorption to the organic poor soils of the hill slope. With regards to the groundwater discharge zone, this result in a limited supply of dominantly labile DOM which is rapidly mineralized by the high microbial activity found in such sub-tropical forests. How this fraction of highly labile DOM remains in solution and is not mineralized along the flow path of the hill slope, however, remain as an unknown.

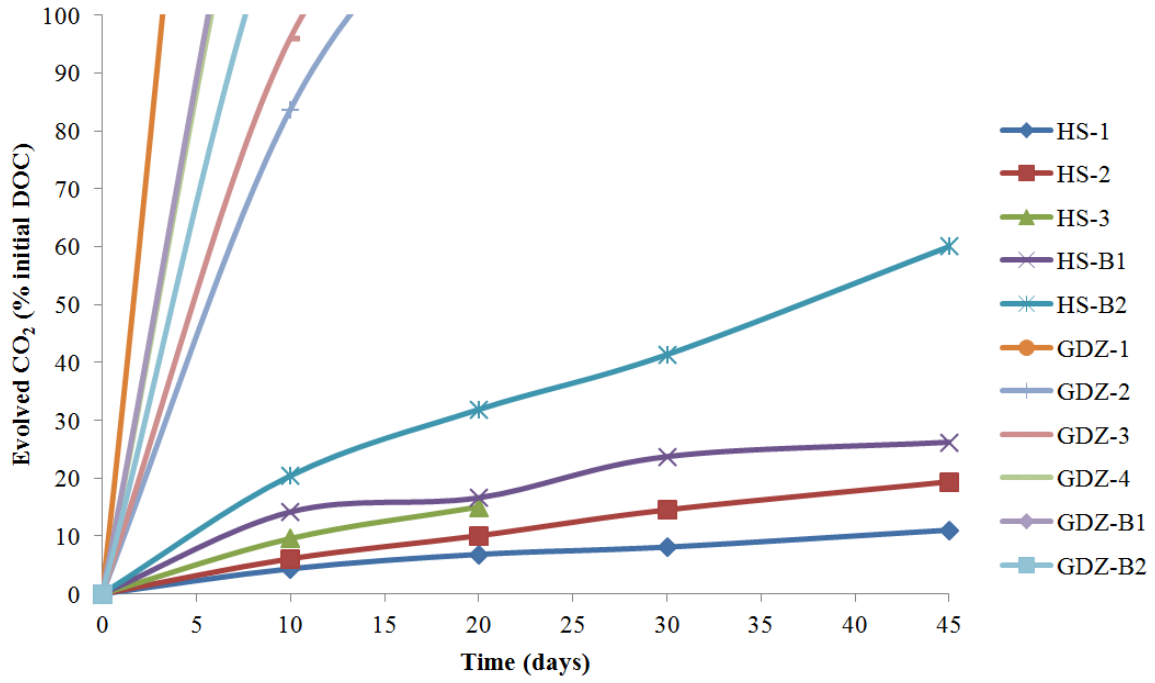

Figure 23: Presentation of the average values of mineralized DOC as relative (%) amounts of evolved CO_2 (mg C) to the initial amount of DOC (mg) for all of the soil-water DOM samples from TSP during the 45 days lasting biodegradation experiment.

4.4.4 Methodical considerations

The experimental setup used to measure biodegradability of the DOM samples is subject to external factors which may have affected the results. Such factors include underestimation of evolved CO_2 resulting from contamination of the sample solution by the NaOH in the alkaline CO_2 trap, uncertainties attributed largely to random variations, and a concentration effects with regards to large differences in the initial DOC concentration of the samples. The following section will deal with the effect of this, in addition to a brief discussion of the relevance of the results from such a laboratory biodegradation experiment to the natural environment of Tie Shan Ping.

4.4.4.1 Exclusion of data resulting from contamination

With the alkaline-trap (1M NaOH), used to capture evolved CO_2, comes the possibility of either contaminating the sample solution with NaOH (aq), or the NaOH-containing tube with the sample solution. NaOH spilled over into the sample solution caused an increase in the solution pH. An increase in pH may result in CO_2 being captured in the sample solution itself. If sample solution came into the NaOH-containing tube, dilution of the aqueous NaOH will result. Thus, in either way, an underestimation of evolved CO_2 would result. By comparing pH measurements conducted on the samples prior and post to the biodegradation experiment, an outlier value among the three replicates of the samples was associated with contamination of NaOH. These cases were found to display an apparent reduced value of evolved CO_2. Sample solution ending up in the NaOH-containing tubes, was observed in that a few of the tubes contained > 3mL solution. Also these samples showed reduced values of evolved CO_2 similar to that of the first type of contamination. This resulted in exclusion of 30 of the 124 sample replicates at any of the four analysis periods of the experiment. It can further be noted that this mainly involves results obtained from the two final analysis series of the incubation experiment. Moreover, such contamination of either the sample- or the NaOH-solutions did not occur for all of the three sample replicates of a sample, except for one of the samples (HS-3) from the final time period of the experiment. Complete list of excluded data and the grounds for exclusion is presented in Appendix D-2.

4.4.4.2 Uncertainties of the results from the biodegradation experiment

The very manual method used for this incubation experiment is prone to variations resulting from the manual execution (e.g. sampling, shaking of the samples etc.), as well as from other external factors (e.g. temperature, differences in jars used with regards to diffusion of CO_2, etc.). In Figure 24, the average value (subtracted by blank) of the absolute amount of CO_2 (mg C) measured from each of the samples from TSP are presented, with the variance resulting from three replicates of each sample (n = 3) illustrated by error bars. For those samples not associated with an error bar, values from certain of the replicates have been excluded based on the findings described in Chapter 4.4.4.1. A clear trend of increasing variance with time is evident. For certain of the samples, even an uncertainty of more than 100 % is stated (HS-B2 and GDZ-B2) for any of the three last days of analysis.

Despite uncertainties associated with these results, the absolute values of evolved CO_2 presented in Figure 24 appear to be significantly greater among the samples from the groundwater discharge zone (GDZ; right) as compared to those from the hill slope (HS, left). This is further especially evident for the results obtained from the first time period of the experiment (day 0 – day 10), which is also the time period found in Chapter 4.4.3.1 in which approximately 100 % mineralization of the samples from the groundwater discharge zone occurred.

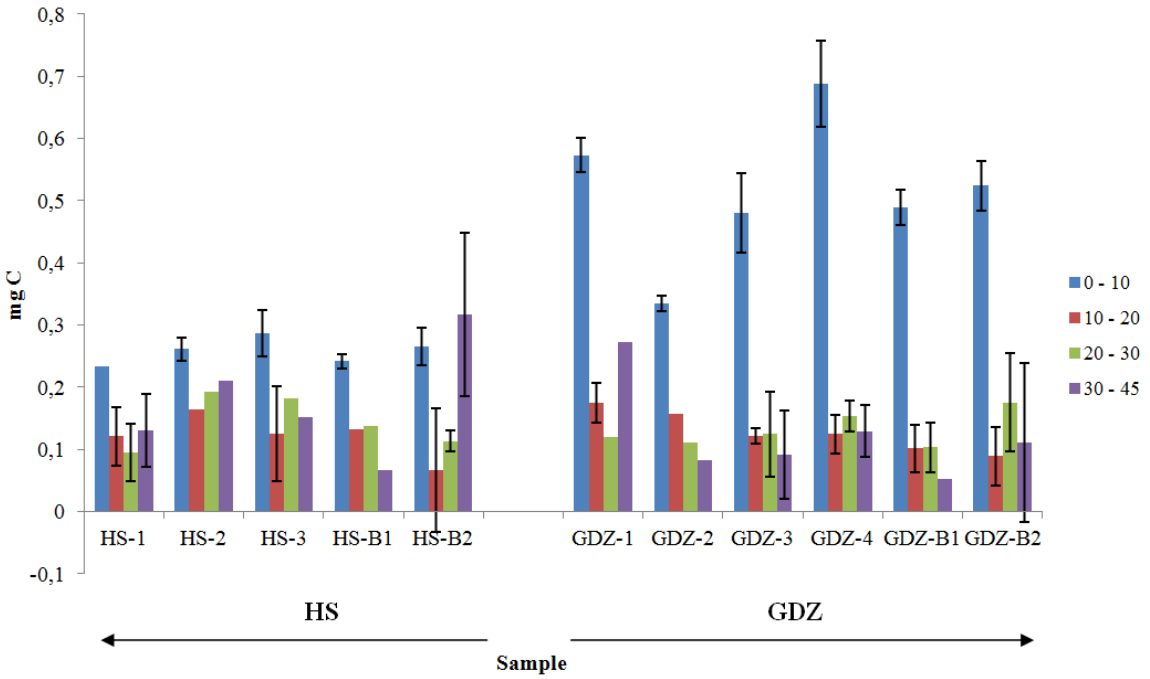

Figure 24: Absolute values of the average amount of evolved CO_2 (mg C) measured for the TSP-samples during the four time periods of the biodegradation experiment (day 0 – day 10, day 10 – day 20, day 20 – day 30, and day 30 – day 45). The variance among the sample replicates of each sample is illustrated by error bars. Note that for those samples not associated with an error bar, less than three replicate values are available.

4.4.4.3 Concentration effect of the biodegradation experiment

From the three reference samples re-dissolved to three different concentrations, a negative correlation is found between the relative amount of DOC biodegraded (%) and the initial amount of DOC in the samples (mg) (Figure 25). The reference sample with the lowest initial concentration of DOC gave the highest values of relative mineralization (%). This indicates a possible overestimation of mineralized DOC in the samples of low initial concentrations of DOC. The extent of such an effect could be especially critical as it is confounding with the differences observed in the biodegradability of DOM between the samples originating from the hill slope and the groundwater discharge zone.

In order to investigate the effect of this, the ratio between the average relative (%) amount of biodegraded DOM between the samples from the hill slope and the groundwater discharge zone was calculated and compared with the ratio between the reference sample with the lowest initial DOC (highest % mineralized) and of the highest initial DOC (lowest % mineralized). The values of the two ratios are presented in Table 10, and it appears that the value for the TSP-samples (9) is more than double of that of the reference samples (4).

These findings could indicate the large differences in biodegradability between DOM from the hill slope and the groundwater discharge zone may be enhanced by this effect, but the differences are not, however believed to be accounted for solely by this concentration effect.

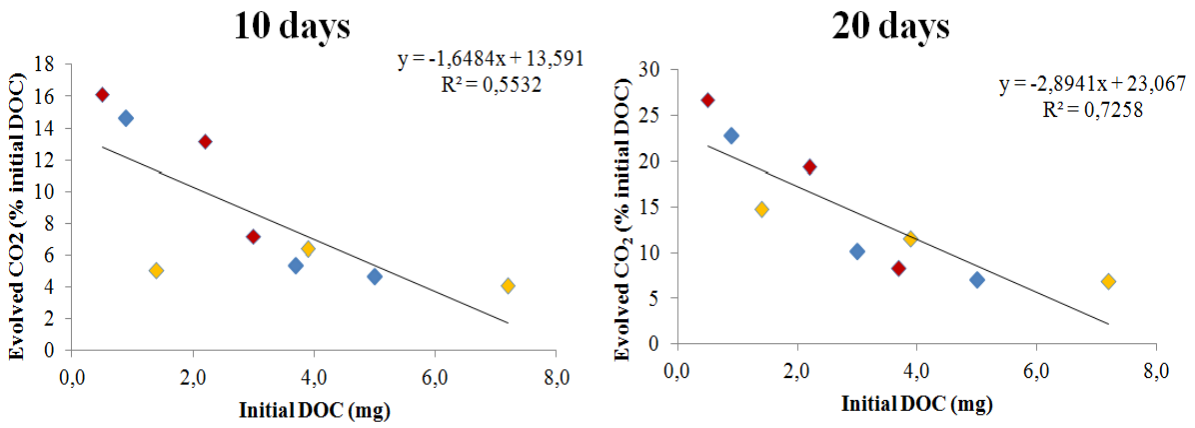

Figure 25: The non-linear correlation between the initial content of DOC (mg) and the amount of evolved CO_2 (mg C) measured after 10 and 20 days of incubation for the three reference samples re-dissolved to three different concentrations (red = Maridalsvannet, blue = Trehørningen, Green = Hieatjäervi Fall).

Table 10: Ratio of the average value of relative mineralization (mg C-CO_2 / mg DOC) measured during the first time period of the biodegradation experiment (day 0 – day 10) between the TSP-samples from the Groundwater Discharge Zone (GDZ) and the Hill Slope (HS) compared with the ratio between the reference samples of lowest and highest value of initial DOC concentrations.

TSP-samples	Reference samples
GDZ:HS	Low DOC:high DOC
9	4

4.4.4.4 Relevance to the natural environment

In the natural environment, the process of biodegradation is, in addition to the intrinsic properties of DOM, governed by numerous interconnected factors, such as water flow, distribution among micro- and macro soil-pores, microbial activity and composition, temperature, nutrients, redox-conditions, and input of fresh organic matter (Zsolnay 1996; Kalbitz et al. 2000; Haider et al. 2009; Madigan et al. 2012). Such factors are site-specific, and may induce differences in the biodegradation of DOM, in which the extent of these are

not covered in this study. However, by measuring biodegradability of DOM under controlled conditions in the laboratory, the effect of the different intrinsic properties of DOM among the samples is obtained. Furthermore, by retaining the natural pH, ionic strength, and initial concentration of DOC in the samples, which could affect the microbial productivity, the natural properties of DOM is maintained to the greatest extent possible. Thus, although the absolute rates of mineralization obtained from this biodegradation experiment should not be extrapolated from the laboratory to ecological settings (Torn et al. 2009), the relatively large differences found in biodegradability between the soil-water DOM samples makes it reasonable to assume that the intrinsic properties of DOM plays a large role in determining the extent of biodegradability of DOM in the field of TSP.

4.5 "The carbon budget"

During the process of biodegradation, DOC will be removed from the water both as CO_2 and as being incorporated into biomass through dissimilative and assimilative metabolism, respectively. Thus, by only considering the fraction transformed into CO_2 an underestimation of biodegraded DOC will occur (Paul and Clark 1996). In order to capture the fraction of DOC converted into biomass, all samples were analyzed for TOC and DOC (filtration[15] through 0.2µm) after completing the biodegradation experiment. Values from these two measurements (including all three sample replicates from the biodegradation experiment) are presented in Figure 26, along with the DOC concentrations obtained prior to the biodegradation experiment. Variance between the measurement replicates (n = 3) are illustrated by error bars. Due to problems with the baseline of the TOC-analyzer, all values are subtracted by the average value obtained from the total of 19 blank samples from the biodegradation experiment (Appendix E-1).

The samples originating from the hill slope (except one of the replicates of HS-B2) display a clear trend of subsequent decreasing concentrations of organic-C between the three measurements (prior > post unfiltered > post filtered). For the samples from the groundwater discharge zone, however, concentrations of organic-C decrease between the measurement conducted prior and post (unfiltered) to the biodegradation experiment, whereas the values of

[15] Filtration of the samples post to the biodegradation experiment was performed in agreement with the method described in Chapter 3.3.1

the final measurement is found to increase (post filtered). This would imply that the DOC is greater than the TOC, which is not sound. This inconsistency is assumed to result from analytical problems associated with the TOC-analyzer or from possible contamination occurring post to filtration. Regardless of the cause for the increase, this can be assumed to have occurred for the samples from the hill slope as well. With the low initial DOC of the samples from the groundwater discharge zone, the effect is more pronounced for these samples. Based on these findings, it will be impossible to estimate the amount of DOC assimilated by the bacteria.

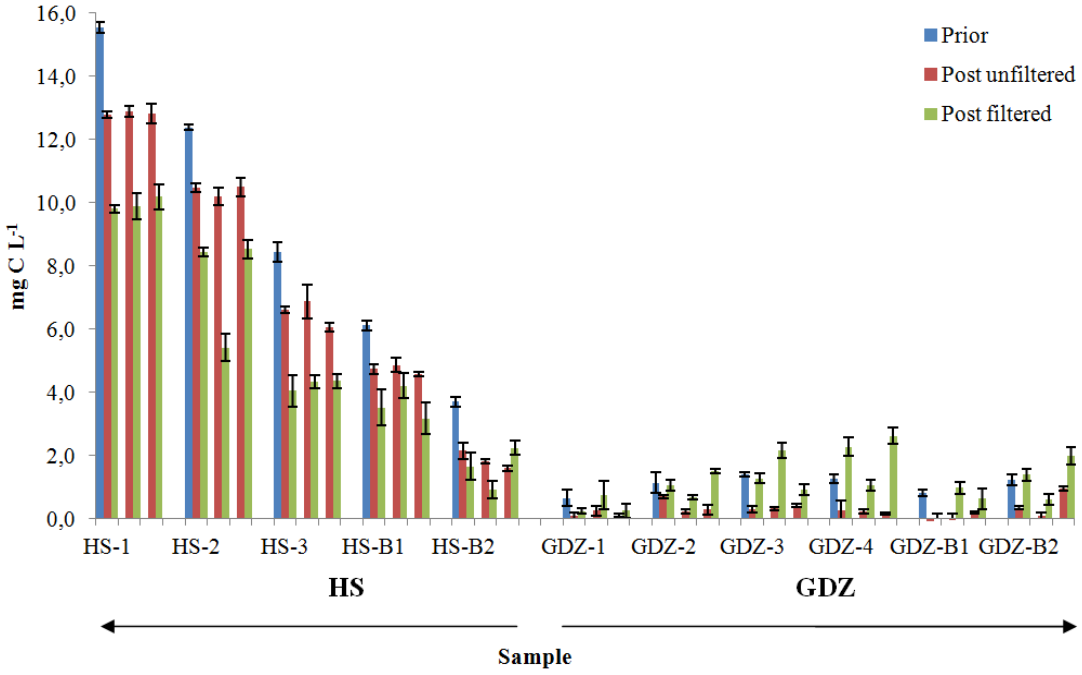

Figure 26: Values for the concentration of organic-C (mg C L^{-1}) measured prior (blue) and post to the biodegradation experiment for unfiltered (red) and filtered samples (green) originating from the Hill Slope (HS) and the Groundwater Discharge Zone (GDZ). Variance between the measurement replicates (n = 3) are presented by error bars.

4.6 Changes induced by the process of biodegradation

The process of biodegradation may induce changes in the water chemistry as well as in the structural properties of DOM. For the water chemistry, such changes may include the release of elements bound to DOM, uptake of essential elements by the microorganisms, and shifts in the redox potential and thereby alterations in redox sensitive species; nitrate, iron, and sulphate. With regards to the intrinsic properties of DOM, changes are largely assumed to render the DOM more recalcitrant (aromatic and condensed), resulting from preferential biodegradation of the less aromatic and hydrophobic fractions. In this study, such possible changes are investigated by repeating the analyses determining the concentration of major anions, and UV-Vis absorbency and fluorescence. The results obtained for the reference samples are presented in Appendix E-1 though E-3 (UV-Vis Fluorescence analysis was not repeated for these samples).

4.6.1 Redox species (nitrate and sulphate)

In order to investigate possible changes in the redox conditions in the samples, concentrations of nitrate and sulphate obtained prior and post to the biodegradation experiment are compared in Figure 27. For the measurement conducted post, average values of the three sample replicates from the biodegradation experiment are presented, with the variance among the replicates illustrated by error bars. The amount of nutrients added (0.1mM NH_4NO_3) in the biodegradation experiment was subtracted from the concentration of nitrate measured after the incubation. The values denominated as post are obtained after filtration (0.2µm).

From the figure, it appears that no significant changes have occurred in the concentration of neither of these two anions. This is further confirmed for nitrate using the paired sample t-test (C = 95%, d.f: 10). With regards to sulphate however, the paired t-test indicates a significant decrease. With nitrate being the preferential electron acceptor over sulphate (Appelo and Postma 2005), this is assumed to result from day-to-day variation in the IC used for these analyses. With regards to the reference samples, a significant change in the concentration of both nitrate and sulphate was detected using the paired t-test (C = 95 %, d.f: 18). The difference may be enhanced in the reference samples containing lower concentrations of all of the anions as compared to the samples from TSP. Based on this finding it can be stated that

the conditions within the incubated sample jars sustained aerobic during the time course of the biodegradation experiment.

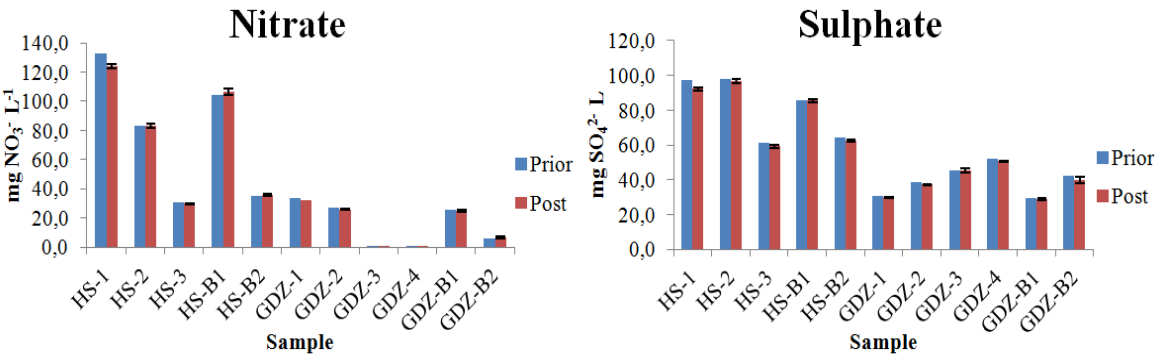

Figure 27: Concentration (mg L^{-1}) of nitrate (left) and sulphate (right) measured prior (blue) and post (red) to the biodegradation experiment in the soil-water samples from TSP. Average values of the three incubation sample replicates are presented, with the variation of the three replicates illustrated using error bars.

4.6.2 Aromaticity

Measurement of DOM absorbency within the UV (λ = 254nm) and Visible (λ = 400 and 600nm) region of the electromagnetic spectrum were repeated on filtered (0.2µm) samples after the biodegradation experiment, with subsequent calculation of the two indices of specific absorbency; sUVa ((Abs_{254nm} /[DOC])*100) and sVISa ((Abs_{400nm}/[DOC]) *1000). The concentration of organic-C measured on unfiltered samples post to the biodegradation experiment is used to calculate these indices, based on the findings from Chapter 4.5.

For the TSP-samples from the groundwater discharge zone and the reference samples, values of absorbency at λ = 254 nm had generally not found to have changed, whereas the values of absorbency at λ = 400 nm had increased. This could indicate that the aromatic entities of DOM, responsible for absorbance in the UV-region were not prone to biodegradation, whereas the increase at λ = 400nm may result from biotic/abiotic polymerization reactions. With regards to the TSP-samples from the hill slope, however, the values of absorbency at both λ = 254 and 400nm appear to decrease. This could indicate that also the aromatic and thus more refractory material in the samples from the hill slope is in fact biodegraded. Data available in Appendix E-3.

The two indices of specific absorbency, sUVa and sVISa, are presented in Figures 28a and b respectively, for the TSP-samples originating from the Hill Slope (HS) and the Groundwater

Discharge Zone (GDZ). All three sample replicates from the biodegradation experiment are included, except for those in which the concentration of C was detected as zero. Variance resulting from the determination of DOC is included as error bars. From these two figures, there appear to be no significant change in the values of these indices for the samples from the hill slope, whereas a remarkable increase is evident for the samples originating from the groundwater discharge zone. These findings corroborate the findings from the values of absorbency addressed above, in that the fraction of aromatic compounds (both lower and higher molecular weight) still remaining in solution in the samples from the groundwater discharge zone are not prone to biodegradation. The practically complete mineralization of the non-aromatic fraction thus causes a strong increase in sUVa and sVIsa.

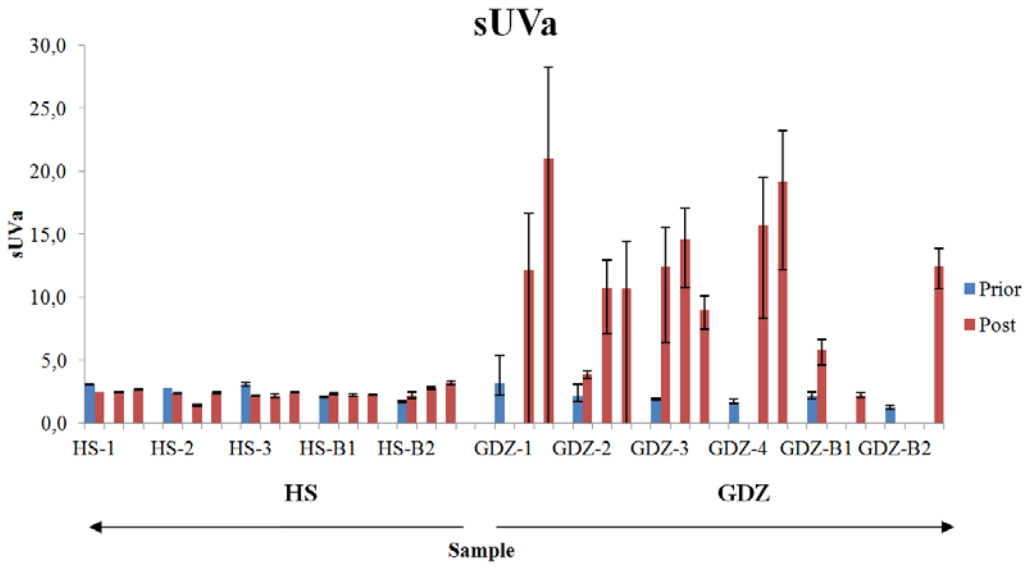

Figure 28a: Values for Specific UV Absorbency, sUVa ($(Abs_{254nm}/[DOC])*100$), measured prior and post to the biodegradation experiment for the TSP-samples originating from the Hill Slope (HS) and the Groundwater Discharge Zone (GDZ). Variance resulting from determination of DOC is illustrated by error bars.

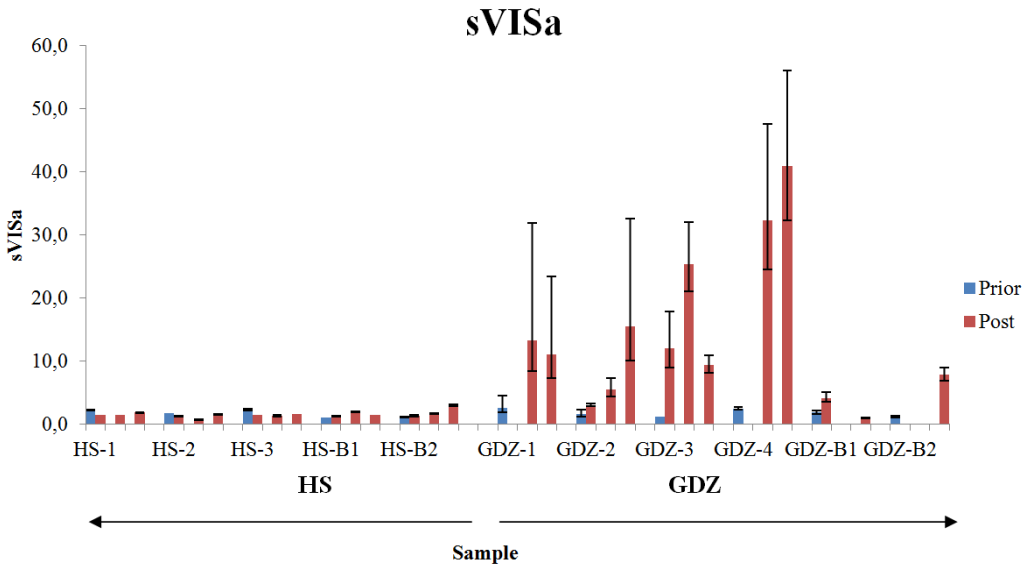

Figure 28b: Values for Specific VISible Absorbency, sVISa ((Abs$_{400nm}$/[DOC])*1000), measured prior and post to the biodegradation experiment for the TSP-samples originating from the Hill Slope (HS) and the Groundwater Discharge Zone (GDZ). Variance resulting from determination of DOC is illustrated by error bars.

4.6.3 Humic and Fulvic acids deduced from Fluorescence EEM spectra

Fluorescence Excitation-Emission Matrix (EEM) spectra obtained on the DOM material after the biodegradation experiment are presented for the samples originating from the Hill Slope (HS) and the Groundwater Discharge Zone (GDZ) in Figures 29a and b, respectively. Note that the sequence of the spectra for the samples is presented in accordance with their origin in the field. Intensities (I) and locations ($\lambda_{ex}/\lambda_{em}$) of the two peaks, A and B, are presented in Table 11, in addition to the relative difference in intensity compared with measurements performed prior to the biodegradation experiment, ΔI (%).

Overall, a decrease in the fluorescence intensity in addition to a reduction in the broadening of the spectra appears for all of the samples as compared to the EEM spectra obtained prior to the biodegradation experiment (Chapter 4.4.2; Figures 18a and b). This reduction in fluorescence may either be due to microbial degradation of fluorophore-containing DOM, or due to quenching of fluorescence by organic molecules synthesized during the course of the biodegradation experiment (Saadi et al. 2006).

For the samples originating from the hill slope, both the peaks A and B, in addition to the weak signal for shoulder C, appear in the spectra. The locations of peak A and B were further

consistent with those found prior to the biodegradation experiment. The consistency of the peak locations is also reported by others studying DOM biodegradation, e.g. Saadi et al. (2006). A relative decrease in the intensity of the two peaks (A and B) is found. This decrease becomes greater down through the plots of the hill slope. The largest decrease was found for peak A (Table 11). With peak A stated to represent the more aromatic and hydrophobic humic acids, these results are quite surprising. With regards to the samples from the groundwater discharge zone, virtually no peaks are evident in the spectra (Figure 29b), with only very weak signals of fluorescence detected. In accordance with the samples from the hill slope, it appears that the fluorescence intensity within the area of peak A is almost completely lost.

The relatively large reduction in fluorescence intensity of both the samples from the hill slope and the groundwater discharge zone is associated with microbial degradation of DOM. However, as these results are not consistent with those from UV-Vis absorbency, it cannot be stated that the reduction is caused by microbial utilization of these fluorescing chromophores. Moreover, with a greater reduction in fluorescence intensity being evident for peak A (humic acids) as compared to peak B (fulvic acids) this reduction is assumed to be caused by some other process, possibly by quenching of fluorescence caused by synthesis of organic molecules during the biodegradation experiment.

Table 11: Locations ($\lambda_{ex}/\lambda_{em}$) and intensities (I) of the two fluorescence peaks A and B for the samples originating from the hill slope (HS) and the groundwater discharge zone (GDZ) post to the biodegradation experiment. Absolute decrease in the two peak intensities (ΔI) compared with the values obtained prior to the biodegradation experiment are also included.

	Peak A				Peak B			
Sample	λ_{ex}	λ_{em}	Intensity (I)	ΔI (%)	λ_{ex}	λ_{em}	Intensity (I)	ΔI (%)
HS-1	341	420	71	17	250	422	63	2
HS-2	342	418	58	23	248	422	63	7
HS-3	341	422	38	28	246	427	51	15
HS-B1	337	416	26	24	247	410	33	18
HS-B2	(339)	(409)	13	24	244	410	22	21
GDZ-1	324	408	4	33	247	421	7	30
GDZ-2					247	430	9	25
GDZ-3	329	418	7	0	230	420	15	6
GDZ-4					244	424	8	0
GDZ-B1					246	420	7	13
GDZ-B2	322	406	3	0	249	416	6	0

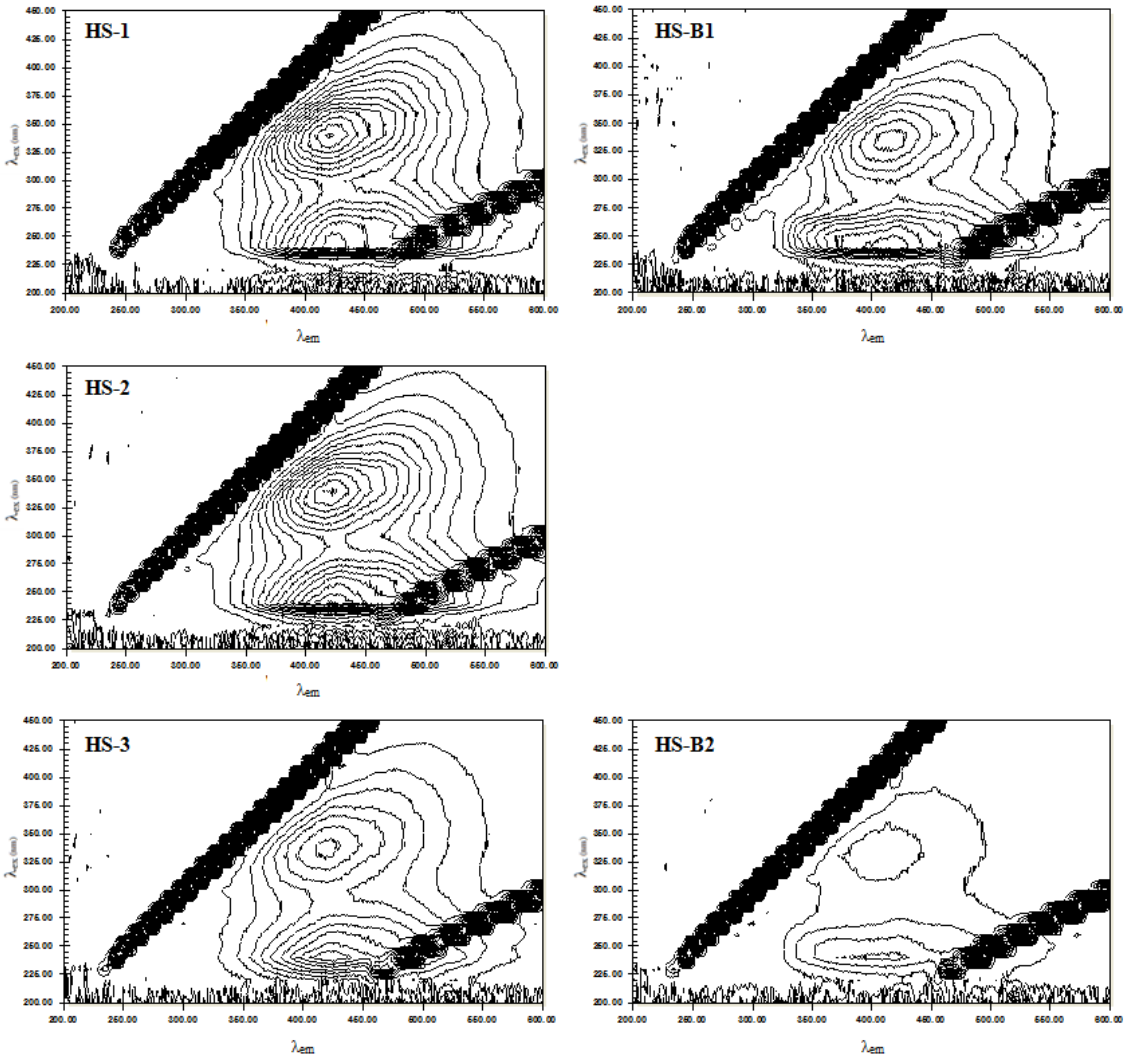

Figure 29a: Fluorescence Excitation-Emission Matrix (EEM) spectra for the samples from the hill slope (HS) post to the biodegradation experiment. All spectra are presented with 200 lines, and are obtained with intensity maximum of 100, except from HS-B2 (I_{max} = 40).

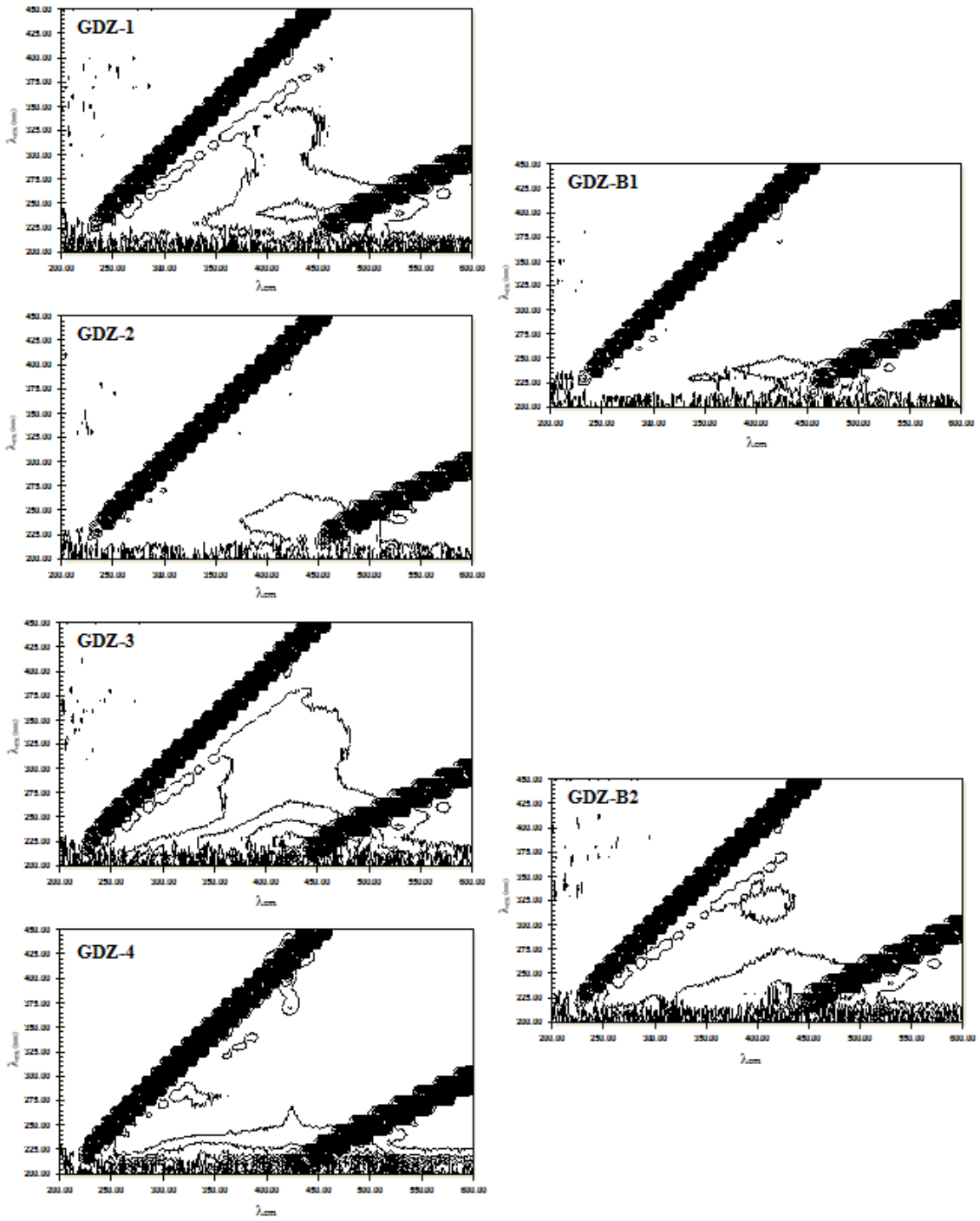

Figure 29b: Fluorescence Excitation-Emission Matrix (EEM) spectra for the samples from the groundwater discharge zone (GDZ) post to the biodegradation experiment. All spectra are obtained with Intensity maximum of 40, and 200 lines.

4.7 Biodegradation of DOM in relation to its physico-chemical characteristics

With biodegradation of DOM conducted under controlled laboratory conditions, any differences in biodegradability between various DOM samples may be attributed to differences in the physico-chemical characteristics of the DOM itself. Thus, by analyzing the correlation between the relative amount of biodegraded DOM (expressed as relative amounts of evolved CO_2 (mg C/ mg DOC)) and the physico-chemical characteristics of DOM, intrinsic factors determining its biodegradability may be revealed. The effect on biodegradation from differences in physico-chemical properties among DOM-samples is generally stated to be most profound during the initial stages of decomposition. For this reason, in addition to the increasing uncertainties with time associated with the results from the biodegradation experiment (Chapter 4.4.3.2), correlation analysis is performed using only mineralization data from the two first time periods of the incubation experiment (day 0 – day 10 and day 0 – day 20).

For this assessment of correlation, only the Reverse Osmosis (RO) isolated DOM reference samples were included. The characterization parameters obtained in this study is supplemented with the large number of data made available from the two respective projects in which the two sets of samples originate from (Gjessing et al. 1999; Vogt et al. 2001). Due to the general lack of consistency in the definition of characterization parameters for the analysis of DOM, the two sets of samples were investigated separately. Since the biodegradation experiment was conducted with the samples sustaining their natural pH and DOC concentration, these two solution properties were also included in the study of correlation.

The reason for excluding the soil-water DOM samples from TSP in this context results from the explanatory parameters from the hill slope and the groundwater discharge zone being clustered in the correlations. This causes practically all the data to co-variate, since the explanatory- and response parameters differ more between the two sites than within each site. Moreover, with the close to complete mineralization measured for all of the samples from the groundwater discharge zone, no sane correlation can be obtained for these data.

4.7.1 Reference DOM samples

Spearman's rank correlation coefficient (r_s) describing the relation between the biodegradability of the reference-DOM samples and the solution- and intrinsic parameters determined in this study are presented in Table 12. Note that all of the resulting coefficients are of significance (p) greater than 0.025.

Both pH and initial DOC are negatively correlated with the amount of biodegraded material in the reference-DOM. The correlation with pH (r_s = -0.45 and -0.29) could be due to that the microorganisms of the added inoculum were adapted to more acidic conditions (pH < 5) than what was the case for the reference sample solutions (pH ~ 5-7). The somewhat weaker correlation found for the initial concentration of DOC (r_s = -0.34 and -0.38) is possibly attributed to the concentration effect associated with the biodegradation experiment (Chapter 4.4.3.1).

With regards to the intrinsic properties of DOM (sUVa, sVISa, SAR, and A:B), the correlation coefficients are generally weak. The directions of the correlations are however in accordance with the literature, stating non-preferential biodegradation of aromatic (sUVa) compounds, while the smaller molecular size compounds are associated with preferential biodegradation (SAR). This is further corroborated by the negative correlation with the fluorescence peak ratio, A:B, indicating preferential biodegradation of the lower molecular weight, less aromatic, and more hydrophilic fulvic acids over the humic acids.

Table 12: Spearman's rank correlation coefficient (r_s) describing the relation between biodegraded DOM (mg C-CO_2/ mg DOC) and its solution- (pH and initial DOC) and intrinsic (sUVa, sVISa, SAR, and A:B) properties among the DOM reference samples (n = 19).

	Solution		Intrinsic			
	pH	DOC	sUVa	sVISa	SAR	A:B
10 days	-0.45	-0.34	-0.12	-0.19	0.33	-0.26
20 days	-0.29	-0.38	-0.05	-0.09	0.13	-0.28

4.7.1.1 Reference DOM-samples originating from and characterized by the "NOM-typing" project

In Table 13, Spearman's rank correlation coefficients (r_s) describing the relation between biodegraded DOM and its intrinsic properties determined by and within the "NOM-typing" project (Gjessing et al. 1999) are presented. The characterization parameters are divided into categories of elemental-, non-humic-, structural-, fluorescent-, solubility/charge-, and molecular size properties. All of the resulting correlations are of significance at $p > 0.025$.

Increasing values of the two elemental ratios, N:C and H:C, are believed to be associated with greater loss of DOC through biodegradation. This is explained by preferential microbial utilization of N-containing compounds, and that molecules of increased saturation (expressed by increased H:C) (i.e. less aromatic) are more prone to biodegradation (Huang and Hardie 2009). From Table 13, a rather weak positive correlation is found for N:C ($r_s = 0.23$ and 0.12) whereas no correlation appears for the H:C ratio. The relative amount of organic sulphur (%) is further found to correlate positively with biodegradation ($r_s = 0.63$ and 0.60), which could result from S being one of the essential elements for all microorganisms (Madigan et al. 2012).

Contribution of non-humic substances to the pool of DOM is generally acknowledged to increase its biodegradability (Bolan et al. 2011). From Table 13 it appears that the content of carbohydrates ($r_s = 0.45$ and 0.67) and proteins ($r_s = 0.41$ and 0.21) increase biodegradation of the reference-DOM, whereas a negative- or no correlation is found for the content of amino acids and amino sugars. The reason for this lack of correlation between biodegraded DOM and these latter two compound classes is unknown.

With regards to the structural parameters, biodegradation of DOM was found to decrease with increasing ratio of aromatic- to aliphatic-H moieties ($r_s = -0.46$ and -0.42). This is in accordance with the literature, stating preferential biodegradation of the less conjugated systems (Marschner and Kalbitz 2003). No significant correlation with biodegradability is however found for the ratio of aromatic- to aliphatic-C, with the reason for this being unknown. The amount of aromatic and aliphatic compounds in these reference DOM-samples have further been determined using a second technique of analysis. From these data no significant correlation is found for the content of aromatics, whereas a rather weak negative correlation appears between the content of aliphatics ($r_s = -0.32$ and -0.42). These deviating

results for the same parameters determined by different analytical methods reflect the lack of consensus in the science of DOM characterization.

Further structural information is obtained from the three fluorescence peak ratios, A:B, A:C, and B:C, calculated from EEM spectra. The A:B ratio, representing the relative amount of humic over fulvic acids, display the strongest correlation with the biodegradability of DOM (r_s = -0.45 and -0.45). This is in accordance with the literature stating preferential biodegradation of less aromatic and more soluble compounds (Marschner and Kalbitz 2003). The contribution of humic (A) and fulvic (B) acids relative to the amount of more highly conjugated aromatic compounds ("shoulder" C) (A/C and B/C) showed no significant correlations with biodegradability of the DOM. This is likely due to that the content of the more extensively humified (C) material is found to be generally low among these samples.

Hydrophilic structures of DOM are believed to be preferentially biodegraded over the more hydrophobic (Marschner and Kalbitz 2003), since the more hydrophilic compounds are more accessible for microbial attack. The ratio of hydrophilic to hydrophobic DOM (Hphi:Hpho) is thus postulated to correlate positively with biodegradation. Still no significant correlation is found between the biodegradability of the reference DOM and the data for this ratio obtained from the "NOM-typing" project. The net charge of the reference DOM, correlates positively with biodegradability of the DOM (r_s = 0.40 and 0.43). This indicates that the more charged entities of DOM, which are also more inherently soluble, are preferentially biodegraded over the neutral and thus more hydrophobic entities.

Molecular dimensional properties such as weight and size are frequently stated to affect biodegradation of DOM. Decreasing molecular size is generally inferred with increased biodegradation, although the effect may be attributed to the characteristics of the smaller sized molecules rather than to the size itself (Wetzel 2001). Molecular weight (Da) of the reference samples appears to correlate positively with its biodegradability (r_s = 0.43 and 0.55), whereas molecular size (nm) is found to correlate negatively (r_s = -0.47 and -0.63). These contradicting results of correlation with the biodegradability of the DOM obtained for these two different parameters, both describing molecular dimension, is attributed to the challenges associated with characterization of the dynamic and heterogeneous DOM.

Table 13: Spearman's rank correlation coefficient (r_s) describing the relation between biodegraded DOM (mg C-CO_2/ mg DOC) in the reference samples originating from the "NOM-typing" project and the various characterization parameters obtained by and within the project (n = 9). The characterization parameters are separated into categories of elemental-, non-humic-, structural-, fluorescent-, solubility/charge-, and molecular dimensional properties.

	Elemental			Non-humic			
	N:C	H:C	Org.S	Carb.	Proteins	Amino acids	Amino sugars
10 days	0.23	0.07	0.63	0.45	0.41	-0.32	0.01
20 days	0.12	-0.05	0.60	0.67	0.21	-0.18	-0.08

	Structural				Fluorescent		
	Aromatic	Aliphatic	ArC:AlC	ArH:AlH	A:B	A:C	B:C
10 days	0.08	-0.32	0.08	-0.46	-0.45	-0.07	-0.08
20 days	0.05	-0.42	0.10	-0.42	-0.45	-0.07	-0.03

	Solubility/charge		Molecular dimension	
	Hpi:Hpho	Net.Cha	Mwt.	Size
10 days	-0.07	0.40	0.43	-0.47
20 days	-0.08	0.43	0.55	-0.63

4.7.1.2 Reference DOM-samples originating from and characterized by the "NOMiNiC" project

The set of parameters used to characterize the DOM in the "NOMiNiC" project (Vogt et al. 2001) are not identical to those used in the "NOM-typing" project, but describe more or less the same properties of DOM. Spearman's rank correlation coefficients, r_s, describing the relation between data on the biodegradability of DOM and the physico-chemical characteristics obtained from the "NOMiNiC" project are presented in Table 14. The parameters are divided into categories of elemental-, non-humic-, humic-, molecular-, structural-, fluorescent-, and fulvic-/humic properties.

In accordance with the literature and the results for the DOM-samples from the NOM-typing project, the relative amount of N to C correlates positively with biodegradability of DOM (r_s = -0.46 and -0.45; expressed as C:N).

The content of the non-humic biochemical moieties of amino acids correlates negatively with the biodegradability of the DOM (r_s = -0.53 and -0.45). This is in contradiction to what is stated in the literature (Huang and Hardie 2009), but it is in accordance with the findings for the samples from the "NOM-typing" project. No significant correlation is found between the content of polysaccharides and the biodegradability of DOM, although this class of molecules is assumed to be easily biodegradable (Huang and Hardie 2009). This is most likely due to the very low content of these molecules found in the DOM. The content of Humic Substances (HM) is further found to correlate positively with biodegradability (r_s = 0.55 and 0.17). Humic substances are not intuitively associated with increased biodegradability, due to its highly condensed and complex nature (MacCarthy 2001).

The content of different types of structural/functional moieties in the DOM is known to affect its biodegradability. The biodegradability of DOM is found to increase with increasing content of phenolic-, ketonic/carbonyl-, and unsaturated aromatic structures (Table 14), as well as with the relative amount of aromatic over aliphatic structural units. Content of phenolic compounds in the DOM is previously found to correlate both positively (Kiikkilä et al. 2011) and negatively (Bu et al. 2011) with biodegradability of DOM. These contradicting findings could result from the dual characteristics of such compounds, in that its charge contribution eases biodegradation by rendering DOM more hydrophilic, whereas the aromatic character reduces biodegradability. The electron withdrawing capacity of the

Ketonic/carbonyl functional group would theoretically result in lower biodegradability of compounds containing such functional groups. The charge of the oxygen atom may however contribute with charge to the whole of DOM, resulting in increased biodegradability through solubilisation. The content of aromatic moieties, being one of the most profoundly recognized parameters found to decrease biodegradability of DOM (Bolan et al. 2011), appears however from these data to correlate positively with the amount of biodegraded DOM. This is found both with the amount of unsaturated aromatics and with the relative contribution of aromatic to aliphatic compounds (Arom:Aliph), determined by a different method. The reason for this is unknown. Carboxylic functional groups and amides are both believed to be rather easily biodegraded, and the electron donating character of alkyl functional groups is assumed to increase biodegradation of DOM. Nevertheless, the content of carboxylic along with amide and alkyl in the DOM were not found to correlate significantly with the biodegradability of the DOM.

Fluorescent DOM was measured within the "NOMiNiC" project using two different modes of analysis, providing these samples with spectra of both 3-D EEM and 2-D emission. From the 3-D EEM, the three peak ratios A:B, A:C, and B:C were obtained, whereas the latter spectra was used to calculate the Humification Index, HIX_{em}. The three peak ratios are not found to correlate significantly with biodegradability of the DOM. This is in contrast to the samples from the "NOM-typing" project even though this particular analysis was performed by the same method and by the same research groups within the two respective projects. The HIX_{em} indicates the relative complexity and condensation of the molecules constituting DOM, and is thus inferred to indicate the degree of humification of the DOM samples. Even though the process of humification is recognized to render the DOM more recalcitrant towards biodegradation, no significant correlation appears between this index and biodegradability of the DOM.

Increasing values of molecular spin is associated with higher degree of aromatization and lower content of carboxylic functional groups, and can thus serve as a proxy for the relative contribution of humic- to fulvic like material. One should therefore expect the spin to be negatively correlated to the biodegradability of DOM. From Table 14 it appears that increasing values of spin reduces biodegradation of DOM among these samples (r_s = 0.75 and -0.46), in accordance with the theory. This is furthermore the strongest correlation found between DOM characterization parameters and the biodegradability of DOM, and the

correlation coefficient increases further when the values of spin are expressed in relative terms (r_s = 0.80 and -0.40).

Table 14: Spearman's rank correlation coefficient (r_s) describing the relation between biodegraded DOM (mg C-CO_2/mg DOC) in the reference samples from the "NOMiNiC" project and the various characterization parameters obtained by and within the project (n = 10). The parameters are separated into categories of elemental-, non-humic-, molecular-, structural-, fluorescent-, and fulvic-/humic properties.

	Elemental	Non-humic		Humic	Molecular	
	C:N	Amino a.	Polysac.	HS	Mwt.	Radii
10 days	-0.46	-0.53	-0.29	0.55	-0.3	-0.03
20 days	-0.45	-0.45	0.10	0.17	-0.18	-0.18

	Structural					
	phenolic	Carbox. + amide	Ketnic/carbonyl	Aromatic unsat.	alkyl	Arom:Aliph
10 days	0.59	-0.25	0.51	0.59	-0.35	0.54
20 days	0.16	-0.20	0.24	0.13	0.47	0.13

	Fluorescent					
	A:B	A:C	B:C	HIX_{em}	Spins	Spin density
10 days	0.07	-0.31	-0.26	0.21	-0.75[c]	-0.80[b]
20 days	-0.24	-0.09	-0.04	-0.02	-0.46	-0.40

[b]Significance at $p < 0.01$
[c]Significance at $p < 0.025$

5. Conclusions

It was previously found that the denitrifying bacteria in the Tie Shan Ping forested catchment were substantially more C-limited in the groundwater discharge zone compared to the hill slope recharge zone. The loss of DOM along the soil-water flowpath was hypothesized to be attributed to rapid mineralization, resulting in only the more recalcitrant fraction of DOM ending up in the groundwater discharge zone (Solheimslid 2011). Based on the findings from this present study, this latter hypothesis is rejected. Instead, the loss of DOM along the flowpath is suggested to be attributed to adsorption to the soil. This has implications on the fraction remaining in solution, which is the more hydrophilic and biodegradable DOM rather than the hydrophobic and more recalcitrant fraction.

This conclusion is based on the results from a biodegradation experiment where DOM from the hill slope recharge zone and from the groundwater discharge zone were incubated with an indigenous mixed bacteria inoculum. This experiment showed a practically complete biodegradation of the DOM originating from the groundwater discharge zone as compared to limited biodegradation of the DOM of the samples from the hill slope. Thus, although the quantity of DOM is lower in the groundwater discharge zone, it appears that it is qualitatively more available for the bacteria. Building on the thesis that bulk of the DOM in the groundwater discharge zone is transported from the hill slope, this difference can only, from the present understanding, result from selective adsorption of the more hydrophobic humic matter to the clay-rich and, organic-poor soils on the hill slope. This was collaborated with the results obtained from the structural characterization, using spectroscopic measures, displaying higher relative amounts of more aromatic and higher ratio of humic to fulvic acids in the DOM from the hill slope as compared to the groundwater discharge zone. This is conceptually sound as these structural characteristics are conceived as constituting the more hydrophobic DOM moieties. The extent of DOM adsorption to the soil is furthermore assessed to be enhanced in the studied site due to a very low pH, high concentration of inorganic aluminium, and high ionic strength found in these soil-waters.

It was deduced from a correlation analysis, conducted to reveal intrinsic properties of DOM that governs its biodegradability, that samples possessing higher degree of aromaticity and condensation were less biodegradable, while an elevated content of essential elements such as

N and S, in addition to the degree of solubility correlated positively with biodegradation. The strengths of the correlations were however relatively weak. Moreover, there were opposing results for certain of the parameters describing the same property of DOM, though obtained by means of different analytical principles. This is believed to result from the lack of consensus in the science of DOM characterization. This study calls for more investment in establishing universe definitions of DOM characterization parameters. The need for this is especially evident when considering the global consequences of the environmental processes that are governed by DOM, such as the process of denitrification which is associated with emission of greenhouse gas, nitrous oxide.

6. References

Alberts, J. J. (1982). "The effect of metal ions on the ultraviolet spectra of humic acid, tannic acid and lignosulfonic acid." Water Research **16**(7): 1273-1276.

Appelo, C. A. J. and D. Postma (2005). Geochemistry, groundwater and pollution. Leiden, Balkema.

Bakken, L. and P. Dörsch (2007). Nitrous Oxide Emission and Global Changes: Modeling Approaches. Biology of the Nitrogen Cycle. H. Bothe, S. J. Ferguson and W. E. Newton, Elsevier**:** 381-395.

Barnes, R. B. (1975). "The determination of specific forms of aluminum in natural water." Chemical Geology **15**(3): 177-191.

Beck, A. J., K. C. Jones, et al. (1993). Organic Substances in Soil and Water: Natural Constituents and Their Influences on Contaminant Behavior. [In: Spec. Publ. - R. Soc. Chem., 1993; 135], Royal Soc. Chem.

Blaser, P., A. Heim, et al. (1999). "Total luminescence spectroscopy of NOM-typing samples and their aluminium complexes." Environment International **25**(2–3): 285-293.

Bolan, N. S., D. C. Adriano, et al. (2011). Dissolved Organic Matter: Biogeochemistry, Dynamics, and Environmental Significance in Soils. Advances in Agronomy. L. S. Donald, Academic Press. **Volume 110:** 1-75.

Bu, X., J. Ding, et al. (2011). "Biodegradation and chemical characteristics of hot-water extractable organic matter from soils under four different vegetation types in the Wuyi Mountains, southeastern China." European Journal of Soil Biology **47**(2): 102-107.

Buffle, J. (1977). Les substances humiques et leurs interactions avec les ions mineraux. La Commission d'Hydrologie Appliquee de l'A.G.H.T.M., L'Universite d'Orsay.

Burba, P., B. Jakubowski, et al. (2002). Characterization of refractory organic substances and their metal species by combined analytical procedures, Wiley-VCH Verlag GmbH.

Chen, W., P. Westerhoff, et al. (2003). "Fluorescence Excitation−Emission Matrix Regional Integration to Quantify Spectra for Dissolved Organic Matter." Environmental Science & Technology **37**(24): 5701-5710.

Chen, X. Y. and J. Mulder (2007). "Indicators for Nitrogen Status and Leaching in Subtropical Forest Ecosystems, South China." Biogeochemistry **82**(2): 165-180.

Chilom, G., Rice, J. A. (2009). Organo-Clay Complexes in Soils and Sediments. Biophysico-Chemical Processes Involving Natural Nonliving Organic Matter in Envrionmental Systems. N. Senesi, Xing, B., Huang, P. M. NJ, United States of America, John Wiley & Sons, Inc.**:** 111-145.

Coble, P. G. (1996). "Characterization of marine and terrestrial DOM in seawater using excitation-emission matrix spectroscopy." Marine Chemistry **51**(4): 325-346.

Cornejo, J. and M. C. Hermosín (1996). Interaction of Humic Substances and Soil Clays. Humic Substances in Terrestrial Ecosystems. P. Alessandro. Amsterdam, Elsevier Science B.V.**:** 595-624.

Dawei, Z., T. Larssen, et al. (2001). "Acid Deposition and Acidification of Soil and Water in the Tie Shan Ping Area, Chongqing, China." Water, Air, & Soil Pollution **130**(1): 1733-1738.

Determann, S., R. Reuter, et al. (1994). "Fluorescent matter in the eastern Atlantic Ocean. Part 1: method of measurement and near-surface distribution." Deep Sea Research Part I: Oceanographic Research Papers **41**(4): 659-675.

Driessen, P., Deckers, J., Spaargaren, O., Nachtergaele, F. (2001). Lecture Notes on the Major Soils of the World.

Driscoll, C. T. (1984). "A Procedure for the Fractionation of Aqueous Aluminum in Dilute Acidic Waters." International Journal of Environmental Analytical Chemistry **16**(4): 267-283.

Fellman, J. B., D. V. D'Amore, et al. (2008). "An evaluation of freezing as a preservation technique for analyzing dissolved organic C, N and P in surface water samples." Science of The Total Environment **392**(2–3): 305-312.

Firestone, M. K. and E. A. Davidson (1989). Microbiological Basis of NO and N2O Production and Consumption in Soil. Exchange of Trace Gases between Terrestrial Ecosystems and the Atmosphere. M. O. Andreae and D. S. Schimel, John Wiley & Sons**:** 7-22.

Forster, P., V. Ramaswamy, et al. (2007). Changes in Atmospheric Constituents and in Radiative Forcing. S. Solomon, D. Qin, M. Manning, Z. Chen, M. Marquis, K.B. Averyt, M.Tignor and H.L. Miller. Cambridge, United Kingdom and New York, NY, USA, Cambridge University Press.

Frimmel, F. H. and G. Abbt-Braun (2009). Dissolved organic matter (DOM) in natural environments. Biophysico-Chemical Processes Involving Natural Nonliving Organic Matter in Environmental Systems. N. Senesi, Xing, B., Huang, P. M., John Wiley & Sons, Inc. **2:** 367-406.

Gaffney, J. S., Marley, N. A., Clark, S. B., Ed. (1996). Humic and Fulvic Acids, American Chemical Society.

Galloway, J., N. Raghuram, et al. (2008). "A perspective on reactive nitrogen in a global, Asian and Indian context " Current Science **94**(11): 1375-1381.

Gjessing, E. T., P. K. Egeberg, et al. (1999). "Natural organic matter in drinking water — The "NOM-typing project", background and basic characteristics of original water samples and NOM isolates." Environment International **25**(2–3): 145-159.

Haider, K. and A. Schäffer (2009). Soil biochemistry. Enfield, N.H., Science Publishers.

Hall, S. J. and P. A. Matson (1999). "Nitrogen oxide emissions after nitrogen additions in tropical forests." Nature **400**(6740): 152-155.

Harrell Jr., F. E. and a. w. c. f. m. o. users (2012). Hmisc: Harrell Miscellaneous.

Harris, D. C. (2007). Fundamentals of Spectrophotometry. Quantitative chemical analysis. New York, Freeman**:** 390-398.

Hayes, M. H. B. (2009). Evolution of Concepts of Environmental Natural Nonliving Organic Matter. Biophysico-Chemical Processes Involving Natural Nonliving Organic Matter in Environmental Systems. N. Senesi, Xing, B., Huang, P. M. , John Wiley & Sons, Inc.**:** 1-39.

Hayes, M. H. B. and R. S. Swift (1978). The Chemistry of soil organic colloids. The Chemistry of Soil Constituents. D. J. Greenland, and Hayes, M. H. B., John Wiley & Sons**:** 179-320.

Huang, P. M. and A. G. Hardie (2009). Formation Mechanisms of Humic Substances in the Environment. Biophysico-Chemical Processes Involving Natural Nonliving Organic Matter in Environmental Systems. N. Senesi, Xing, B., Huang, P. M., John Wiley & Sons, Inc.**:** 41-109.

Huffman, E. W. D., Stuber, H. A. (1985). Analytical Methodology for Elemental Analysis of Humic Substances. Humic Substances in Soil, Sediment, and Water. G. R. Aiken, McKnight, D. M., Wershaw, R. L., McCarthy, P. NY, Unitid States of America, John Wiley and Sons**:** 433-455.

Insam, H. (1996). Microorganisms and Humus in Soils. Humic Substances in Terrestrial Ecosystems. P. Alessandro. Amsterdam, Elsevier Science B.V.**:** 265-292.

IPCC (2001). IPCC Third Assessment Report - Climate Change 2001.

ISO-6874 (2004). Water quality - Determination of phosphorous - Ammonium molybdate spectrometric method.

ISO-7888 (1985). Water quality - Determination of electrical conductivity. International Organization for Standardization**:** 6.

ISO-8245 (1999). Water quality - Guidelines for the determination of total organic carbon (TOC) and dissolved organic carbon (DOC). International Organization for Standardization.

ISO-9963-1 (1994). Water quality - Determination of alkalinity - Part 1: Determination of total and composite alkalinity. International Organization for Standardization.

ISO-10304-1 (2007). Water quality - Determination of dissolved anions by liquid chromatography of ions - Part 1: Determination of bromide, Chloride, fluoride, nitrate, nitrite, phosphate and sulfate. International Organization for Standardization, International Organization for Standardization

ISO-10523 (2008). Water quality - Determination of pH. International Organization for Standardization.

ISO-22036 (2008). "Soil quality - Determination of trace elements in extracts of soil by inductively coupled plasma - atomic emission spectrometry (ICP-AES). International Organization for Standardization."

Jin, L., M. Shao, et al. (2006). "Estimation of dry deposition fluxes of major inorganic species by canopy throughfall approach." Chinese Science Bulletin **51**(15): 1818-1823.

Kalbitz, K., Schmerwitz, J., Schwesig, D., Matzner, E. (2003). "Biodegradation of soil-derived dissolved organic matter as related to its properties." Geoderma **113**(3–4): 273-291.

Kalbitz, K., S. Solinger, et al. (2000). "Controls on the dynamics of dissolved organic matter in soils: A review." Journal Name: Soil Science; Journal Volume: 165; Journal Issue: 4; Other Information: PBD: Apr 2000: Medium: X; Size: page(s) 277-304.

Kalff, J. (2002). Hydrology and Climate. Limnology: inland water ecosystems. Upper Saddle River, N.J., Prentice Hall**:** 53-71.

Kiikkilä, O., V. Kitunen, et al. (2011). "Properties of dissolved organic matter derived from silver birch and Norway spruce stands: Degradability combined with chemical characteristics." Soil Biology and Biochemistry **43(**2): 421-430.

Kogel-Knabner, I. and M. Kleber (2011). Mineralogical, Physicochemical, and Microbiological Controls on Soil Organic Matter. Handbook of Soil Sciences. P. M. Huang, Y. Li and M. E. Summer, CRC Press Inc**:** B302-B332.

Larssen, T., L. Duan, et al. (2011). "Deposition and Leaching of Sulfur, Nitrogen and Calcium in Four Forested Catchments in China: Implications for Acidification." Environmental Science & Technology **45**(4): 1192-1198.

Leeben, A., A. Heinsalu, et al. (2010). "High-resolution spectroscopic study of pore-water dissolved organic matter in Holocene sediments of Lake Peipsi (Estonia/Russia)." Hydrobiologia **646**(1): 21-31.

Leenheer, J. A. (1985). Fractionation Techniques for Aquatic Humic Substances. Humic Substances in Soil, Sediment and Water. G. R. Aiken, McKnight, D. M., Wershaw, R. L., McCarthy, P. NY, United Stated of America, John Wiley & Sons, Inc.**:** 409-429.

MacCarthy, P. (2001). The Principles of Humic Substances: An Introduction to the First Principle. Humic Substances: Structures, Models and Functions. E. A. Ghabbour and G. Davies. UK, The Royal Society of Chemistry 19-30.

Madigan, M. T., J. M. Martinko, et al. (2012). Brock biology of microorganisms. Boston, Mass., Pearson.

Maier, R. M. (2000). Bioavaliability and Its Importance to Bioremidation. Bioremidation. J. J. Valdes. The Netherlands, Kluwer Academic Publishers**:** 59-78.

Maier, R. M., I. L. Pepper, et al. (2009). Environmental microbiology. Amsterdam, Academic Press.

Marschner, B. and K. Kalbitz (2003). "Controls of bioavailability and biodegradability of dissolved organic matter in soils." Geoderma **113**(3–4): 211-235.

Martin-Neto, L., D. M. B. P. Milori, et al. (2009). EPR, FTIR, Raman, UV–Visible Absorption, and Fluorescence Spectroscopies in Studies of NOM. Biophysico-Chemical Processes Involving Natural Nonliving Organic Matter in Environmental Systems. N. Senesi, Xing, B., Huang, P. M. , John Wiley & Sons, Inc.**:** 651-727.

McGill, W. B., K. R. Cannon, et al. (1986). "Dynamics of soil microbial biomass and water-soluble organic C in Breton L after 50 years of cropping to two rotations " Canadian Journal of Soil Science **66**(1): 1-19.

Mobed, J. J., S. L. Hemmingsen, et al. (1996). "Fluorescence Characterization of IHSS Humic Substances: Total Luminescence Spectra with Absorbance Correction." Environmental Science & Technology **30**(10): 3061-3065.

Mounier, S., N. Patel, et al. (1999). "Fluorescence 3D de la matière organique dissoute du fleuve amazone: (Three-dimensional fluorescence of the dissolved organic carbon in the Amazon river)." Water Research **33**(6): 1523-1533.

NS-4743 (1993). Water analysis - Determination of total nitrogen after oxidation by peroxodisulphate. Norwegian Standard.

Ohno, T. (2002). "Fluorescence Inner-Filtering Correction for Determining the Humification Index of Dissolved Organic Matter." Environmental Science & Technology **36**(4): 742-746.

Oliver, B. G., E. M. Thurman, et al. (1983). "The contribution of humic substances to the acidity of colored natural waters." Geochimica et Cosmochimica Acta **47**(11): 2031-2035.

Paul, E. A. and F. E. Clark (1996). Soil microbiology and biochemistry. San Diego, Academic Press.

Pavia, D. L. (2009). Ultraviolet Spectroscopy. Introduction to Spectroscopy. Belmont, Calif., Brooks/Cole**:** 381-417.

Qualls, R. G. and B. L. Haines (1992). "Biodegradability of Dissolved Organic Matter in Forest Throughfall, Soil Solution, and Stream Water." Soil Sci. Soc. Am. J. **56**(2): 578-586.

R-Development-Core-Team (2012). R: A Language and Environment for Statistical Computing. Vienna, Austria, R Foundation for Statistical Computing.

Ross, S. (1989). Production of Soil Material through Organic Matter Decomposition. Soil processes: a systematic approach. London, Routledge**:** 39-74.

Saadi, I., M. Borisover, et al. (2006). "Monitoring of effluent DOM biodegradation using fluorescence, UV and DOC measurements." Chemosphere **63**(3): 530-539.

Schecher, W. D. and C. T. Driscoll (1987). "An evaluation of uncertainty associated with aluminum equilibrium calculations." Water Resour. Res. **23**(4): 525-534.
Schnabel, R. R., C. J. Dell, et al. (2002). "Filter, inoculum and time effects on measurements of biodegradable water soluble organic carbon in soil." Soil Biology and Biochemistry **34**(5): 737-739.
Schnitzer, M. and S. U. Khan (1972). Humic substances in the environment. New York, Dekker.
Senesi, N., T. Miano, et al. (1991). Fluorescence spectroscopy as a means of distinguishing fulvic and humic acids from dissolved and sedimentary aquatic sources and terrestrial sources Humic Substances in the Aquatic and Terrestrial Environment. B. Allard, H. Borén and A. Grimvall, Springer Berlin / Heidelberg. **33:** 63-73.
Serkiz, S. M. and E. M. Perdue (1990). "Isolation of dissolved organic matter from the suwannee river using reverse osmosis." Water Research **24**(7): 911-916.
Solheimslid, S. O. (2010). Denitrification and Nitrification Characteristics in a Nitrogen Saturated Subtropical Forest in Southwest China. M.Sc, Norwegian University of Life Sciences.
Steelink, C. (1985). Implications of Elemental Characteristics of Humic Substances. Humic Substances in Soil, Sediment, and Water G. R. Aiken, McKnight, D. M., Wershaw, R. L., McCarthy, P. NY, United States of America, John Wiley & Sons, Inc**:** 457-476.
Stevenson, F. J. (1982). Structural Basis of Humic Substances. Humus Chemistry: Genesis, Composition, Reactions, John Wiley & Sons, Inc.**:** 259.
Stevenson, F. J. (1994). Humus chemistry: genesis, composition, reactions. New York, Wiley.
Stevenson, J. F. (1985). Geochemistry of Soil Humic Substances. Humic substances in soil, sediment, and water. G. R. Aiken, McKnight, D. M., Wershaw, R. L., McCarthy, P. NY, United Stated of America, John Wiley & Sons, Inc.**:** 13-52.
Swift, R. S. (1985). Fractionation of Soil Humic Substances. Humic Substances in Soil, Sediment and Water. G. R. Aiken, McKnight, D. M., Wershaw, R. L., McCarthy, P. NY, United Stated of America, John Wiley & Sons, Inc.**:** 387-408.
Sørbotten, L. E. (2011). Hill slope unsaturated flowpaths and soil moisture variability in a forested catchment in Southwest China. Ms.C, The Norwegian University of Life Sciences.
Thurman, E. M. (1985). Organic geochemistry of natural waters. Dordrecht, Nijhoff.
Tipping, E., H. T. Corbishley, et al. (2009). "Quantification of natural DOM from UV absorption at two wavelengths." Environ. Chem. **6**(Copyright (C) 2012 American Chemical Society (ACS). All Rights Reserved.): 472-476.
Torn, M. S., C. W. Swantson, et al. (2009). Storage and Turnover of Organic Matter in Soil. Biophysico-Chamical Processes Involving Natural Nonliving Organic Matter in Environmen. N. Senesi, Xing, B., Huang, P. M. United States of America, John Wiley & Sons, Inc**:** 219-272.
van Spanning, R. J. M., D. J. Richardson, et al. (2007). Introduction to the Biochemistry and Molecular Biology of Denitrification. Biology of the Nitrogen Cycle. H. Bothe, S. J. Ferguson and W. E. Newton. The Netherlands, Elsevier**:** 1-3.
VanLoon, G. W. and S. J. Duffy (2005). Environmental chemistry: a global perspective. Oxford, Oxford University Press.
Vitousek, P. M., J. D. Aber, et al. (1997). "Human alteration of the global nitrogen cycle: Sources and Consequences." Ecological Applications **7**(3): 737-750.
Vogt, R. D. and E. T. Gjessing (2008). Correlation between Optical and Chemical properties of DNOM. International Meeting of the International Humic Substances Society,

Moscow-Saint Petersburg, Russia, Department of Chemistry, Lomonosov Moscow State University, Russia.
Vogt, R. D., E. T. Gjessing, et al. (2001). Natural organic matter in the nordic countries, Nordtest Report **TR 479**.
Vogt, R. D., S. B. Ranneklev, et al. (1994). "The impact of acid treatment on soilwater chemistry at the HUMEX site." Environment International **20**(3): 277-286.
Weishaar, J. L., G. R. Aiken, et al. (2003). "Evaluation of Specific Ultraviolet Absorbance as an Indicator of the Chemical Composition and Reactivity of Dissolved Organic Carbon." Environmental Science & Technology **37**(20): 4702-4708.
Wetzel, R. G. (2001). Detrius: Organic Carbon Cycling and Ecosystem Metabolism. Limnology: lake and river ecosystems. San Diego, Academic Press**:** 731-783.
Wolters, V. (2000). "Invertebrate control of soil organic matter stability." Biology and Fertility of Soils **31**(1): 1-19.
Young, K. C., K. M. Docherty, et al. (2005). "Degradation of surface-water dissolved organic matter: influences of DOM chemical characteristics and microbial populations." Hydrobiologia **539**(1): 1-11.
Zech, W., G. Guggenberger, et al. (1996). Organic Matter Dynamics in Forest Soils of Temperate and Tropical Ecosystems. Humic Substances in Terrestrial Ecosystems. P. Alessandro. Amsterdam, Elsevier Science B.V.**:** 101-170.
Zsolnay, A. (1996). Dissolved Humus in Soil Waters. Humic Substances in Terrestrial Ecosystems. P. Alessandro. Amsterdam, Elsevier Science B.V.**:** 171-223.

7. Appendix

List of Appendixes

Appendix A. Instrumentation and Calibration

A-1 IC

Calibration solutions were prepared by dissolving the following mineral salts in Type 1 water NaF, NaCl, $NaNO_3$, Na_2SO_4, KH_2PO_4 (dried at 100˚C in ≥ 2h, cooled in hexicator), to final concentrations of 0, 1, 10, 20, 40, and 50 mg NO_3^-, SO_4^{2-}, and Cl^- L^-, and 0, 0.1, 0.3, 0.5, and 0.7 mg F^{-1} L^{-1}.

Table 1: Instrumental settings applied for the IC.

Parameter	Setting
Flow rate	1.0 mL min^{-1}
Temperature	30˚C
Applied current	5mA
Injection volume	5µL
Eluent/ Storage Solution	Methanesulfonic acid (KOH)
No. Replicate	3

Table 2: Values for the inclement (y) and the strength (r^2) of the calibration solutions prepared for the determination of the major anions (fluoride, chloride, sulphate, and nitrate) from the total of five runs using the IC.

	Fluoride (F^-)		Chloride (Cl^-)		Sulphate (SO_4^{2-})		Nitrate (NO_3^-)	
Run	y	R^2	y	R^2	y	R^2	y	R^2
1	1x	0.9988	1x	0.9999	1x	0.9999	1x	0.9998
2	1x	0.9998	1x	0.9998	1x	0.9993	1x	0.9997
3	1x	0.9974	1x	0.9999	1x	0.9997	1x	0.9997
4	1x	0.9983	1x	0.9999	1x	0.9998	0.9914x	0.9996
5	1x	0.9975	1x	0.9999	1x	0.9998	1x	0.9998

Table 3: Limit of Detection (LOD) determined as 3x St.dev. of 11 subsequent measurements of blank sample (type 1 water) using the IC.

Anion	Fluoride (F^-)	Chloride (Cl^-)	Sulphate (SO_4^{2-})	Nitrate (NO_3^-)
LOD (mg L^{-1})	0.0064	0.014	0.021	0.051

A-2 ICP-OES

Table 4: Concentration (mg L^{-1}) range of the four cations (calcium, potassium, magnesium, and sodium) in the calibration solution prepared for the analysis with the ICP-OES.

Analyte	Std 1	Std 2	Std 3	Std 4	Std 5	Std 6
Ca	1.0	2.0	5.0	10.0	25.0	60.0
K	0.5	1.0	2.5	5.0	10.0	20.0
Mg	0.5	1.0	2.5	5.0	10.0	20.0
Na	1.0	2.0	5.0	10.0	20.0	40.0

Table 5: Instrumental settings applied for the ICP-OES

Parameter	Setting
RF Power	0.95kW
Plasma Ar Flow	15.0 L min^{-1}
Auxillary Ar Flow	1.50 L min^{-1}
Nebulizer Ar Flow	1.00 L min^{-1}
Read time	1.00s
Rinse time	45s
Sample update delay	60s
Rump rate	20rpm

Table 6: Wavelength selection for the determination of the major cations (calcium, potassium, magnesium, and sodium) using the ICP-OES. Wavelengths were selected based on the concentration of the analytes, weather it was low ~3 mg L^{-1} of medium ~10 mg L^{-1}.

Analyte	Low	Medium
Ca	393.366	422.673
K	766.491	769.897
Mg	280.270	285.213
Na	588.995	589.592

A-3 TOC-analyzer

Calibration solutions prepared from potassium hydrogen phtalate ($HOOCC_6H_4COOK$), dried for 1h at 110˚C, and dissolved in Type 1 water. The calibration solution covered the following range in concentrations; 0, 5, 10, 50, and 20 mg C L^{-1}. All glass equipment was baked at 500˚C.

The Limit of detection (LOD) of the TOC-analyzer was determined to 0.80 mg C L^{-1}. This was calculated from 3x st.dev. of 10 repeated measurements of blank sample (Type 1 water).

Table 7: Instrumental settings applied for the TOC-analyzer.

Parameter	Setting
Pressure	5bar (500kPa)
Flow rate	150 mL min^{-1}
No. Of injections	3
Max. No. injections	5
Min no. injections	3
No. Of washes	4
Sparge time	1min
Type of catalyst	P/N 638-92069-01

Table 8: Values for the inclement (y) and the strength (r^2) of the calibration solutions prepared for the analyses using the TOC-analyzer. Values are obtained for analysis of the calibration solution after end sample-analysis.

Run	y	R^2
1	1.0041x	0.9981
2	0.998x	0.9947
3	0.8856x	0.9921

A-4 Aluminium fractionation

Calibration solutions were prepared by dissolving $KAl(SO_4)_2$ in Type 1 water to the following concentrations of; 0, 40, 100, 200, 400, 600, 800µg Al L^{-1}.

Table 91: Values for the inclement (y) and the strength (r^2) of the calibration solutions prepared for the aluminium fractionation.

y	R^2
0.9972x	0.9939

A-5 ICP-MS

Table 10: Instrumental settings applied for the ICP-MS (Timing parameters)

Parameter	Setting
Sweeps/Reading	15
Reading/Replicate	1
Number of replicates	2
QC Enabled	yes

Table 11: Instrumental settings applied for the ICP-MS

Analyte	Mass	Scan Mode	Internal Standard	Dwell Time	Mode	Gas A	Gas B	RPq	RPa
Al	26.982	Peak hopping	In	80.0ms	KED	0.0	0.0	0.25	0.000
Fe	55.935	Peak hopping	In	80.0ms	DRC	0.5	0.0	0.85	0.000
Si	27.977	Peak hopping	In	80.0ms	KED	0.0	3.0	0.25	0.000
Mn	54.938	Peak hopping	In	80.0ms	DRC	0.5	0.0	0.75	0.000
Zn	63.929	Peak hopping	In	80.0ms	KED	0.0	3.0	0.25	0.000

Table 12: Instrumental settings applied for the ICP-MS (Signal processing)

Parameter	Setting
Detector Mode	Dual
Measurement Units	Cps
AutoLens:	On
Spectral Peak processing	Average
Signal Profile Processing	Average
Blank Substraction	Substracted after internal standard
Baseline Readings	0
Smoothing	Yes, Factor 5

A-6 Infra Red Gas Analyzer (IRGA)

Calibration solutions were prepared by dissolving sodium carbonate (Na_2CO_3) (dried >12h at 60°c) in 1 M sodium hydroxide (NaOH) to the following concentrations: 0, 100, 200, 500, 1000, and 2000 mg CO_2 L^{-1}.

The IRGA presents the CO_2-concentrations as ppm (mol) gas. The ideal gas law (Pv = nRT) was used to convert the results into values with the denomination of mg m^{-3}. The results were further converted into mg CO_2 L^{-1} (aq) by the values of constant flow for the argon gas (0.5 L min^{-1}) and the peristaltic pump (0.8 mL min^{-1}).

Table 13: Instrumental settings applied for the IRGA detector.

Parameter	Setting
Cell temperature (˚C)	51.3
Cell pressure (kPa)	100
Flow of Argon gas (L min^{-1})	0.50
Pump flow (ml min^{-1})	0.8

Table 142: Values for the inclement (y) and the strength (r^2) of the calibration solutions prepared for the determination of CO_2 using the IRGA detector. Values are presented for the analysis both prior and post to the sample analysis at the four days of analysis during the biodegradation experiment.

	Prior		Post	
Run	y	R^2	y	R^2
Day 10	1.1044x	0.9999		
Day 20	1.1050x	0.9999	1.1522x	0.9987
Day 30	0.9984x	0.9999	0.9227x	0.9999
Day 45	0.9963x	0.9999	0.9581x	0.9997

Appendix B. Raw data

B-1 Biodegradation experiment

Table 15: Readout data for measured concentration of CO_2 (mg L^{-1}) in the two different types of blank samples, with and without inoculum, as well as for the three replicates of glucose control from the four days of analysis (Day 10, 20, 30, and 45) in the biodegradation experiment.

	Replicate	Day 10	Day 20	Day 30	Day 45
Blank	1	184	182	267	212
	2	139	126	200	213
	3	166	278	244	304
	4	210	215	159	299
Inoculu-containing Blank	1	225	245	213	451
	2	166	204	149	252
	3	143	204	240	253
	4	170	278	240	116
	5	128	220	252	279
	6	173	354	225	225
	7	169	312	402	242
	8	173	267	163	337
	9	159	159	193	257
Glucose	1	285	2293	688	422
	2	312	2157	427	159
	3	236	2373	568	426

Table 16: Readout data for concentration of CO_2 (mg L^{-1}) for the soil-water samples from TSP measured at the four days of analysis in the biodegradation experiment (day 10, 20, 30, and 45).

Sample	Replicate	Day 10	Day 20	Day 30	Day 45
HS-1	1		361	389	345
	2	439	367	285	402
	3	450	462	300	487
HS-2	1	455	386	312	328
	2	480	380	423	619
	3	502	354	467	398
HS-3	1	530	307	431	300
	2	541	406	265	437
	3	457	494	268	175
HS-B1	1	445	445	236	351
	2	658	216	358	293
	3	465	377	395	316
HS-B2	1	511	272	361	824
	2	499	241	324	544
	3	443	469	359	546

GDZ-1	1	833	431	343	266
	2	897	450	370	227
	3	849	507	123	904
GDZ-2	1	557	157	372	278
	2	563	451	318	422
	3	586	430		358
GDZ-3	1	668	403	269	277
	2	823	381	386	361
	3	748	411	430	450
GDZ-4	1	1095	369	362	355
	2	975	443	413	456
	3	930	392	415	415
GDZ-B1	1	727	375	288	354
	2	752	325	334	277
	3	795	419	384	94
HDZ-B2	1	815	369	480	302
	2	746	296	478	568
	3	840	409	313	291

Table 17: Readout data for concentration of CO_2 (mg L^{-1}) for the reference samples originating from the "NOM-typing" project measured at the four days of analysis in the biodegradation experiment (day 10, 20, 30, and 45). Note that the samples re-dissolved to two additional concentrations are included and denoted by min (minimum concentration) and max (maximum concentration).

Sample	Replicate	Day 10	Day 20	Day 30	Day 45
Tre min	1	274	266	286	501
	2	297	357	334	492
	3	277	275	258	174
Tre	1	374	270	279	296
	2	390	357	260	453
	3	353	212	311	422
Tre max	1	388	352		659
	2	511	333	344	431
	3	273	352	314	529
Hem	1	622	436	390	735
	2	522	615	411	1018
	3	544	469	415	620
Aur	1	340	311	313	262
	2	309	288	298	338
	3	295	327	247	285
Mar min	1	236	256	55	100
	2	219	307	293	366
	3	228	265	230	715

Mar	1	455	174	203	178
	2	397	246	48	111
	3	506	286	347	380
Mar max	1	342	341	326	325
	2	325	347	328	440
	3	395	317	287	339
Bir	1	517	353	75	75
	2	527	402	358	348
	3	400	430	354	197
Hum	1	503	513	421	443
	2	506	496	392	454
	3	529	467	321	330
Gjl	1	454	270	426	326
	2	345	368	456	287
	3	358	390	274	123
Gju	1	505	326	304	321
	2	440	313	345	285
	3	404	334	351	432
Heo	1	429	389	376	397
	2	562	399	317	510
	3	486	428	371	252

Table 18: Readout data for concentration of CO_2 (mg L^{-1}) for the reference samples originating from the "NOMiNiC" project measured at the four days of analysis in the biodegradation experiment (day 10, 20, 30, and 45). Note that the samples re-dissolved to two additional concentrations are included and denoted by min (minimum concentration) and max (maximum concentration).

Sample	Replicate	Day 10	Day 20	Day 30	Day 45
Bir-F	1	422	494	311	132
	2	411	370	294	260
	3	394	330	210	139
Bir-S	1	526	365	268	130
	2	497	298	305	298
	3	606	361	367	344
Val K-F	1	409	393	368	457
	2	522	397	293	400
	3	378	111	84	153
Val K-S	1	382	304	224	258
	2	380	367	318	310
	3	473	384	458	355
Hie-F min	1	230	480	233	579
	2	146	298	245	354
	3	273	318	243	121

Hie F	1	449	449	305	373
	2	395	475	317	342
	3	382	377	300	335
Hie-F max	1	432	597	384	340
	2	440	357	378	409
	3	494	343	215	197
Hie-S	1	410	330	284	307
	2	121	81	80	159
	3	410	320	212	409
Svart-F	1	313	470	370	334
	2	338	357	435	255
	3	351	416	378	340
Svart-S	1	460	369	413	513
	2	581	420	86	222
	3	542	359	298	219
Skj-F	1	476	419	410	412
	2	514	420		382
	3	541	363	380	60
Skj-S	1	376	294	63	61
	2	450	410	272	319
	3	395	308	60	145

Appendix C. Results obtained prior to the biodegradation experiment

C-1 Soil-water samples from Tie Shan Ping (TSP)

Table 193: Complete results for the characterization parameters (water characterization, and UV-Vis abs) obtained for the soil-water samples from TSP

Sample	HS-1	HS-2	HS-3	HS-B1	HS-B2	GDZ-1	GDZ-2	GDZ-3	GDZ-4	GDZ-B1	GDZ-B2
pH	3.63	3.66	3.74	3.83	3.90	4.28	4.26	4.92	4.74	4.77	4.90
Conductivity (µS/cm)	454.00	385.00	222.00	358.00	211.00	142.40	146.10	107.70	122.10	121.60	114.50
Temperature (°C)	22.3	21.3	21.4	21.4	21.3	21.2	21.2	21.2	21.3	21.2	21.3
Alkalinity (mmol/L)								0.041	0.021	0.031	0.033
Ala (ug/L)	18069.4	14935.2	7640.4	17404.5	9136.4	1576.1	1765.3	766.6	542.8	782.1	681.5
Ali (ug/L)	17483.5	14362.5	7352.1	16802.5	8838.9	1491	1693.5	741.2	526.3	744.5	663.5
Alo (ug/L)	585.9	572.6	288.3	602	297.5	85.1	71.4	25.3	16.5	37.6	17.9
F (mg/L)	1.1	0.8	0.5	0.7	0.7	0.3	0.4	0.1	0.0	0.2	0.1
Cl (mg / L)	4.3	7.1	1.3	4.1	1.5	2.6	2.7	1.0	1.1	2.6	2.3
SO4 (mg /L)	97.7	98.0	61.5	85.6	64.2	30.9	39.0	45.6	52.1	29.8	42.4
NO3 (mg /L)	132.8	83.4	30.4	104.2	35.4	33.6	27.2	0.0	0.0	25.8	6.1
Ca (mg /L)	30.4	20.8	10.6	21.3	10.4	11.4	12.2	9.9	6.8	11.1	9.3
Mg (mg /L)	3.6	4.0	1.9	2.6	2.3	4.4	4.6	3.7	2.6	4.3	3.6
K (mg /L)	5.8	5.5	1.4	3.7	0.9	0.3	0.6	0.1	0.6	0.3	0.6
Na (mg /L)	0.6	0.9	0.4	0.6	0.6	1.2	1.3	1.2	1.4	1.2	1.7
TOC (mg /L)	15.53	12.37	8.44	6.11	3.69	0.65	1.13	1.40	1.26	0.82	1.23
Tot-N (mg /L)	31.8	19.6	10.05	24.3	8.05	7.6	6.1	0.09	0.5	5.9	1.66
Tot-P (ug/L)	6.6	7.0	6.8	9.4	8.7	7.0	2.2	1.8	1.6	2.1	1.7
PO4 (ug P /L)	0.7	0.9	0.7	1.1	1.1	0.5	1.0	1.2	1.3	0.9	1.3
Al (ug /L)	165552	14954.6	7752.7	16729.2	8851.8	1384.6	1545.8	379.8	350.7	765.6	372.1
Fe (ug /L)	254.4	105.1	201.9	0	21.7	0	166	175.7	9466.1	181.5	2178
Si (ug /L)	0	0	0	0	0	0	0	0	0	0	0
Mn (ug /L)	2567.2	583.3	796	1562.5	1318.5	647.1	877	1740.6	1152.1	747.9	1223.7
Zn (ug /L)	409.8	636.5	562	357.7	189.1	103.9	264.8	206.4	237	238.9	208.2
Abs 254nm	0.474	0.345	0.259	0.125	0.063	0.021	0.024	0.026	0.021	0.018	0.015
Abs 400nm	0.035	0.022	0.020	0.007	0.004	0.002	0.002	0.002	0.003	0.002	0.001
Abs 600nm	0.002	0.001	0.002	0.001	0.001	0.000	0.001	0.000	0.003	0.001	0.001
sUVa	3.05	2.79	3.07	2.05	1.70	3.16	2.15	1.86	1.68	2.14	1.23
sVISa	2.27	1.76	2.34	1.12	1.17	2.66	1.62	1.24	2.49	1.88	1.17
SAR	13.5	15.8	13.1	18.4	14.5	11.8	13.3	15.0	6.7	11.4	10.5

C-2 Reference samples

Table 20: Complete results for the characterization parameters (water characterization, and UV-Vis abs) obtained for the reference samples originating from the "NOM-typing" project

Sample	Tre min	Tre	Tre max	Hem	Aur	Mar min	Mar	Mar max	Bir	Hum	Gjl	Gju	Heo
pH	6.15	6.76	6.81	6.06	6.80	5.77	6.16	6.09	4.92	5.30	5.31	4.89	4.59
Conductivity (µS/cm)	17.44	33.60	63.4	20.50	33.20	21.4	40.60	80.2	43.70	26.90	30.50	30.00	23.20
Temperature (°C)	21.3	22.1	21	21.3	21.6	21.3	20.9	21.5	21.5	21.7	21.8	21.6	21.4
Alkalinity (mmol/L)		0.146		0.082	0.114		0.058		0.022	0.049	0.042	0.037	0.009
Ala (ug/L)									83.1	78.9	412.3	91.3	117.2
Ali (ug/L)									46.7	19.4	67.7	25.7	46.3
Alo (ug/L)									36.4	59.5	344.6	65.6	71
F (mg/L)	0.0	0.1	0.1	0.0	0.1	0.0	0.1	0.2	0.0	0.0	0.1	0.0	0.0
Cl (mg/L)	0.8	1.8	3.5	1.2	1.8	1.7	3.5	7.0	5.0	4.5	2.5	2.2	0.8
SO4 (mg/L)	2.2	4.9	9.6	2.2	5.3	3.9	8.0	15.8	7.3	1.4	6.1	5.7	2.6
NO3 (mg/L)	0.0	0.4	0.9	0.2	0.7	0.5	1.5	3.0	0.6	0.0	0.3	0.1	0.1
Ca (mg/L)	0.9	1.0	2.1	1.8	0.3	0.1	0.1	0.4	0.0	0.4	0.1	0.0	0.0
Mg (mg/L)	0.2	0.4	0.8	0.3	0.1	0.0	0.1	0.2	0.0	0.0	0.1	0.0	0.0
K (mg/L)	0.3	0.7	1.3	0.3	0.4	0.2	0.4	0.8	0.1	0.3	0.2	0.1	0.0
Na (mg/L)	2.6	5.2	9.8	1.8	6.1	4.0	7.8	14.6	7.2	4.7	5.2	5.0	2.8
TOC (mg/L)	2.6	8.64	14.4	12.29	8.22	1.5	6.21	10.5	6.42	12.60	8.07	9.95	13.23
Tot-N (mg/L)	0.18	0.34	0.66	0.43	0.41	0.88	0.57	1.2	0.32	0.25	0.33	0.29	0.23
Tot-P (ug/L)		2.5		1.1	1.6		1.9		1.7	1.4	2.3	1.3	1.6
PO4 (ug P/L)		1.1		1.0	1.1		0.9		1.2	1.2	1.3	1.1	0.9
Al (ug/L)	42.6	70.4	200	322.9	52.4	21.6	15.9	64.7	146.5	177.1	195.8	191.6	257.1
Fe (ug/L)	13.6	34.4	105.4	234	66.8	22.6	53.6	149	77.7	178.9	143.5	181.6	207.6
Si (ug/L)	478.3	1140.2	2144.9	1305.2	987.3	21.9	168.3	292.7	290.3	534.8	420.2	1199.5	1169
Mn (ug/L)	2.9	23.8	81.3	3.4	5.6	0	0	36.5	0	0	0	0	0
Zn (ug/L)	13.6	15.7	54.8	69.4	15.2	7	7.6	49.3	11.4	6.3	4.3	4	5.5
Abs 254nm		0.3187		0.5553	0.3035		0.1728		0.2236	0.5346	0.3192	0.4006	0.5289
Abs 400nm		0.0338		0.0733	0.0321		0.0154		0.0226	0.075	0.0367	0.0479	0.0622
Abs 600nm		0.0031		0.0065	0.0037		0.0018		0.0015	0.0114	0.0039	0.0048	0.0061
sUVa		3.7		4.5	3.7		2.8		3.5	4.2	4.0	4.0	4.0
sVISa		3.9		6.0	3.9		2.5		3.5	6.0	4.5	4.8	4.7
SAR		9.4		7.6	9.5		11.2		9.9	7.1	8.7	8.4	8.5

Table 21: Complete results for the characterization parameters (water characterization, and UV-Vis abs) obtained for the reference samples originating from the "NOMiNiC" project

Sample	Bir-F	Bir-S	Val K-F	Val K-S	Hie-F min	Hie-F	Hie-F max	Hie-S	Svart-F	Svart-S	Skj-F	Skj-S
pH	4.73	4.99	5.30	5.50	6.28	6.25	6.82	6.71	6.22	4.97	5.36	4.90
Conductivity (µS/cm)	33.20	41.20	28.40	28.60	9.54	18.05	34.4	21.40	20.30	18.38	21.20	34.10
Temperature (°C)	21.5	21.6	21.8	21.6	21.1	21.6	21.1	21.8	21.6	21.6	21.6	21.7
Alkalinity (mmol/L)	0.020	0.032	0.047	0.050		0.096		0.120	0.068	0.029	0.052	0.029
Ala (ug/L)	100	68.3	29.4	22						70	91.3	77.9
Ali (ug/L)	34	24.3	5.7	5.2						24.5	20.8	20.4
Alo (ug/L)	66	44	23.7	16.8						45.5	70.5	57.5
F (mg/L)	0.000	0.021	0.029	0.024	0.0	0.044	0.1	0.055	0.087	0.014	0.006	0.011
Cl (mg/L)	3.731	6.800	1.386	1.141	0.2	0.472	1.0	0.626	0.690	0.313	3.275	6.776
SO4 (mg/L)	4.641	4.825	6.434	6.729	1.0	1.819	3.6	2.365	4.037	2.730	0.797	1.343
NO3 (mg/L)	0.252	0.500	0.138	0.000	0.0	0.089	0.0	0.023	0.134	0.028	0.028	0.043
Ca (mg/L)	0.000	0.183	0.088	0.128	0.1	0.145	0.4	0.062	0.185	0.111	0.542	0.080
Mg (mg/L)	0.007	0.057	0.004	0.014	0.0	0.000	0.0	0.000	0.034	0.007	0.013	0.000
K (mg/L)	0.081	0.022	0.080	0.017	0.0	0.060	0.2	0.056	0.127	0.000	0.011	0.064
Na (mg/L)	5.244	6.954	5.366	5.296	2.3	3.794	7.3	4.672	3.905	2.635	3.455	5.559
TOC (mg/L)	8.25	6.42	10.46	10.54	4.0	11.10	20.5	10.11	6.82	13.12	13.05	11.77
Tot-N (mg/L)	0.26	0.29	0.35	0.27	0.11	0.18	0.46	0.24	0.17	0.2	0.22	1
Tot-P (ug/L)	1.8	1.6	1.1	2.8		1.5		6.0	7.9	6.0	7.1	6.2
PO4 (ug P/L)	0.9	1.0	1.2	1.3		1.1		0.7	1.0	0.8	1.0	0.8
Al (ug/L)	201.1	143.9	66.5	76.2	20.3	15.1	59.5	36.6	15.1	163.8	221	186
Fe (ug/L)	256.8	132.6	231.2	178	83.8	167.5	374.7	58.5	214.3	338.1	252.6	138.7
Si (ug/L)	953.6	396.2	560.7	517.1	231.2	541.4	2027.8	2581.7	579.5	1590.5	555.2	523.8
Mn (ug/L)	0	0.1	0	0	0	0	41.2	0	0	0	0	0
Zn (ug/L)	3.3	5.7	6.9	10.6	7.3	9.8	49.2	8.3	9.5	9.2	6.9	14.6
Abs 254nm	0.3311	0.2104	0.4509	0.4116		0.4		0.3558	0.316	0.5897	0.5795	0.5061
Abs 400nm	0.0351	0.0223	0.0551	0.0497		0.0491		0.0415	0.0424	0.0777	0.0819	0.0694
Abs 600nm	0.0041	0.0032	0.0084	0.0068		0.0097		0.0044	0.0062	0.0096	0.0108	0.0086
sUVa	4.0	3.3	4.3	3.9		3.6		3.5	4.6	4.5	4.4	4.3
sVISa	4.3	3.5	5.3	4.7		4.4		4.1	6.2	5.9	6.3	5.9
SAR	9.4	9.4	8.2	8.3		8.1		8.6	7.5	7.6	7.1	7.3

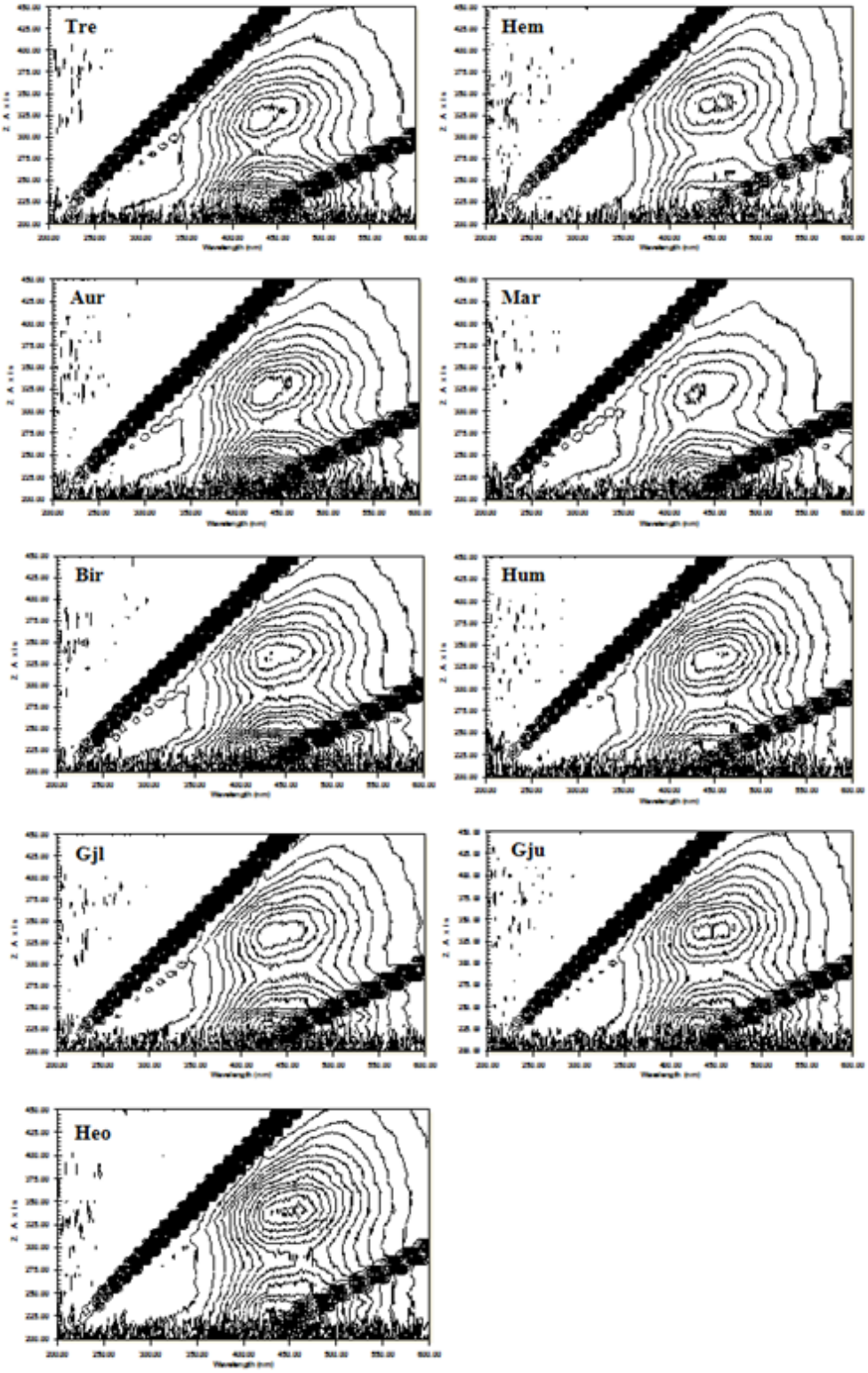

Figure 1: Fluorescence Emission-Excitation Matrix (EEM) spectra obtained for the reference samples originating from the "NOM-typing" project. Intensity maximum (I_{max}) set to 100.

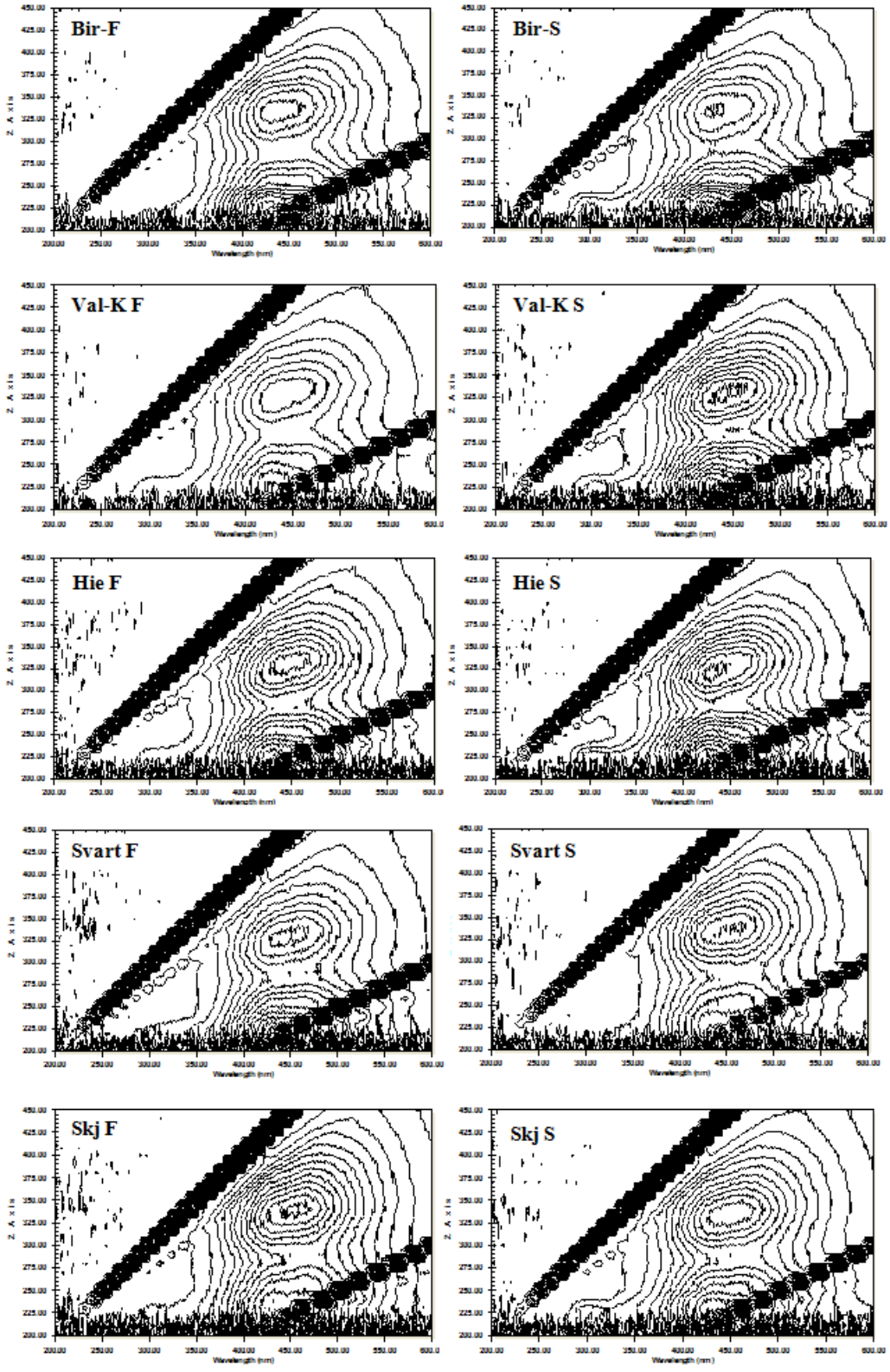

Figure 2: Fluorescence Emission-Excitation Matrix (EEM) spectra obtained for the reference samples originating from the "NOM-typing" project. Intensity maximum (I_{max}) set to 100.

Table 22: Location ($\lambda_{ex}/\lambda_{em}$) of peak A and B, absolute and relative intensity of these two peaks for the reference samples.

	Peak A				Peak B			
Sample	λ_{ex}	λ_{em}	Intensity (I)	Std. I (I/DOC)	λ_{ex}	λ_{em}	Intensity (I)	Std. I (I/DOC)
Tre	320	430	29	3.4	232	422	49	5.7
Hem	340	454	27	2.2	235	425	28	2.3
Aur	327	430	28	3.5	237	427	49	6.0
Mar	322	424	18	2.9	231	424	36	5.7
Bir	333	428	24	3.8	231	425	44	6.8
Hum	344	460	27	2.1	237	429	30	2.4
Gjl	336	432	25	3.0	234	428	37	4.6
Gju	339	438	27	2.7	238	424	35	3.5
Heo	341	444	30	2.3	238	436	29	2.2
Bir-F	330	438	29	3.5	232	423	43	5.2
Bir-S	336	432	23	3.6	235	432	41	6.4
Val K-F	333	439	29	2.8	236	432	37	3.5
Val K-S	333	445	30	2.9	234	427	41	3.9
Hie-F	339	445	26	2.3	231	425	31	2.8
Hie-S	327	432	28	2.8	232	421	38	3.8
Svart-F	333	447	21	3.1	235	426	30	4.4
Svart-S	343	459	31	2.4	237	432	26	2.0
Skj-F	342	454	28	2.2	244	433	25	1.9
Skj-S	339	447	29	2.5	233	430	32	2.7

Appendix D: The biodegradation experiment

D-1 Blank Samples

Table 234: Contribution of CO_2 (mg C) from the two types of blank samples included in the biodegradation experiment during the four days of analysis (day 10, 20, 30, and 45). B 1-4 = Blank without inoculum, BI 1-9 = with inoculum. Values from the latter type only, were used to subtract from the sample values. Possible outliers marked.

Sample	Day 10	Day 20	Day 30	Day 45
B 1	0.151	0.149	0.219	0.174
B 2	0.114	0.103	0.164	0.174
B 3	0.136	0.228	0.2	0.249
B 4	0.172	0.176	0.13	0.245
BI 1	0.184	0.201	0.174	0.369
BI 2	0.136	0.167	0.122	0.206
BI 3	0.117	0.167	0.197	0.207
BI 4	0.139	0.228	0.197	0.095
BI 5	0.105	0.18	0.206	0.228
BI 6	0.142	0.29	0.184	0.184
BI 7	0.138	0.256	0.329	0.198
BI 8	0.142	0.219	0.134	0.276
BI 9	0.13	0.13	0.158	0.21
Average	0.131	0.204	0.172	0.206
St.Dev	0.013	0.050	0.031	0.014

D-2 Basis for exclusion of data from the biodegradation experiment

In the following section the grounds for exclusion of data from the biodegradation experiment, largely based on increase in pH resulting from NaOH contamination in the sample solution.

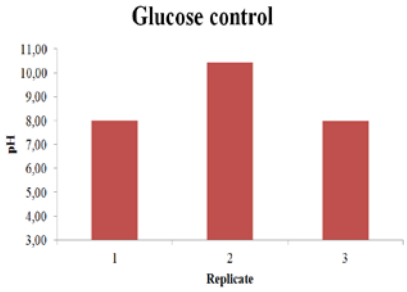

Figure 3: pH measured post to the biodegradation experiment for the three replicates of the glucose control solution.

Table 24: Results for glucose control solutions.

Replicate	Day 10	Day 20	Day 30	Day 45
1	0,102	1,673	0,392	0,140
2	0,124	1,562	0,178*	-0,076*
3	0,062	1,739	0,294	0,143

*Data excluded based on correlation between peak in pH and negative result for CO_2

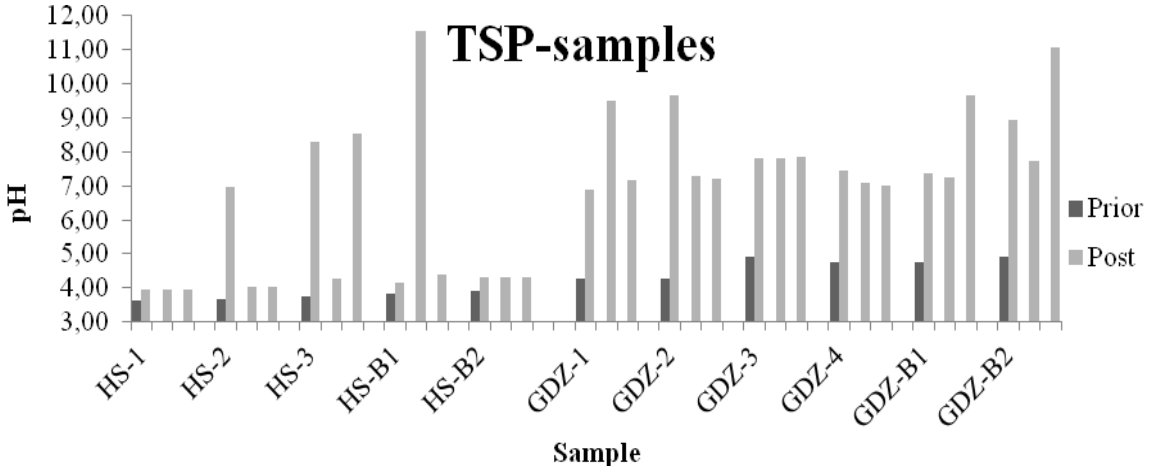

Figure 4: Values for pH measurements performed on the samples originating from the Hill Slope (HS) and the Groundwater Discharge Zone (GDZ) prior and post to the biodegradation experiment.

Table 255: Total amount of CO_2 (mg C) measured for the soil-water samples originating from the Hill Slope (HS) and the Groundwater Discharge Zone (GDZ) from the four days of analysis (day 10, 20, 30, and 45). Values excluded based findings indication NaOH contamination in the samples solution (*), contamination of samples solution in the NaOH (**) or for samples lost during transportation to UMB (***).

Sample	Replicate	Day 10	Day 20	Day 30	Day 45
HS-1	1	***	0.0915	0.147	0.0767
	2	0.228	0.0965	0.0619	0.123
	3	0.237	0.174	0.0742	0.193
HS-2	1	0.241	0.0473*	0.0840*	0.0628*
	2	0.262	0.128	0.175	0.301
	3	0.28	0.200	0.211	0.120
HS-3	1	0.303	0.0473	0.181	0.0399*
	2	0.312	0.128	0.0455**	0.152
	3	0.243	0.200	0.0480**	-0.0625*
HS-B1	1	0.233	0.160	0.122	0.0816
	2	0.408	-0.0272*	0.0218*	0.0342*
	3	0.250	0.105	0.152	0.0530
HS-B2	1	0.287	0.0187	0.124	0.469
	2	0.277	0.000	0.0939	0.240
	3	0.232	0.180	0.123	0.241
GDZ-1	1	0.551	0.149	0.109	0.012
	2	0.603	0.164	0.132	-0.0199*
	3	0.564	0.211	***	0.534
GDZ-2	1	0.325	-0.0755*	-0.0707*	0.0219*
	2	0.330	0.165	0.133	0.140
	3	0.349	0.148	0.0889	0.0874
GDZ-3	1	0.416	0.126	0.0488	0.0211
	2	0.543	0.108	0.145	0.0898
	3	0.481	0.132	0.181	0.163
GDZ-4	1	0.765	0.098	0.125	0.0849
	2	0.667	0.159	0.167	0.168
	3	0.630	0.117	0.168	0.134
GDZ-B1	1	0.464	0.103	0.0644	0.0841
	2	0.485	0.0621	0.102	0.0211
	3	0.520	0.139	0.143	-0.129*
GDZ-B2	1	0.536	0.0981	0.222	0.0415
	2	0.480	0.0383	0.220	0.259
	3	0.557	0.131	0.0848	0.0325

*Data excluded based on correlation between peak in pH and negative result for CO_2
**Data excluded based on observation of > 3ml NaOH at the day of analysis
***Sample lost through transportation to UMB

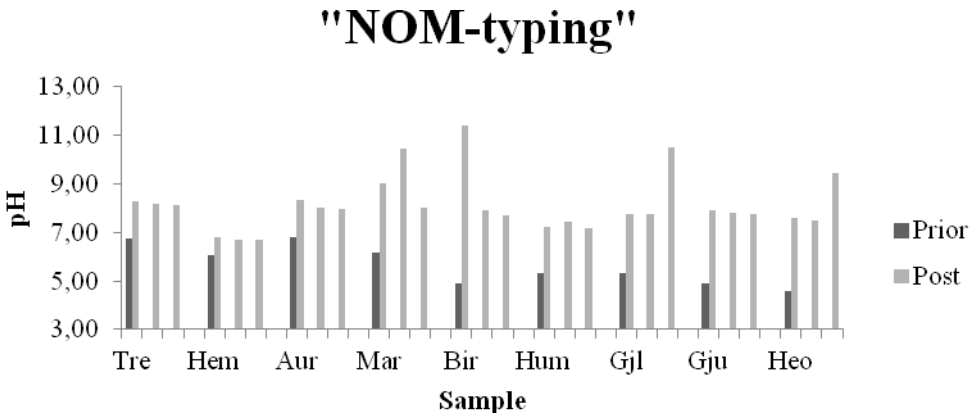

Figure 5: pH measurements performed prior (blue) and post (post) to the biodegradation experiment for the reference samples originating from the "NOM-typing" project.

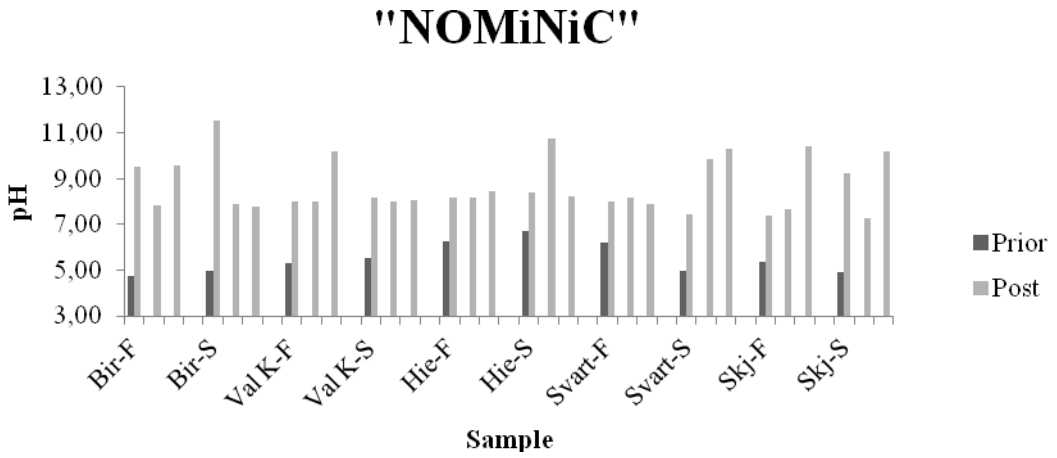

Figure 6: Measurements of pH conducted prior (blue) and post (red) to the biodegradation experiment for the reference samples from the "NOMiNiC" project.

Table 26: Total amount of CO_2 (mg C) measured for reference samples originating from the "NOM-typing" project from the four days of analysis (day 10, 20, 30, and 45). Values excluded based findings indication NaOH contamination in the samples solution (*), contamination of samples solution in the NaOH (**) or for samples lost during transportation to UMB (***).

Sample	Replicate	Day 10	Day 20	Day 30	Day 45
Trehørningen (Tre)	**1**	0.217	0.047	0.088	0.069
	2	0.232	0.128	0.070	0.215
	3	0.197	-0.00672**	0.118	0.186
Hellerudmyra (Hem)	**1**	0.447	0.201	0.191	0.477
	2	0.354	0.367	0.211	0.741
	3	0.375	0.232	0.214	0.371
Aurevann (Aur)	**1**	0.185	0.085	0.119	0.037
	2	0.156	0.064	0.105	0.109
	3	0.143	0.100	0.058	0.060
Maridalsvann (Mar)	**1**	0.292	-0.04192*	0.0169*	-0.0404*
	2	0.238	0.118	-0.127*	-0.103*
	3	0.339	0.155	0.151	0.147
Birkenes (Bir)	**1**	0.349	0.124	-0.102*	-0.136*
	2	0.358	0.169	0.161	0.118
	3	0.241	0.196	0.158	0.164
Humex B (Hum)	**1**	0.336	0.272	0.220	0.206
	2	0.339	0.257	0.193	0.216
	3	0.360	0.230	0.127	0.101
Gjerstad limed (Gjl)	**1**	0.291	0.047	0.225	0.097
	2	0.190	0.138	0.253	0.061
	3	0.201	0.159	0.083*	-0.0911*
Gjerstad unlimed (Gju)	**1**	0.338	0.099	0.111	0.092
	2	0.277	0.087	0.150	0.060
	3	0.245	0.106	0.154	0.195
Hellerudmyra Oct. (Heo)	**1**	0.361	0.158	0.178	0.164
	2	0.391	0.167	0.123	0.268
	3	0.321	0.194	0.173	0.028

*Data excluded based on correlation between peak in pH and neg. Result
**Data excluded based on observation of > 3ml NaOH at the day of analysis
***Sample lost through transportation to UMB

Table 27: Total amount of CO_2 (mg C) measured for reference samples originating from the "NOMiNiC" project from the four days of analysis (day 10, 20, 30, and 45). Values excluded based findings indication NaOH contamination in the samples solution (*), contamination of samples solution in the NaOH (**) or for samples lost during transportation to UMB (***).

Sample	Replicate	Day 10	Day 20	Day 30	Day 45
Birkenes Fall (Bir-F)	1	0.261	0.255	0.118	-0.0829**
	2	0.251	0.140	0.102	0.036
	3	0.235	0.103	0.023	-0.0764*
Birkenes Spring (Bir-S)	1	0.358	0.135	0.077	-0.0846*
	2	0.331	0.073	0.112	0.071
	3	0.432	0.132	0.170	0.114
Valkea Kotinen Fall (Val K-F)	1	0.249	0.161	0.171	0.219
	2	0.354	0.165	0.101	0.166
	3	0.220	-0.101*	-0.937*	-0.0633*
Valkea Kotinen Spring (Val K-S)	1	0.224	0.078	0.037	0.034
	2	0.222	0.137	0.124	0.082
	3	0.309	0.153	0.254	0.124
Hieatäjervi Fall (Hie-F)	1	0.286	0.214	0.112	0.141
	2	0.236	0.237	0.123	0.112
	3	0.224	0.196	0.108	0.105
Hieatjäervi Spring (Hie-S)	1	0.250	0.103	0.092	0.080
	2	-0.0190*	-0.129*	-0.0969*	-0.0584*
	3	0.250	0.093	0.0259**	0.174
Svartberget Fall (Svart-F)	1	0.160	0.233	0.172	0.105
	2	0.183	0.128	0.233	0.031
	3	0.195	0.182	0.180	0.110
Svartberget Spring (Svart-S)	1	0.296	0.139	0.213	0.271
	2	0.409	0.187	-0.0912*	0.000580*
	3	0.372	0.130	0.105	-0.00188*
Skjervatjern Fall (Skj-F)	1	0.311	0.186	0.209	0.177
	2	0.346	0.187	***	0.150
	3	0.372	0.133	0.181	-0.150*
Skjervatjern Spring (Skj-S)	1	0.218	0.0694*	-0.112*	-0.149*
	2	0.287	0.177	0.082	0.091
	3	0.236	0.0825*	-0.116*	-0.0707*

*Data excluded based on correlation between peak in pH and neg. Result
**Data excluded based on observation of > 3ml NaOH at the day of analysis
***Sample lost through transportation to UMB

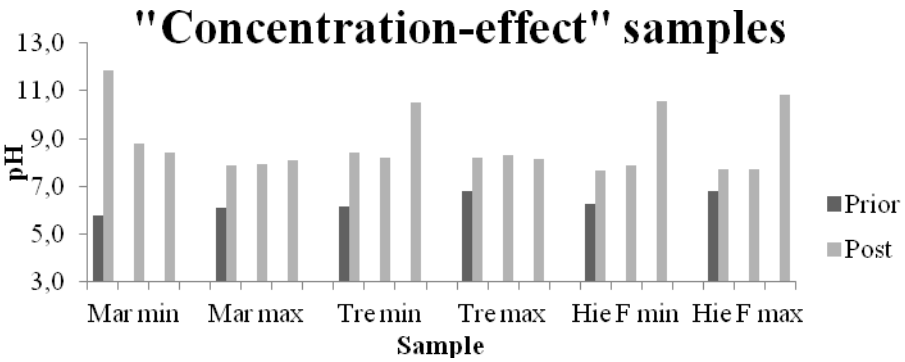

Figure 7: Comparison of pH measured on the reference samples re-dissolved to two additional concentrations, minimum (min) and maximum (max), measured prior (blue) and post (red) to the biodegradation experiment.

Table 28: Total amount of CO_2 (mg C) measured for reference samples originating from the "NOMiNiC" project from the four days of analysis (day 10, 20, 30, and 45). Values excluded based findings indication NaOH contamination in the samples solution (*), contamination of samples solution in the NaOH (**) or for samples lost during transportation to UMB (***).

Sample	Replicate	Day 10	Day 20	Day 30	Day 45
Maridalsvann (Mar) min	1	0.0883	0.0342	-0.121*	-0.112*
	2	0.0727	0.0817	0.101	0.134
	3	0.0809	0.0424	0.0423	0.459
Maridalsvann (Mar) max	1	0.187	0.113	0.132	0.0964
	2	0.171	0.119	0.133	0.203
	3	0.236	0.0907	0.095	0.109
Trehørningen (Tre) min	1	0.124	0.0432	0.095	0.260
	2	0.145	0.128	0.139	0.252
	3	0.126	0.051	0.068	-0.0440*
Trehørningen (Tre) max	1	0.229	0.123	***	0.407
	2	0.344	0.105	0.149	0.195
	3	0.123	0.123	0.120	0.286
Hieeatjärvi Fall (Hie-F) min	1	0.0826	0.242	0.0455	0.332
	2	0.00478	0.0727	0.0562	0.123
	3	0.123	0.0915	0.0545	-0.0936*
Hieatjärvi Fall (Hie-F) max	1	0.270	0.351	0.152	0.110
	2	0.277	0.128	0.180	0.174
	3	0.328	0.114	0.0283**	-0.0223*

*Data excluded based on correlation between peak in pH and neg. Result
**Data excluded based on observation of > 3ml NaOH at the day of analysis
***Sample lost through transportation to UMB

D-3 Mineralization curves for the reference samples

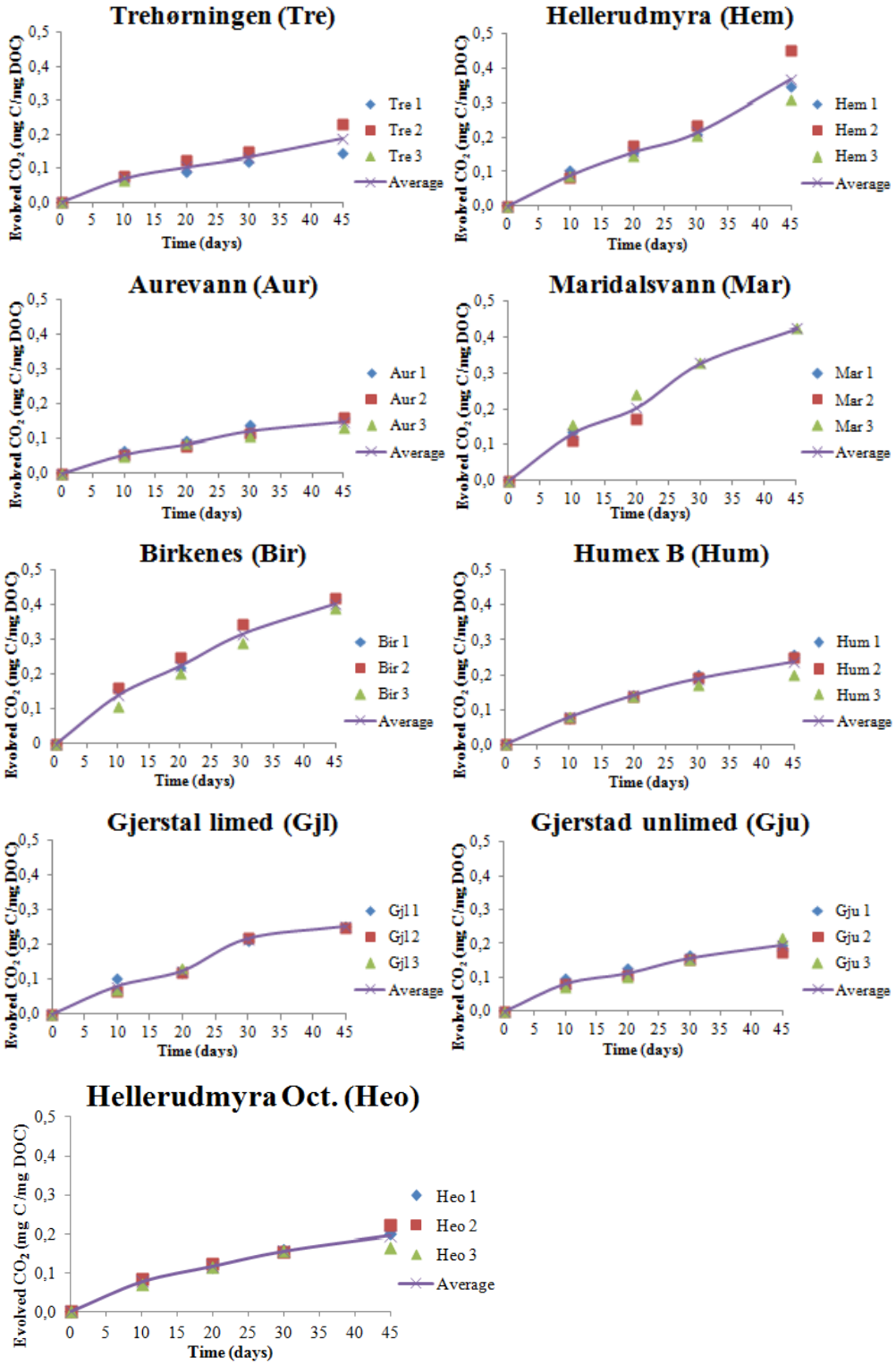

Figure 8: Mineralization curves presenting the relative amount of DOM biodegraded (mg C-CO_2/ mg DOC) for the reference samples originating from the "NOM-typing" project for the time course of the experiment (days).

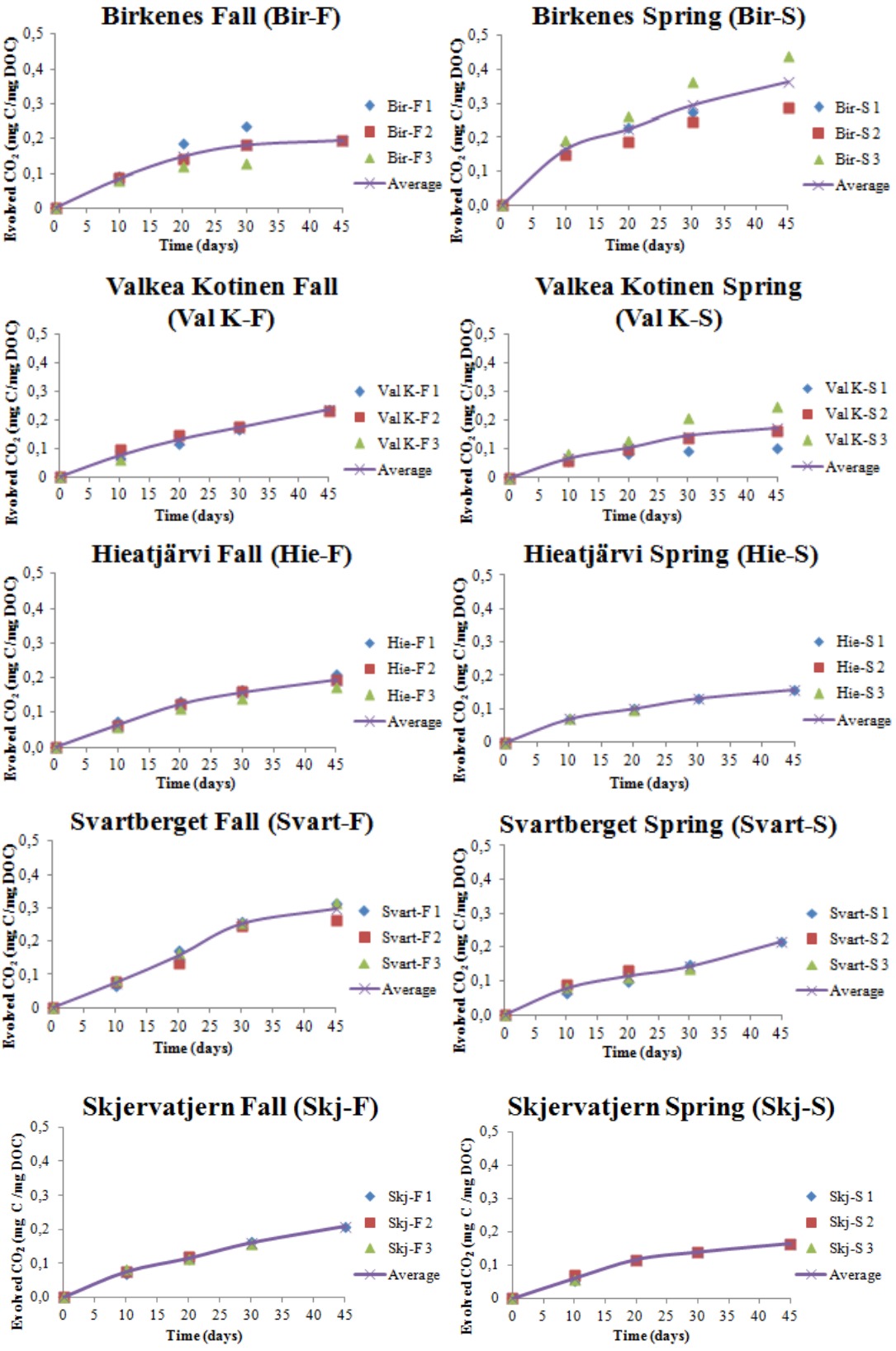

Figure 9: Mineralization curves presenting the relative amount of DOM biodegraded (mg C-CO_2/ mg DOC) for the reference samples originating from the "NOM-typing" project for the time course of the experiment (days).

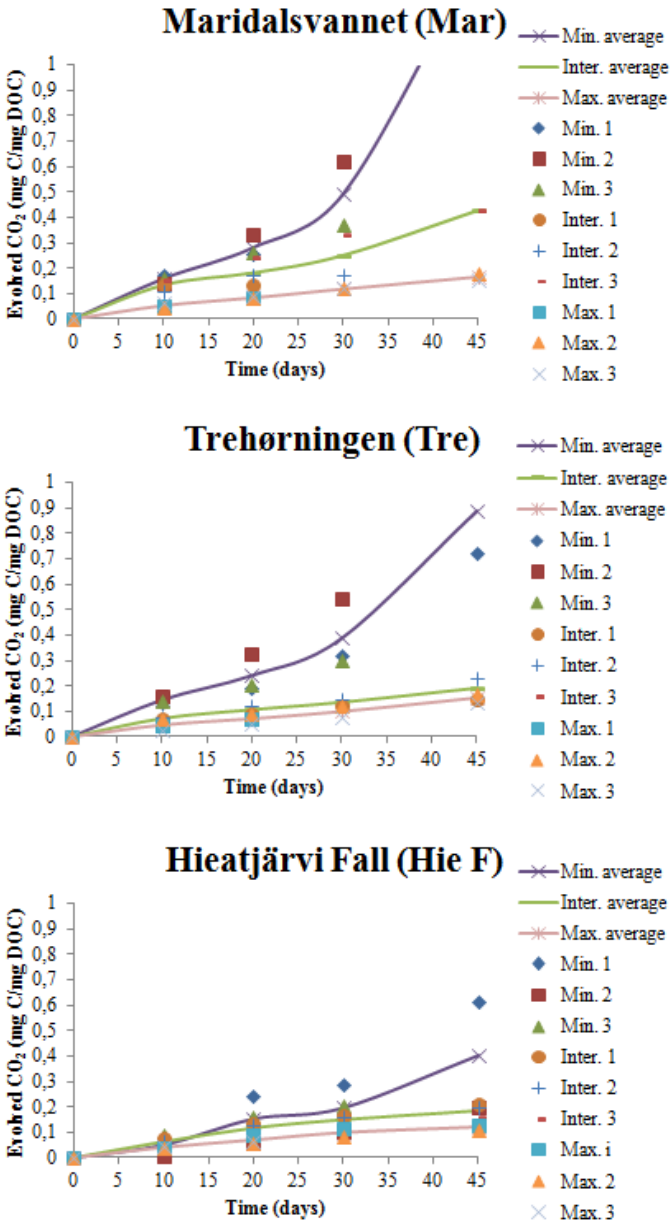

Figure 10: Mineralization curves presenting the relative amount of DOM biodegraded (mg C-CO_2/ mg DOC) for the reference samples re-dissolved to three different concentrations (minimum, intermediate, maximum) for the time course of the experiment (days).

Table 29: Mineralization rate constants for the re-dissolved RO isolated reference samples originating from the "NOM-typing" and the "NOMiNiC" projects, from the first time period of the biodegradation experiment, and for the total

Sample	k (10)	k (45)
Tre min	-15.6E-03	-21.5E-03
Tre	-7.38E-03	-4.47E-03
Tre max	-4.72E-03	-3.74E-03
Hem	-9.56E-03	-8.70E-03
Aur	-5.78E-03	-3.39E-03
Mar N	-17.3E-03	-98.2E-03
Mar	-14.3E-03	-9.00E-03
Mar X	-5.51E-03	-3.67E-03
Bir	-15.2E-03	-9.47E-03
Hum	-8.15E-03	-5.41E-03
Gjl	-8.39E-03	-5.91E-03
Gju	-8.59E-03	-4.50E-03
Heo	-8.04E-03	-4.46E-03
Bir-F	-9.02E-03	-4.52E-03
Bir-S	-18.2E-03	-8.28E-03
Val K-F	-7.79E-03	-5.22E-03
Val K-S	-7.06E-03	-3.89E-03
Hie-F min	-5.17E-03	-9.55E-03
Hie-F	-6.62E-03	-4.40E-03
Hie-F max	-4.16E-03	-2.62E-03
Hie-S	-7.31E-03	-3.88E-03
Svart-F	-7.80E-03	-6.90E-03
Svart-S	-8.15E-03	-5.10E-03
Skj-F	-7.80E-03	-4.70E-03
Skj-S	-6.19E-03	-3.47E-03

Appendix E. Changes due to biodegradation

E-1 Dissolved- and Total Organic Carbon (TOC/DOC)

Table 306: Concentration of Organic-C (mg C L^{-1}) measured on unfiltered and filtered blank samples; without (B1-4) and with inoculum (BI1-9) included in the biodegradation experiment. The average value was used to subtract from the sample values. This was performed due to analytical problems with the baseline of the TOC-analyzer.

Sample	Unfiltered	Filtered
B1	1,66	1,21
B2	1,30	1,98
B3	0,67	1,58
B4	1,21	0,98
BI 1	0,83	0,71
BI 2	0,78	0,91
BI 3	1,00	1,05
BI 4	1,26	1,75
BI 5	1,53	0,82
BI 6	1,14	1,39
BI 7	1,03	0,95
BI 8	1,23	1,42
BI 9	1,18	1,73
Average	1,14	1,27
St.Dev	0,28	0,40
RSD (%)	24,8 %	31,9 %

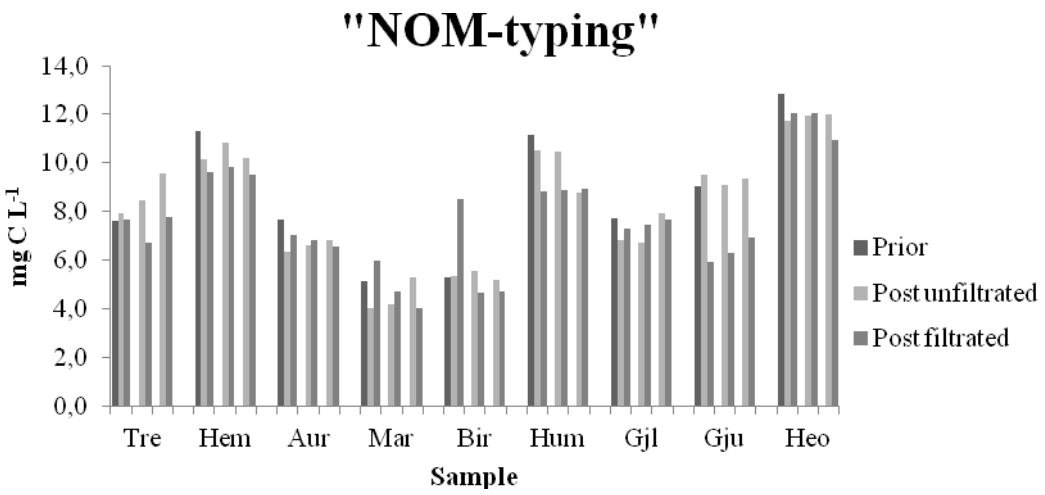

Figure 11: Concentration of DOC (mg C L^{-1}) measured in the reference samples originating from the "NOM-typing" project prior (blue) and on unfiltered (red) and filtered samples (green) post the biodegradation experiment.

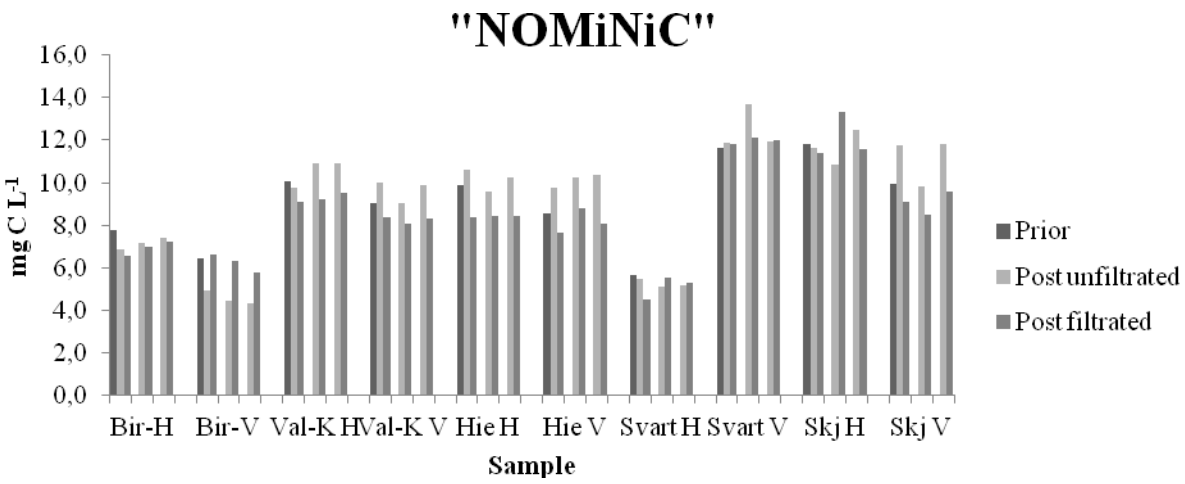

Figure 12: Concentration of DOC (mg C L^{-1}) measured in the reference samples originating from the "NOMiNiC" project prior (blue) and on unfiltered (red) and filtered samples (green) post the biodegradation experiment.

E-2 Concentration of Major Anions

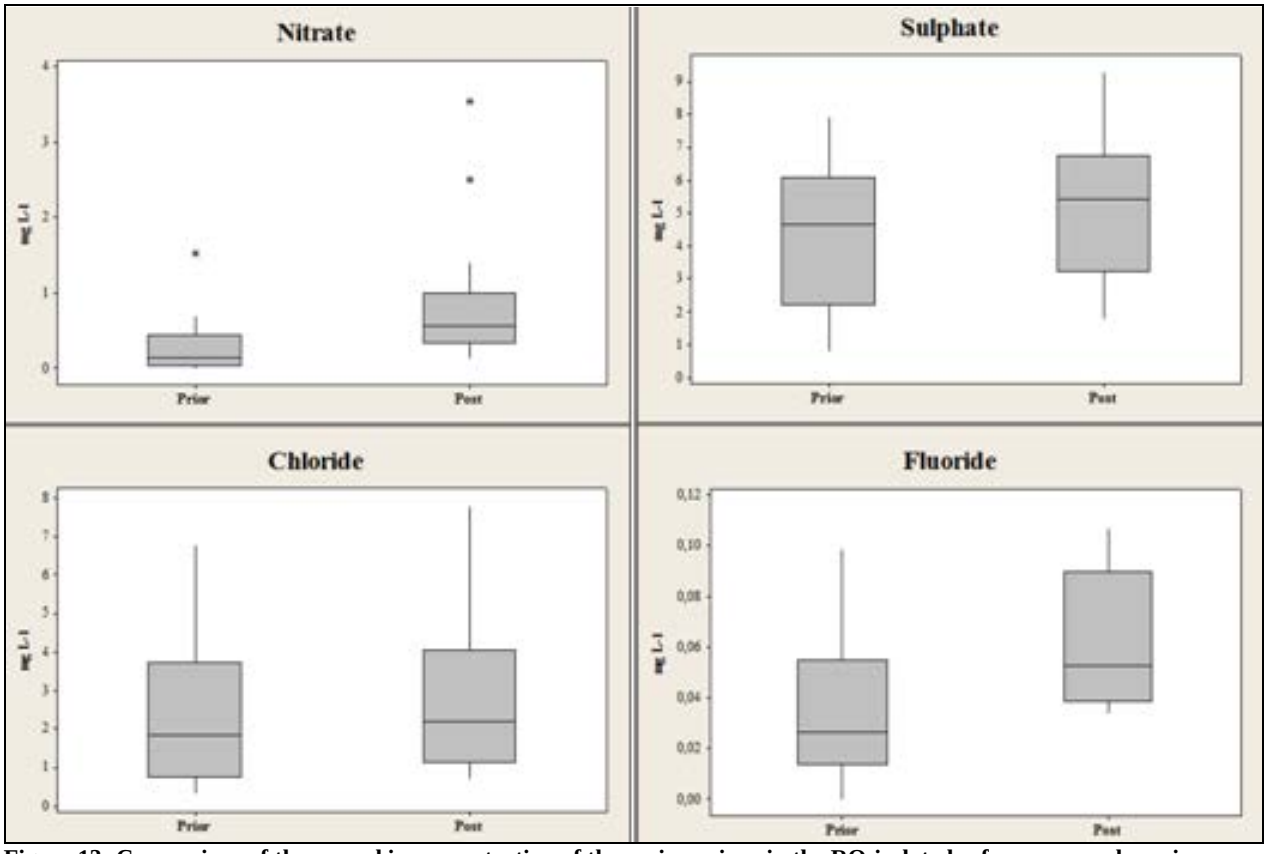

Figure 13: Comparison of the spread in concentration of the major anions in the RO-isolated reference samples prior and post to the biodegradation experiment. Above: nitrate (left), and sulphate (right). Below: Chloride (left), and Fluoride (right).

E-3 UV-Vis Absorbency

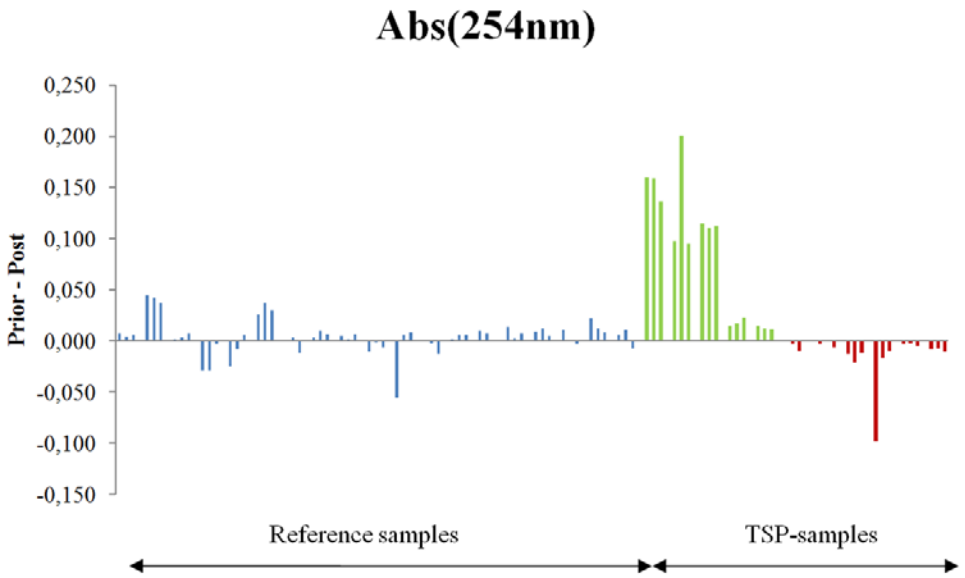

Figure 14a: Difference in absorbency at λ= 254nm measured prior and post to the biodegradation experiment for the reference samples (blue) and the TSP samples originating from the Hill Slope (green) and the groundwater discharge zone (red).

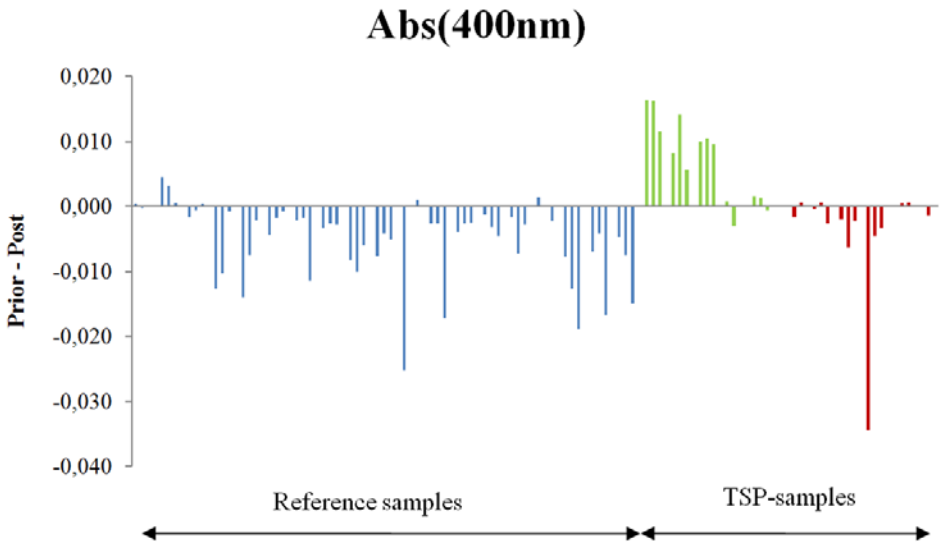

Figure 15b: Difference in absorbency at λ= 400nm measured prior and post to the biodegradation experiment for the reference samples (blue) and the TSP samples originating from the Hill Slope (green) and the groundwater discharge zone (red).

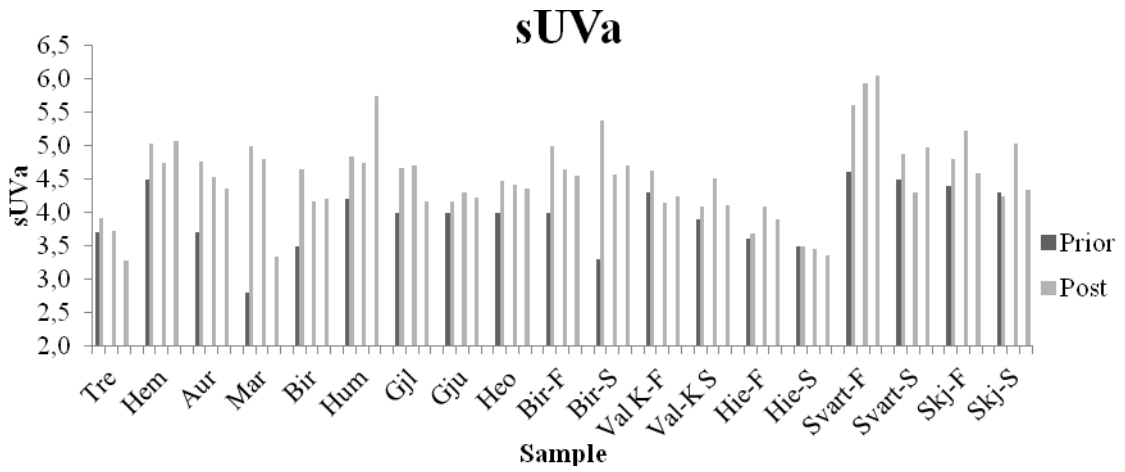

Figure 15: Comparison of the values for the specific UV absorbency (sUVa; Abs_{254nm}/[DOC]*100) measured prior (blue) and post (red) to the biodegradation experiment for the reference samples originating from the "NOMiNiC" project.

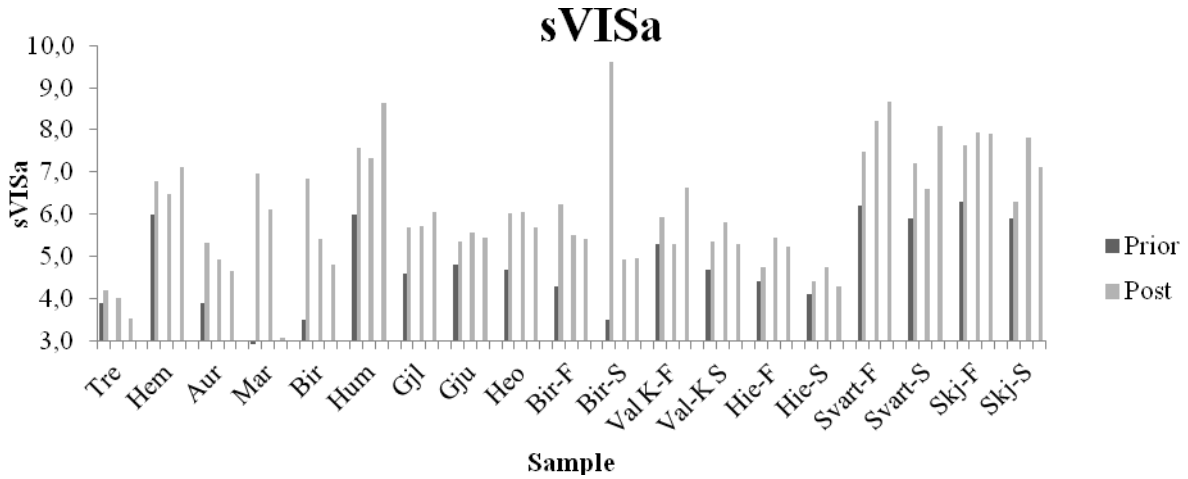

Figure 16: Comparison of the values for the specific VISible absorbency (sVISa; Abs_{400nm}/[DOC]*1000) measured prior (blue) and post (red) to the biodegradation experiment for the reference samples originating from the "NOMiNiC" project.

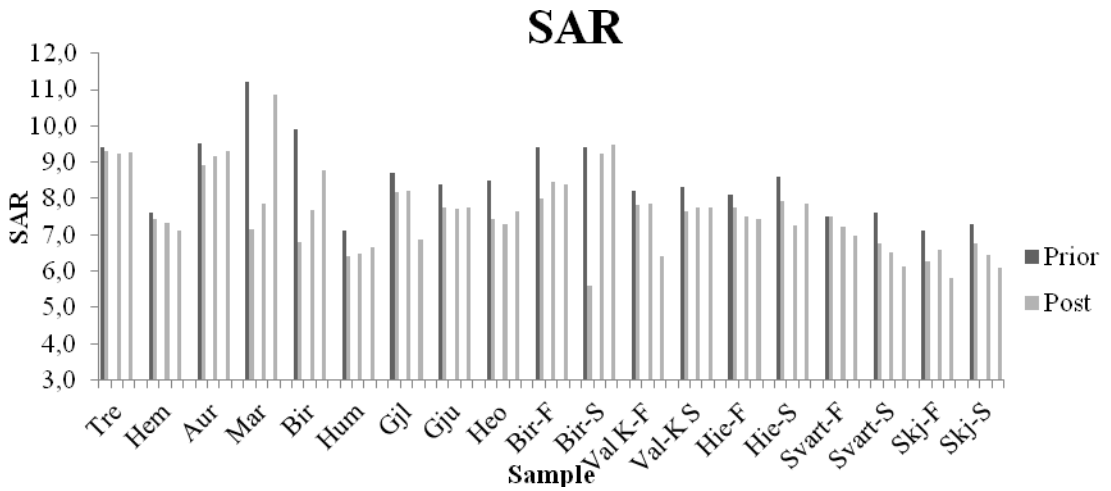

Figure 17: Comparison of the values for the Specific Absorbency Ratio (SAR; Abs_{400nm}/Abs_{400nm}) measured prior (blue) and post (red) to the biodegradation experiment for the reference samples originating from the "NOMiNiC" project.

E-4 Fluorescence EEM spectra for blank samples from the biodegradation experiment

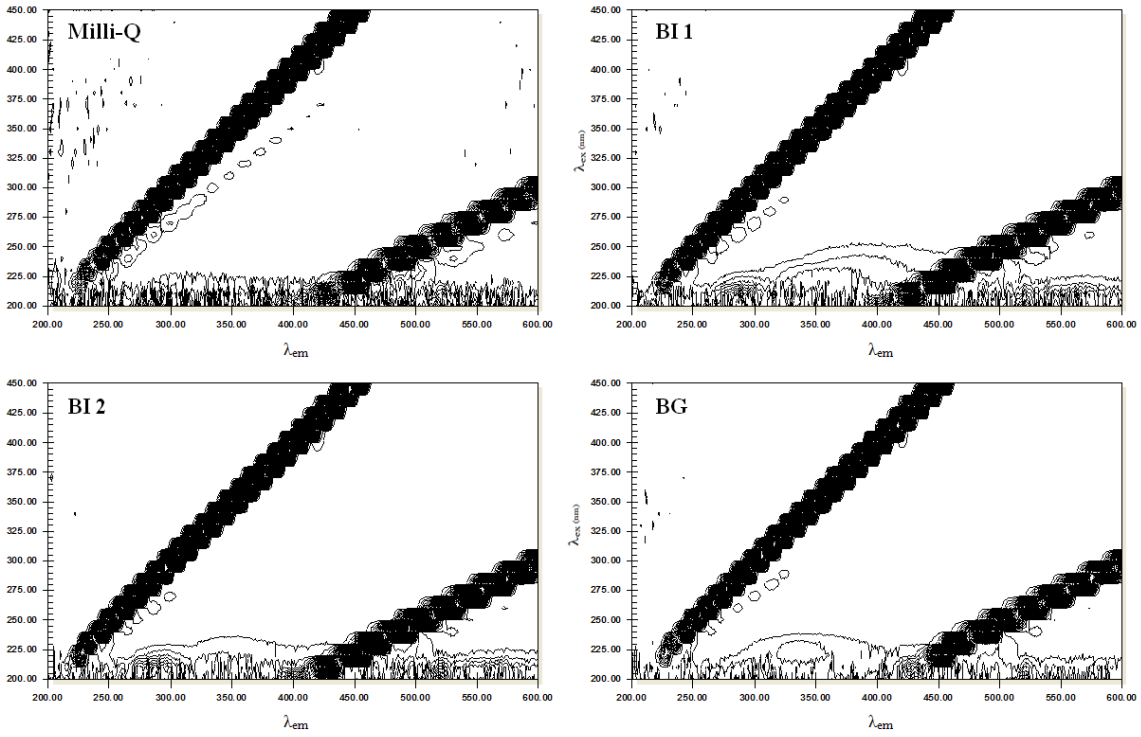

Figure 19: Fluorescence Excitation-Emission Matrix (EEM) spectra obtained for the measurement blank (Milli-Q), two replicates of the incubation-blanks (BI 1 and 2), and of the glucose solution (BG) post to the incubation experiment.